MICROCOPY RESOLUTION TEST CHART

NATIONAL BUREAU OF STANDARDS-1963-A

OFFICE OF NAVAL RESEARCH

Research Contract No. N00014-K-0576

TECHNICAL REPORT No. 13

C_2H_n FRAGMENTS ON METAL SURFACES

by

Jerome Silvestre and Roald Hoffmann

Prepared for Publication

in

Physical Review Letters

Laboratory of Atomic and Solid State Physics
Cornell University
Ithaca, NY   14853

AD-A151 474

DTIC FILE COPY

DTIC
ELECTE
MAR 2 0 1985

A

85   03   04   076

REPORT DOCUMENTATION PAGE	READ INSTRUCTIONS BEFORE COMPLETING FORM

1. REPORT NUMBER 13	2. GOVT ACCESSION NO.	3. RECIPIENT'S CATALOG NUMBER

4. TITLE (and Subtitle) C_2H_n Fragments on Metal Surfaces	5. TYPE OF REPORT & PERIOD COVERED Interim
	6. PERFORMING ORG. REPORT NUMBER

7. AUTHOR(s) Jerome Silvestre and Roald Hoffmann	8. CONTRACT OR GRANT NUMBER(s) N00014-82-K-0576

9. PERFORMING ORGANIZATION NAME AND ADDRESS Laboratory of Atomic and Solid State Physics Cornell University Cornell, Ithaca, N.Y. 14853	10. PROGRAM ELEMENT, PROJECT, TASK AREA & WORK UNIT NUMBERS

11. CONTROLLING OFFICE NAME AND ADDRESS	12. REPORT DATE February 22, 1985
	13. NUMBER OF PAGES 111

14. MONITORING AGENCY NAME & ADDRESS(If different from Controlling Office)	15. SECURITY CLASS. (of this report)
	15a. DECLASSIFICATION/DOWNGRADING SCHEDULE

16. DISTRIBUTION STATEMENT (of this Report)

Approved for public release; distribution unlimited.

17. DISTRIBUTION STATEMENT (of the abstract entered in Block 20, if different from Report)

18. SUPPLEMENTARY NOTES

Submitted to Physical Review Letters.

19. KEY WORDS (Continue on reverse side if necessary and identify by block number)

20. ABSTRACT (Continue on reverse side if necessary and identify by block number)

The chemisorption of an acetylene (HCCH), a vinylidene (CCH_2) and an ethylidyne (CCH_3) on metal surfaces, especially Pt(111) is analyzed in some detail, with an emphasis on the electronic rearrangements ensuing. The bonding is described in terms of semi-localized states, in turn obtained via a deconvolution of the total density of states into fragment orbitals of the hydrocarbon and the surface. The geometrical choices made by the various fragments on surfaces are analyzed by simple perturbation theory. It is found that in general the bonding within both the hydrocarbon fragment and the surface is dramatically weakened,

as indicated by the changes in overlap populations that result. The more
surface atoms are involved in anchoring the adsorbate, the weaker the bond-
ing within the surface becomes. A non-dissociative chemisorption is the re-
sult of a compromise and is operative when the price of the binding energy is
evenly distributed over the loss of bonding within the adsorbate and the surface.

Surface reconstruction and dissociative chemisorption are to be expected
as a consequence of the two extreme situations that may occur: a filling of
metal-metal antibonding states leading to surface reconstruction, whereas ex-
cessive population of carbon-carbon antibonding orbitals would drive a diss-
ociative chemisorption. The two patterns are illustrated by a would-be 4-fold
adsorption of C_2H_2 on Pt(111) and the chemisorption of C_2H_2 on Fe(100) respect-
ively. In the latter it is shown that the entire carbon-carbon bonding energy is
passed to the metal-carbon bonds, in a kind of bonding transfer. We find a
special role for the bulk-centered states, that of a reservoir which can be
alternatively filled or emptied depending on the metal atoms constituting the
surface.

Throughout the paper a comparison is made between the binding of the
fragments to the metallic surface and to discrete transition metal fragments
in organometallic chemistry.

C_2H_n FRAGMENTS ON METAL SURFACES

Jérôme Silvestre and Roald Hoffmann

Department of Chemistry and Materials Science Center
Cornell University, Ithaca, NY 14853

Abstract: The chemisorption of an acetylene (HCCH), a vinylidene
(CCH_2) and an ethylidyne (CCH_3) on metal surfaces, especially
Pt(111) is analyzed in some detail, with an emphasis on the
electronic rearrangements ensuing. The bonding is described
in terms of semi-localized states, in turn obtained via a decon-
volution of the total density of states into fragment orbitals
of the hydrocarbon and the surface. The geometrical choices
made by the various fragments on surfaces are analyzed by
simple perturbation theory. It is found that in general the
bonding within both the hydrocarbon fragment and the surface is
dramatically weakened, as indicated by the changes in overlap
populations that result. The more surface atoms are involved
in anchoring the adsorbate, the weaker the bonding within the
surface becomes. A non-dissociative chemisorption is the re-
sult of a compromise and is operative when the price of the
binding energy is evenly distributed over the loss of bonding
within the adsorbate and the surface.

Surface reconstruction and dissociative chemisorption
are to be expected as a consequence of the two extreme situations
that may occur: a filling of metal-metal antibonding states
leading to surface reconstruction, whereas excessive population

of carbon-carbon antibonding orbitals would drive a dissociative chemisorption. The two patterns are illustrated by a would-be 4-fold adsorption of C_2H_2 on Pt(111) and the chemisorption of C_2H_2 on Fe(100) respectively. In the latter it is shown that the entire carbon-carbon bonding energy is passed to the metal-carbon bonds, in a kind of bonding transfer. We find a special role for the bulk-centered states, that of a reservoir which can be alternatively filled or emptied depending on the metal atoms constituting the surface.

Throughout the paper a comparison is made between the binding of the fragments to the metallic surface and to discrete transition metal fragments in organometallic chemistry.

Chemistry has been enriched in the last two decades by an exponentially growing literature dealing with small molecules chemisorbed on metal surfaces. The reason for this expansion of our knowledge lies in a combination of three factors: i) an advancing technology which has allowed the development of highly sophisticated spectroscopic tools relevant to surface studies,[1] ii) an increased interest in many catalysis-related phenomena[2], iii) the general feeling induced by numerous experimental results, that discrete metallic clusters and metal surfaces should and do exhibit similar reactivity patterns, the so-called cluster-surface analogy[3,4]. In this context, a much investigated topic is that of the bonding and reactivity of acetylene on metal surfaces[5]. A large body of experimental information has now become available for different metal atoms constituting the surfaces as well as for systems involving a variety of crystal faces.

Let us review briefly the results and conclusions of these experimental studies. A number of techniques (Low Energy Electron Diffraction, Electron Energy Loss Spectroscopy, photoelectron spectroscopy, photoemission) have been used to ascertain the geometry and the adsorption site of C_2H_2 on Pt(111). Although believed at one time to be sitting on top of one metal atom[6], the acetylene is now considered most likely to occupy a bridging position of the hexagonal lattice of Pt(111)[4d]. The geometry is that depicted in 1. Note the bending of the hydrogens away from the surface. Also, the HCCH plane is not perpendicular to the surface; the C_2H_2 "leans" over a third metal atom,
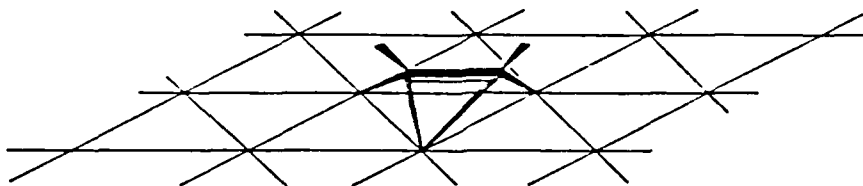
1

presumably to gain some extra bonding. The acetylene is essentially in a di-σ/π type of geometry similar to that observed in several trinuclear complexes[7]. Upon heating, the next species clearly detected on the surface is an ethylidyne fragment (C-CH_3) lying on top of a 3-fold hollow, as in 2. The step taking 1 into 2 is thought to transit via a vinylidene species[5f] which ultimately picks up a coadsorbed hydrogen atom. The formation of a C-CH_2 fragment on the surface has found some support in the recent literature[8].
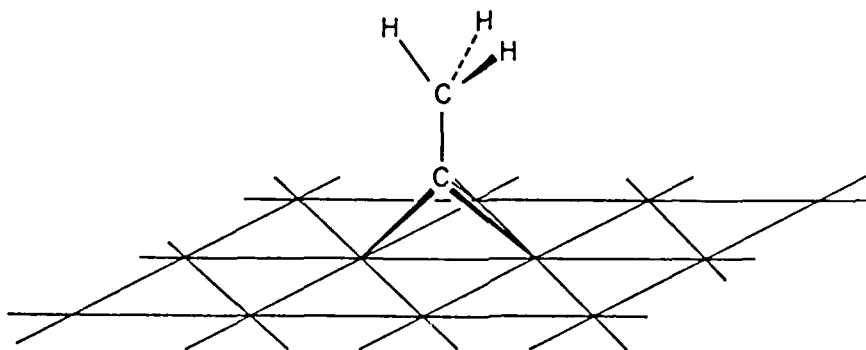

2

It is interesting to compare the overall behavior of C_2H_2 on Pt(111) and on other surfaces. For example, it has been demonstrated[5o] that the acetylenic bond is cleaved at low temperature on the square lattice of the Fe(100) surface. The hydrocarbon there is initially bound in a 4-fold manner, 3.
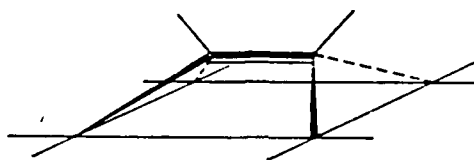
3

However, on Cu(111), featuring the same topology as Pt(111), C_2H_2 has been suggested[5s] to be 2-fold coordinated to the surface, as pictured in 4. The acetylene was shown[5v,9] to
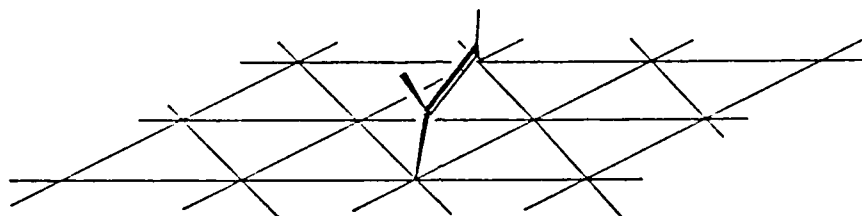

4

desorb intact at 350 K. Finally, on Ni(111), also hexagonal, the C_2H_2 unit is adsorbed in a similar way as on Cu(111), with some slight distortion of the hydrogens leading to a decrease in the overall symmetry as inferred from spectroscopic evidence[10]. In contrast to the adsorption on Cu(111), the hydrocarbon on Ni(111) undergoes some bond breaking processes upon heating; it does not desorb intact.

These experimental observations raise many questions. In this contribution we will dwell specifically on the following points: i) the electronic factors governing the geometrical choice made by C_2H_2, CCH_2 and CCH_3 on Pt(111), ii) the reasons for a different adsorption site and ractivity of C_2H_2 when chemisorbed on Pt(111), Cu(111) and Ni(111), iii) the

tremendous lowering of the barrier for the dissociation of C_2H_2 into two C-H fragments upon chemisorption on Fe (100). We shall try to generalize our conclusions and provide a general picture for the phenomenon of chemisorption in terms of the electronic changes occurring in both the adsorbate and the metallic surface.

We should direct the reader here to a number of excellent previous theoretical studies of the acetylene-metal surface system. Due in most part to A.B. Anderson[11] and Simonetta[12], these cluster calculations[13] were devoted primarily to the energetics of the system. We shall focus on the nature of the bonding between the chemisorbed species and the surface as well as the electron reorganization induced by chemisorption. Our arguments are based primarily on symmetry and overlap considerations supplemented by calculations of the tight-binding[14] type, within the formalism and framework of the extended Hückel method[15]. The geometrical and computational details not mentioned in the main body of the text may be found in Appendix 1 and 2 respectively.

Since one of the problems we want to tackle is that of the choice made by C_2H_2 for its adsorption site[16] on a hexagonal surface, let us first enumerate the different possibilities available. In 5a-d are drawn from a top view, an on-top, a 2-fold bridging, a 3-fold bridging and a 4-fold bridging

(a)   (b)   (c)   (d)
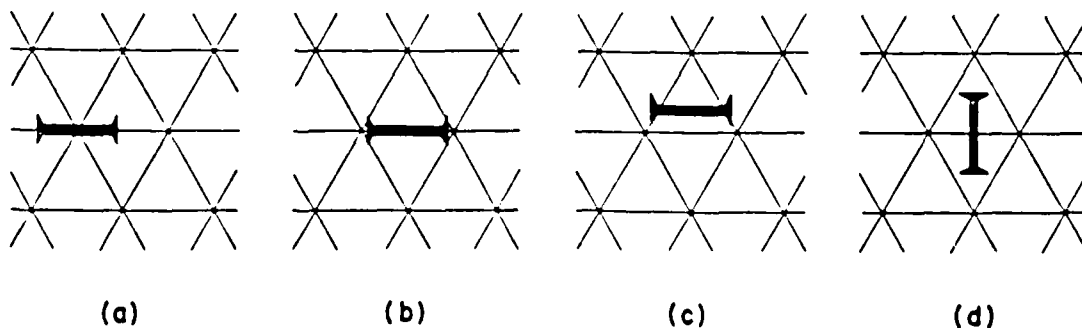
geometry - no consideration is yet made of the coverage of the surface. In 5 and the remainder of the paper, the stick with the two triangles at its ends represents an acetylene with the two hydrogens bent away from the surface, in a top view. One could imagine that the bonding in 5a-d is simply modelled by what we know about discrete transition metal complexes. Indeed, there is certainly an analogy between 5a-c and an acetylene bound to a mono-, bi-, and tri-nuclear complex, respectively. In 5d C_2H_2 may be considered as attached to a binuclear frame in a perpendicular fashion, as opposed to 5b, where the C-C bond is parallel to a metal-metal bond. However, these similarities hold only locally. The surface represents in fact a cluster, but one of infinite nuclearity. The conventional interaction diagram generated by combinations of discrete levels is not applicable and must be substituted by interaction between groups of states. We will return to this point later. It turns out, however, that the analysis of the interactions in the solid is made easier by prior knowledge of the related interactions taking place in discrete complexes. For this reason we turn now to a brief review of the forces holding together an acetylene and a mono-, bi- and tri-nuclear transition metal fragment. Another justification for going through this process is our intent eventually to compare the bonding of C_2H_2 with transition metal fragments and metal surfaces.

C_2H_2 on Discrete Transition Metal Fragments

In this section, we would like to extract the essence of
the electronic requirements for the formation of acetylene com-
plexes. First the topology of the transition metal fragment
orbitals in these systems is reviewed. The fragments under
consideration here are those which <u>locally</u> mimic the adsorption
sites described in 5a-c, that is a mono-, bi- and tri-nuclear
fragment, respectively. In Figure 1 are displayed the frontier
orbitals of prototype ML_n, M_2L_{2n} and M_3L_{3n} units for which
acetylene complexes are well established[17]. Before commenting
further on Figure 1, let us remind the reader of the orbitals
of a coordinated acetylene. In increasing order of energy,
one finds π, π_σ, π_σ^* and π^* all depicted in 6. The detailed

π π_σ π_σ^* π^*
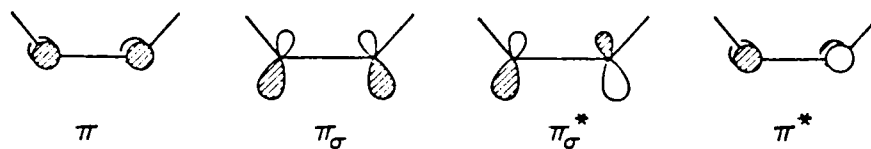
6

description of this pattern may be found elsewhere[17b]. With the
convention of using a neutral acetylene as ligand, only π and
π_σ are filled, each with two electrons. Returning to Figure 1,
at left are the valence orbitals of both a d^{10} - ML_2 and a
d^9 - ML_3 fragment[18]. Next, a schematic picture has been used
to display the frontier orbitals of a M_2L_{2n} unit[17b]. The

reason for the two different entries (and) will become

apparent shortly. Finally on the right-hand side of Figure 1,

---
Figure 1 here
---

the upper frontier orbitals of a D_{3h} M_3L_{3n} unit are dis-

played[19]. The splitting of the M_2L_{2n} case into two distinct

possibilities is motivated by the differentiation that has to

be made between a parallel acetylene, 7a, and a perpendicular

one, 7b.

(a)   (b)
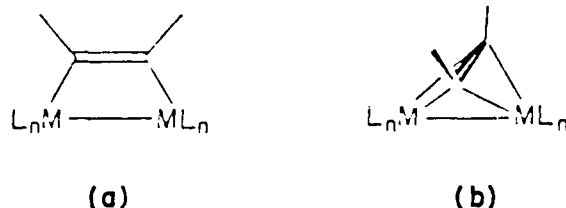
7

Upon coordination of an acetylene, the orbitals boxed by

a dashed line in Figure 1 combine with π_σ and π_σ^*, to produce

the MO's shown in 8 and 9. The reader will have noticed that

the forward donation components from the acetylene to the metals

are gathered in 8 whereas the back-donating ones are displayed

on the right, in 9. What we have done in 8 and 9 is simply to

extract for each complex the two interactions lying at the

heart of the universally known Dewar-Chatt-Duncanson model[20].

Beyond this apparent simplicity and similarity in the bond-

ing scheme of all these systems, there are differences. The

latter will have important ramifications when we deal with the

case of an acetylene on a metal surface, and therefore deserve

further comments. First, we have ignored in the previous con-

The bare surface

Let us discuss here the electronic structure of our chunk of Pt metal without the acetylene layer. Most of the information is cast in Figure 2 which displays the DOS curve of the slab. On the left is the contribution of s states, on the right that of the p states. What is not s or p is metal d. In this paper we will use alternatively "contribution" or "projection" to single out the participation of a subset of atoms, atomic orbital or fragment molecular orbitals in the overall DOS plot. The dashed

Figure 2 here

lines in Figure 2 refer to the total DOS curve. The darkened areas indicate the contribution of the projected states. The dotted lines are integration curves, running from 0 to 100%. These are to be interpreted in the same way as NMR integrations --they additively count the number of states across the energy scale.

From Figure 2 it is clear that a substantial number of s and p states penetrate the d band. At the Fermi level (indicated by ϵ_F in Figure 2), the electron distribution on an inner layer atom and a surface one is indicated in Table 2. Note that on average, any Pt atom has its s band approximately $\frac{1}{3}$ filled, reminiscent of the conventional d^9s^1 configuration. Also, the surface is negatively charged relative to the bulk. This is not a new result, but has been discussed at length on several

Table 2 here

used ($\frac{1}{2}$). Although we will return to this point, note that in
$\underline{17}$ the black triangles are not aligned with the solid line
representing the C-C bond. For this geometry alone the H-C-C-H
plane was chosen not to make an angle of 90.0° with the surface.
The views in $\underline{17}$-$\underline{19}$ also display the hexagonal symmetry of the
lattice, and indicate the coordinate system used. The z axis
sticks out of the plane of the paper, i.e., is perpendicular
to the surface. For future reference, each structure shows the
numbering of the Pt atoms on the surface in the unit cell
(shaded).

The following assumptions are made throughout in terms of the geometry and the coverage of the surface: the acetylenic C-C bond is kept at a constant value of 1.34 Å; the acetylene hydrogens are bent back so that the C-C-H is 140.0° and the closest Pt-C distance is 2.03 Å. Experimentally, the LEED pattern for the metastable C_2H_2 layer is 2×2. This simply means that the metallic film is ¼ covered. The unit cell of the chemisorbed surface is thus quadrupled with respect to that of the bare metallic slab. Our computation will use the same coverage. This complicates our calculations somewhat but prevents the introduction of spurious effect due to short acetylene-acetylene contacts.

Four geometries corresponding to 5a-d were investigated. Each is redrawn in 16-19, taking into account the coverage

16   17

18   19
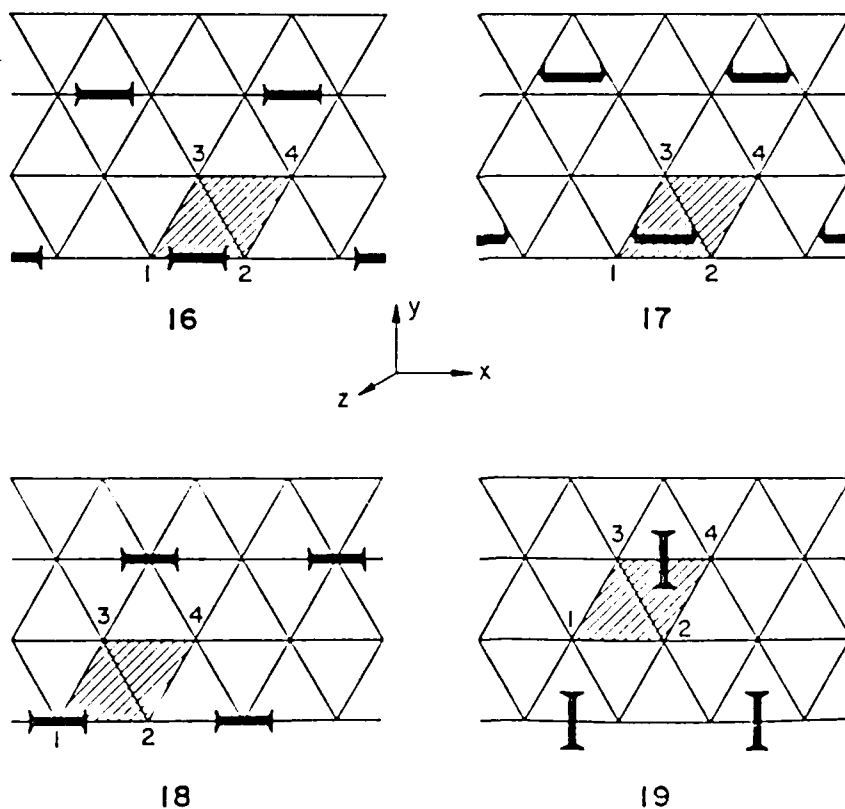
C_2H_2 on Pt(111)

As mentioned in the introductory lines of this paper, an enormous amount of experimental work has been devoted to this system.[29] Numerous calculations of the cluster-type have also been performed. We prefer to model the surface by a two-dimensional slab of finite thickness so as to simulate better the semi-infinite nature of the system.[30] The choice of the thickness of the slab is the result of a compromise between computational economy and reasonable accuracy. Exploratory calculations lead to the conclusion that a 3-layer film is an appropriate choice: changes in the Fermi level, charge distributions and overlap populations are small on going from a 3- to a 4-layer slab.

The (111) face of Pt is a closed-packed structure of hexagonal symmetry. Along the perpendicular to the surface, one has successive layers with a stacking sequence A B C . In 15 is shown in a top view the atomic arrangement. The bold solid line represents layer A, the dashed line is B, one "floor"
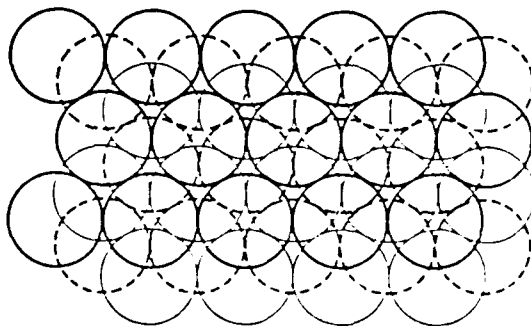
15

below, and the thin solid line is C, the bottom layer.

the edges of the Brillouin zone the band must be flat.[27] The
flatness of the band at these points translates into peaks in
the DOS curve. The states at the bottom of the band are bonding,
those in middle non-bonding, roughly, and those near the top
antibonding between nearest neighbors in the chain. There is a
natural "clumping" of levels near the bottom and top of a band,
and this leads naturally to a focussing on these band extremes.
Looking at one DOS plot, one may further ask of each state,
sweeping up across the energy scale, how much it contributes
to the bonding between two specified atoms. The result may be
plotted and has been called the Crystal Orbital Overlap Population.
in short COOP.[28] The integration of this curve up to a given
level provides the overlap population between the two prespecified
atoms for the corresponding band filling.

used by solid state physicists: an energy level diagram becomes

a density of state (DOS from now on) plot, the HOMO is named the

Fermi level, etc. Because at any arbitrary k-point a crystal

orbital is represented by a complex function of k, one may be

scared by the loss of physical and pictorial insight that ensues.

In other words, can we still apply frontier orbital ideas when

one deals with bonding in the solid? The answer in an informal

way is "Yes, if one gets used to thinking about the properties

of bunches of levels", and the density of states formalism is

the right way to do this.

Let us examine the simplest example. In 13 and 14 are

drawn a band and the corresponding DOS associated with it. This

13   14
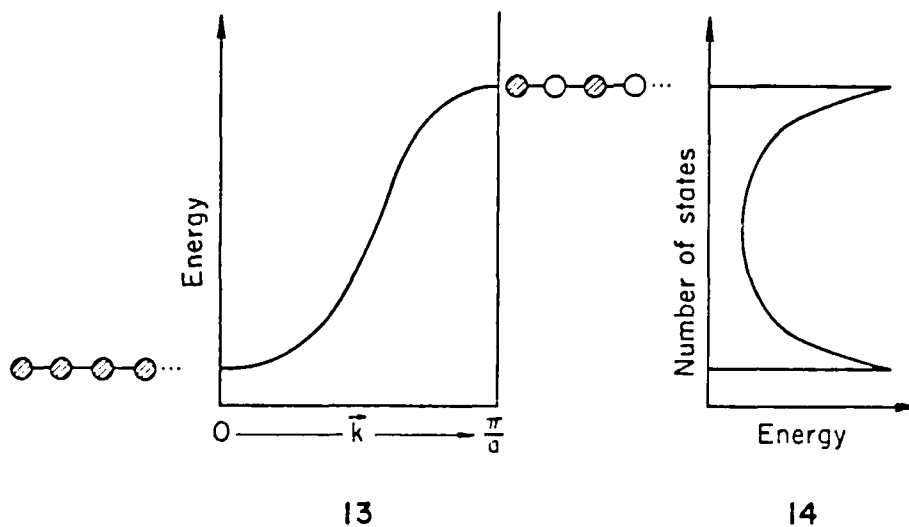
could represent the 1s band of a hypothetical one-dimensional

chain of hydrogen atoms. Also indicated is the nodal structure

of the crystal orbital at $k = 0$ and at the zone boundary,

$k = \frac{\pi}{a}$. A fundamental property of an energy band is that at

Concepts and Tools

A metallic surface, with or without a chemisorbed species on it, is a 2-dimensional solid[23]. As such, and within the usual approximation of a perfect lattice, it possesses the fundamental property of any crystal, namely translational symmetry. A wave function, if it is to represent a particular electronic state of such a system, must reflect this periodicity. One has therefore to utilize to the so-called Bloch functions. The latter, beside the fact that they conveniently[24] meet the previous requirement, depend on the location in reciprocal space of the wave under consideration. Any Bloch function representing a state n is characterized by an index, k, and written $\psi_k^{(n)}(r)$. The crucial consequence of this double index dependence is that any single state, any eigenvalue of the Schrödinger equation for the unit cell, generates as a function of k a very large[25] number of levels all representing eigenstates of the Schrödinger equation for the solid; a band is born. Thus, it is clear that the number of bands is equal to the number of basis function in the unit cell. In other words, each molecular orbital of the unit cell generates one band. Each particular k-point along this band is associated with a particular nodal structure of the crystal orbital. From these considerations[26], it is apparent that one cannot, in the electronic structure description of a solid, deal with one level at a time. As mentioned earlier, one is forced to talk in terms of groups of states. This is conveniently done by borrowing the language

spirit of this study, the behavior of C_2H_2 on other surfaces is examined. The emphasis at that point will be put on reactivity rather than on static interactions. In our attempt to understand the influence of the d-band filling of the metal, the choice of the Fe(100) and Cu(111) surfaces was guided by the reasonably large amount of experimental information available for these two systems.

numbers is that in the process of forming 12a and 12b, the
driving interactions are different in the two cases. Clearly
in the d^{10}-ML_2 system π_σ^* is occupied to a greater extent
in the early stages of the reaction than π_σ is depopulated.
The reverse phenomenon occurs for the d^8-ML_3 complex. In
general one can say that with respect to acetylene, a d^{10}-ML_2
fragment is a better base, in the Lewis sense, and a d^8-ML_3
unit is a better acid. The conclusion emerging from this dis-
cussion is that the direction in which the ultimate synergistic
motion of the electrons is initiated depends substantially
on the d-electron count of the transition metal fragment. Using
the same line of thought, for a given ML_n unit the sense of
the initial flux of electron is governed by the energy of the
frontier orbitals of the incoming ligand relative to those of
the metals.

We next want to see how these considerations translate
when the metallic fragment is substituted by a metallic surface.
At this point, a word must be said about the organization of the
rest of the paper. We first review the concepts and tools used
throughout the remaining part of this work. Next, a detailed
study of the chemisorption of C_2H_2 onto a Pt(111) is under-
taken. The electronic features associated with each particular
adsorption site are analyzed. Using then the C_2H_2/Pt(111)
problem as a "worked example", the adsorption of CCH_2 and
CCH_3 on Pt(111) is described at a somewhat faster pace.
Finally, the reader being then acquainted with the general

Table 1. Occupation of π_σ and $\pi_\sigma{}^*$ in 12a-b.

ML_n	$d^{10} - ML_2$	$d^8 - ML_3$
Occupation of π_σ	1.83	1.69
Occupation of π_σ^*	0.53	0.13

stages of the reaction taking a free C_2H_2 molecule to a complexed form with a d^{10} - ML_2 unit, the dominant interaction is <u>not</u> the one involving forward donation from π_σ of C_2H_2 into this sp hybrid but rather that involving the back-donation component. This follows because of a much better energy match between the donor of the metal and π_σ^*. In the case of a metal-d centered acceptor, the initial stabilization is due to the forward donation term[22]. Maybe we can provide a more quantified illustration of these considerations by the following: let us take $(CO)_2Pt(C_2H_2)$ and $H\,Pt(CO)_2(C_2H_2)^+$ in a geometry before 100% of the bonding between Pt and C_2H_2 is turned on, for

(a)   (b)
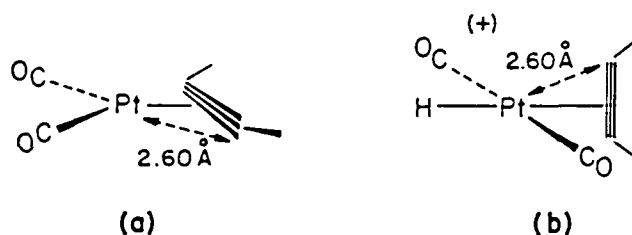
12

instance at a Pt-C(acetylene) distance of 2.60 Å (see <u>12a-b</u>). The two structures represent examples of incipient $C_2H_2\,d^{10}$ -ML_2 and $C_2H_2\,d^8$ -ML_3 complexes. The direction of the electron density flow may be measured by computing in the two systems the occupation of π_σ and π_σ^*. The numerical values are gathered in Table 1. The implication of these

Table 1 here

π and π^* components of C_2H_2 have been shown recently to be active participants in the electronic structure of mononuclear complexes[21], it seems that their contributions are more important as the nuclearity of the metallic fragment increases. We will see soon how this translates in the surface case.

The second point we would like to discuss concerns the orbital pattern of the metallic units. From both Figure 1 and 8-9, it is quite clear that the metal fragment must present in one form or another some type of low-lying vacant orbital of the appropriate symmetry to accept the flux of electrons from π_σ. Similarly a filled metal-centered MO must be present to back-donate into π_σ^*. In other words, the transition metal fragment has to be both electronically and coordinatively unsaturated. However, a careful look shows that in this respect the d^{10} - ML_2 case is unique. The acceptor orbital is not metal d centered, but rather a sp hybrid on the metal. The d-shell of the metal is filled before interaction with an acetylene. Because of its constitution, this sp hybrid lies perforce relatively high in energy in comparison to π_σ. Recall that from the simple perturbation expression:

$$\Delta E = \frac{|H_{ij}|^2}{E_i^0 - E_j^0}$$

the stabilization of the lower orbital in a 2-orbital interaction is governed by the energy difference between the two levels before interaction and by the overlap between the two wavefunctions representing these two states. What this implies is that in the initial

(a) $3a_1 + \pi_\sigma$ $b_2 + \pi_\sigma^*$ ML$_2$

(b) $2a_1 + \pi_\sigma$ $a_2 + \pi_\sigma^*$ ML$_3$

(c) L$_n$M——ML$_n$ $a_1 + \pi_\sigma$ L$_n$M——ML$_n$ $b_1 + \pi_\sigma^*$ M$_2$L$_{2n}$ //

(d) L$_n$M——ML$_n$ $a_1 + \pi_\sigma$ L$_n$M——ML$_n$ $b_2 + \pi_\sigma^*$ M$_2$L$_{2n}$ $\perp$

(e) $2a_1 + \pi_\sigma$ $2e(A) + \pi_\sigma^*$ M$_3$L$_{3n}$
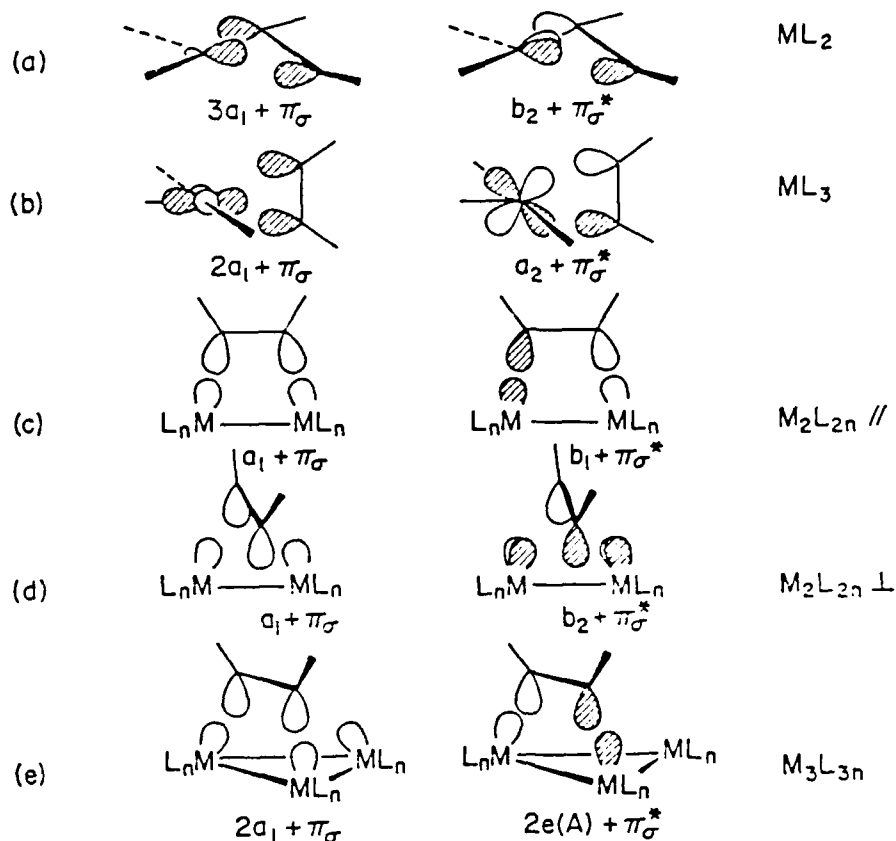
8   **9**

siderations the role of the perpendicular π-type orbitals,

π and π*. The reason is that the extent of their involve-

ment in the overall picture varies considerably, depending on

the transition metal fragment the C_2H_2 is bound to. A detailed

study of the binuclear and trinuclear systems[17b,19] shows that

π and π* are allowed to mix into π_σ and π_σ^*, respectively.

Such is the case for trinuclear complexes of type 10. An

interaction such as 11 (given here only as a representative

example), is crucial in this system. Although the perpendicular
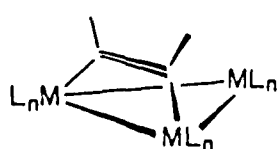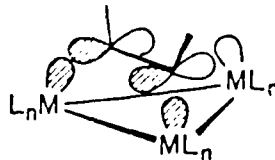
10   11
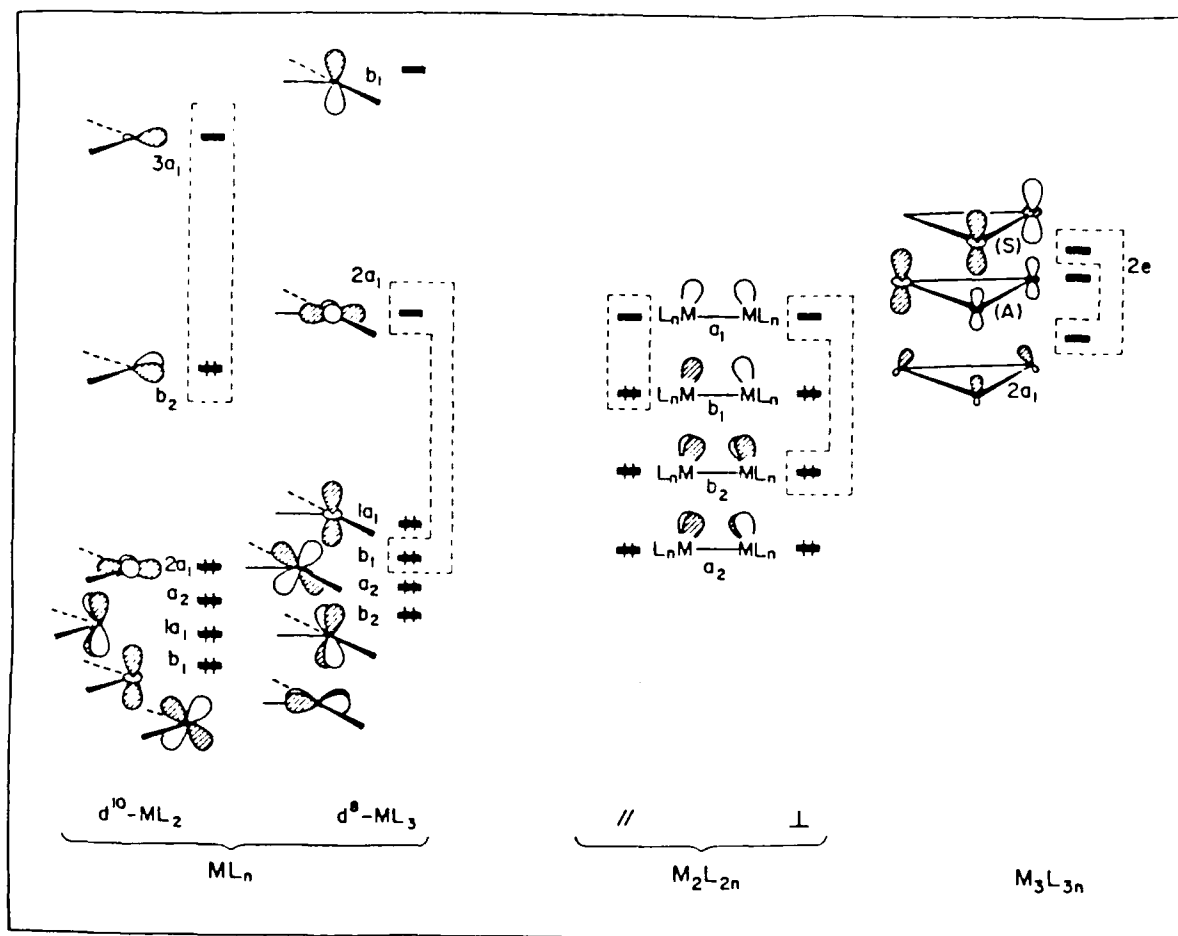
Figure 1. Frontier orbitals of d^{10}-ML_2, d^8-ML_3, M_2L_{2n} and M_3L_{3n} fragments.

Table 2. Population of Surface and Inner Pt Orbitals.

	s	p	d	total
surface layer Pt	0.686	0.064	9.375	10.125
inner layer Pt	0.604	0.088	9.058	9.750

occasions.[31] Its explanation in short is that any inner atom feels the influence of more neighbors than a surface one. Thus the states of inner or bulk atoms are more spread out; in particular a few of them go above the Fermi level and are therefore empty, relative to a 10 electron uncharged reference.

We are now in the position to bring in a layer of acetylene molecules.

The 2-fold geometry. 16

In order to understand better the electron changes associated with the covering of the surface by C_2H_2 (the coverage is that shown in 16), we show in Figure 3 the DOS curves of the d-orbitals of the surface atoms before and after the interaction ((a) and (b) respectively) as well as the distribution of the acetylene states prior to the contact with surface and after ((d) and (c) respectively). The peaks for curve (d) here are reduced to single lines. The reasons for this lie in the fact that there is essentially no overlap between different acetylenes with the

---
Figure 3 here
---

coverage used. All the crystal orbitals are at the same energy, the energy of the relevant MO in the isolated molecules. The pattern in (d) follows directly from what was displayed in 6. The stick at -16.0 eV corresponds to one combination of the C-H bonds.

Let us concentrate first on the total DOS curves. These are the dashed lines. It is important to realize that a number of states lying just above the Fermi level (arrow) in (a) have dissappeared in (b). Conversely, the dip existing at -12.0 eV in the DOS of the slab-only has vanished and many more states are now present in this energy region. Interestingly, the loss of the feature at -10.0 eV upon chemisorption of C_2H_2 is experimentally observed by Plummer and coworkers using angle-resolved photo-electron spectroscopy. This is certainly encouraging as far as the overall accuracy of our calculation is concerned.
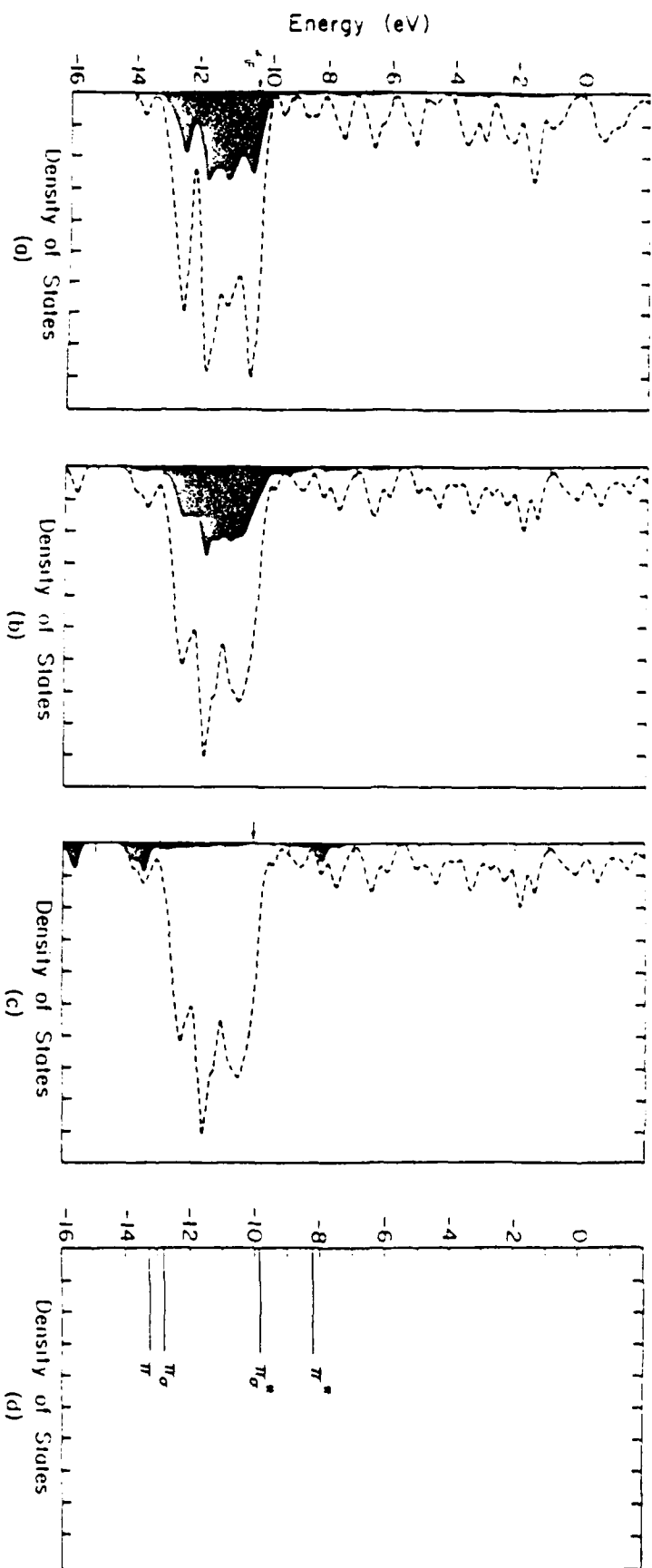
Figure 3. a) Contribution of the surface d-states in the slab before interaction.

b) Contribution of the surface d-states in the overall system after interaction.

c) Contribution of the acetylene states in the overall system after interaction.

d) Density of states of the acetylene layer only.

The area under each contribution curve is darkened.

Looking now at the projection curves, Figure 3(b) clearly establishes that this transfer of states from -10.0 eV to -12.0 eV primarily involves surface d-states. Also it is apparent that these states are more spread out after chemisorption than before as the result of the interaction with C_2H_2. Turning to the acetylene levels, Figure 3(c) displays in the dard area under the curve the states contributed by C_2H_2 to the overall DOS. This is to be compared with Figure 3.(b) Gone is the clear-cut separation of π, π_σ, π_σ^*, and π^* . The surface "dilutes" all these states. In particular, note the total disappearance of what used to be π_σ^* before adsorption.

One would like to know what is the fate of each of these acetylene states in the process of adsorption. Figure 4 is illuminating in this regard. From left to right is plotted the contribution to the total DOS separately of π, π_σ, π_σ^* and π^* . The curves have been magnified by a constant ratio for better viewing. Since the emphasis here is on how the states have been shifted by adsorption, the total DOS curves

---

Figure 4 here

---

are omitted. However, the integration curves are left in the pictures. The Fermi level is indicated by an arrow. Also, we indicate by a stick mark the position of the corresponding states in the absence of interaction between the acetylene layer and the slab. The following observations can be made. The bonding π orbital does not interact much; it is slightly
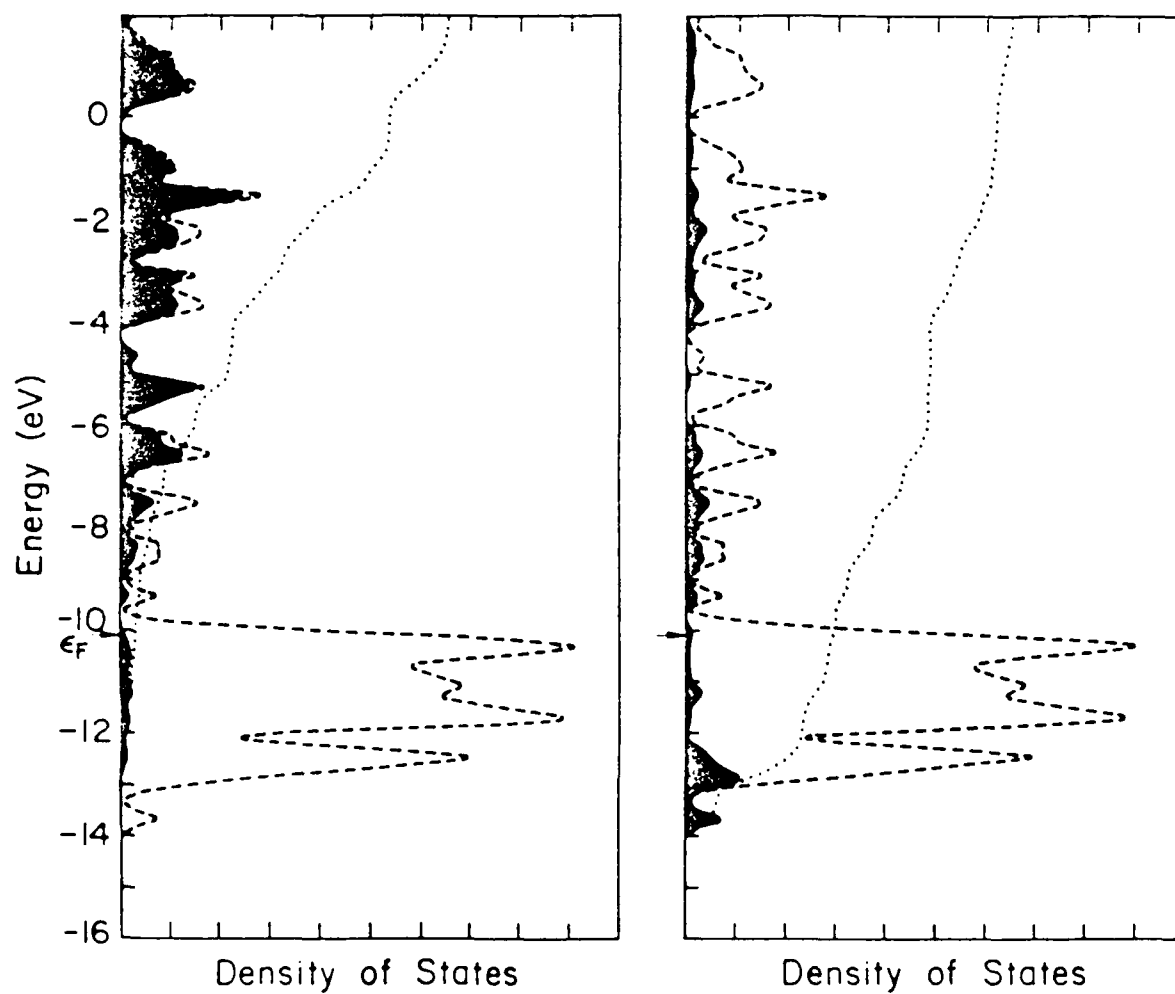
Figure 2. Left: contribution of the s states to the total DOS of the bare Pt(111) slab.
Right: contribution of the p states to the total DOS of the bare Pt(111) slab.

pushed down in energy by a few tenths of an eV. From the inte-
gration curve, one sees that only 20% of the states are some-
what dispersed but most of them are still filled, since they
wind up lying below the Fermi level. The other bonding MO
is more involved and experiences a lot of interaction: 70%
of the states are shifted down in energy by more than 3 eV.
Also, at the Fermi level roughly 20% of them are empty. In
other words some forward donation from C_2H_2 to the surface
has occurred.

It is however in the behavior of π_σ^* that we find the
most drastic electronic effects due to adsorption. Initially
all empty, more than 50% of the corresponding states are now
filled. The contact of C_2H_2 with the surface has spread the
π_σ^* band broadly. Starting at -9.8 eV as a single peak, this
band has now a width of ~7 eV ranging from -13.5 eV to -6.5 eV!
This interaction is the source of a tremendous amount of back-
donation from the metallic film to the acetylene; an occupation
of 1.059 electrons is computed for the initially empty π_σ^*
orbital. Finally, π^* is pushed up as a result of the inter-
action of C_2H_2 with the surface by ~0.5 eV. The extent of
π^* involvement in the overall picture appears to be small;
however, as indicated by the integration curve, approximately
8% of the state fall below the Fermi level and thus π^* is
occupied with 0.160 electrons.

Now that we understand better what has happened to the
acetylene levels, let us try to unearth which of the surface d-
states are responsible for the observed changes.

If one recalls that the 2-fold geometry resembles that of
a parallel binuclear complex, one has the intuitive idea that
the two sets of Pt atoms in the unit cell, {1,2} and {3,4}
(see the numbering of the surface atoms 16) play a totally
different role in binding the acetylene. In particular, Pt_1
and Pt_2 should be the principal actors in the process. This
is nicely confirmed by looking separately at the dispersion of
the d-bands on {Pt_1, Pt_2} and {Pt_3, Pt_4}. Schematically,
the picture is that of 20. Here we draw side by side
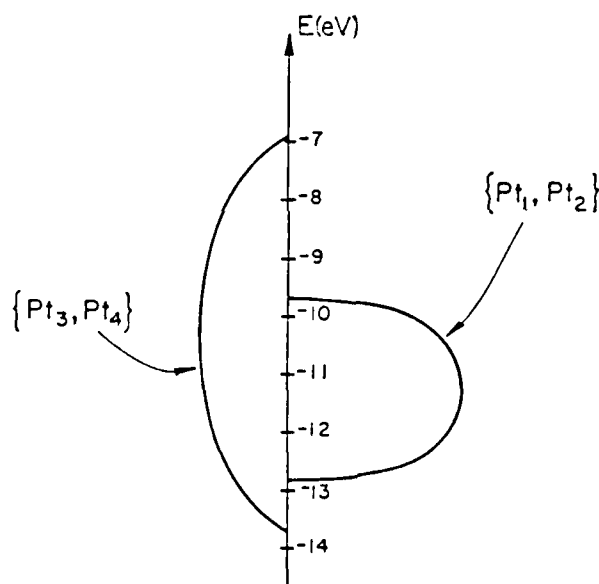
20

diagrammatic representations of the d-band widths in each case:
{Pt_1, Pt_2} at left, {Pt_3, Pt_4} at right. The curves stand
for an approximate envelope of the corresponding densities of
states. The curves were cut off in such a way that the number
of states range from 3% to 95%. In other words, outside the
curves one finds the first 3% and the last 5% of the d-states
for the two sets of metal atoms. Referring to Figure 3(a),

it is clear that the d states of $\{Pt_3, Pt_4\}$ do not interact much with C_2H_2. We shall see, however, that they feel the acetylene a little.

Let us now see if we can single out specifically those states out of $\{Pt_1, Pt_2\}$ surface subset which interact strongly with the states of C_2H_2. Figure 5 shows the curve describing the distribution of those d-states of Pt_1 and Pt_2 which are z^2 in character. We also show the states corresponding to π_σ and π_σ^* again for a comparative purpose. We shall adopt the

---

Figure 5 here

---

convention of drawing the atomic orbitals (e.g. d_{z^2}) as labels for the plot they refer to with no shading. The reason is that each point of the DOS curve corresponds to many states, each of different nodal character.

One can see that the peak of the bottom of the z^2 band perfectly matches the peak of π_σ, at -13.8 eV. Similarly the z^2 band has a nice feature at -9.0 eV which finds some counterpart in the π_σ^* curve. The change of slope in the integration line of π_σ^* reflects an accumulation of states around -9.0 eV. Finally, between -12.0 and -13.0 eV, one finds peaks common to π_σ^* and z^2. What we have in hand here is an interaction between the whole z^2 band of $\{Pt_1, Pt_2\}$ and both π_σ and π_σ^*. We may depict this in the more usual frame of an interaction diagram as in 21. The dashed line refers to the Fermi level. Note that in the main block, primarily d-centered
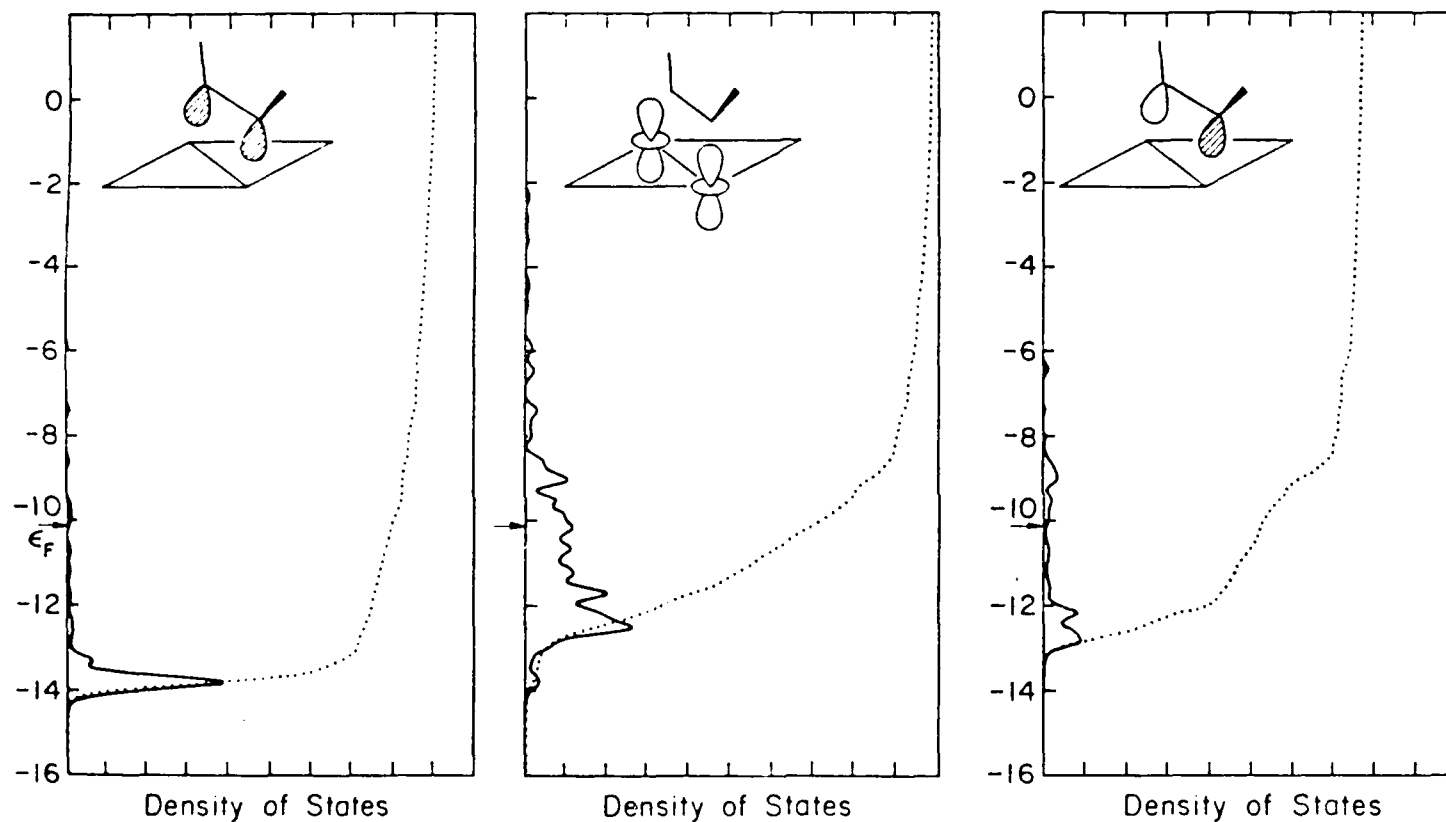
Figure 5. From left to right: contributions of π_c, z^2 (Pt$_1$, Pt$_2$) and $\pi_\sigma*$ to the DOS of the C$_2$H$_2$/Pt(111) system the 2-fold geometry. The curves are magnified by a factor of 10.
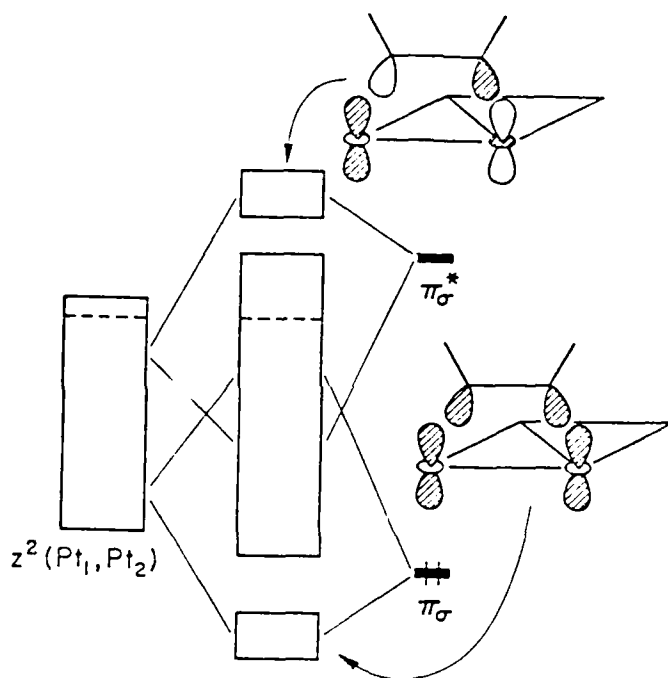
21

there should be a few states carrying π_σ^* character <u>below</u>

states involving π_σ. Also, from this simple picture it is

clear that the z^2 band is depleted of some of its electron dens-

ity upon coordination of C_2H_2. Both Pt_1 and Pt_2 actually

see their electron density charge in z^2 reduced by 0.282 elec-

trons each.

Representative interactions may be drawn out, as shown in

<u>21</u>. The two combinations depicted are certainly analogous

to those encountered in the parallel binuclear system, <u>8c</u>, <u>9c</u>.

There is an essential difference however. The interaction

$a_1 + \pi_\sigma$ in <u>8c</u> is a 2-electron stabilizing one. In the surface

case the z^2 band is initially almost completely filled (1.810

electrons). Mixing in of the s and p bands generates only a

few empty states. In that respect the surface behaves rather as the d^{10} - ML_2 case, where the d-orbital of the right symmetry to receive electrons from π_σ is filled. In the discrete complex, the high-lying sp hybrid provides an alternative acceptor. For the surface, a few s and p states penetrate the d band, hybridize with z^2 and are tied up in the so-called "dangling bonds" pointing towards the adsorbate.

What is the fate of and where are the electrons which are destabilized by the antibonding component of the $z^2-\pi_\sigma$ interaction? Mostly into the bulk. Around the Fermi level there are many levels involving interactions between surface atoms and the inner layer ones. These states act as an empty "reservoir" and mop up the overflow of electrons generated by the z^2/π_σ interaction. Neighboring metal atoms on the surface not engaged in bonding with the adsorbate act in a similar fashion. On the average, an inner-layer atom is computed to gain 0.150 electron in the process of acetylene chemisorption in this geometry. To put it in another way, electrons are transferred from filled states of the surface to empty states in the bulk via the intermediacy of π_σ. The interaction at work here was encountered and discussed in a previous study.[31]

So far we have described the σ-type of interaction. Let us investigate the less dramatic action taking place with π and π^*. Figure 6 uses a similar arrangement to that of Figure 5 and displays the distribution of the d_{yz} states of Pt_1 and Pt_2 after adsorption. Again for convenience the π and π^* curves are included. As already noticed in Figure 3,

the states in π and π^* are grouped more together. The
corresponding DOS curves are more peaked. This allows a nice
resolution of the d_{yz} curve which exhibits a central portion
(between -13.0 eV and -10.0 eV) plus two small features at

Figure 6 here

-13.5 and -8.0 eV, nicely matching the peaks of π and π^*
respectively. We had already noted that π and π^* were not
shifted by much in terms of energy. This follows from a
relatively small overlap between the d_{yz} crystal orbitals and
those generated by π and π^*. Following 21, we can cast the
interaction between d_{yz} and π and π^* in the diagram 22.
Representative combinations are drawn out.
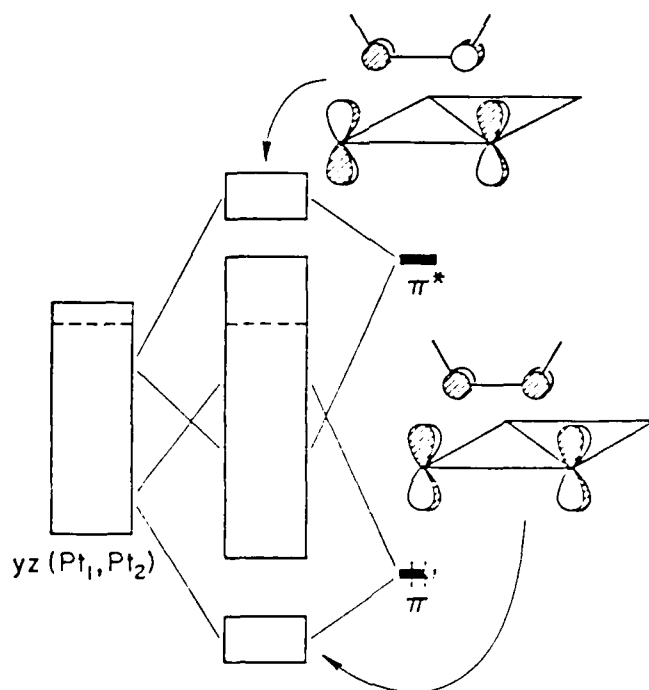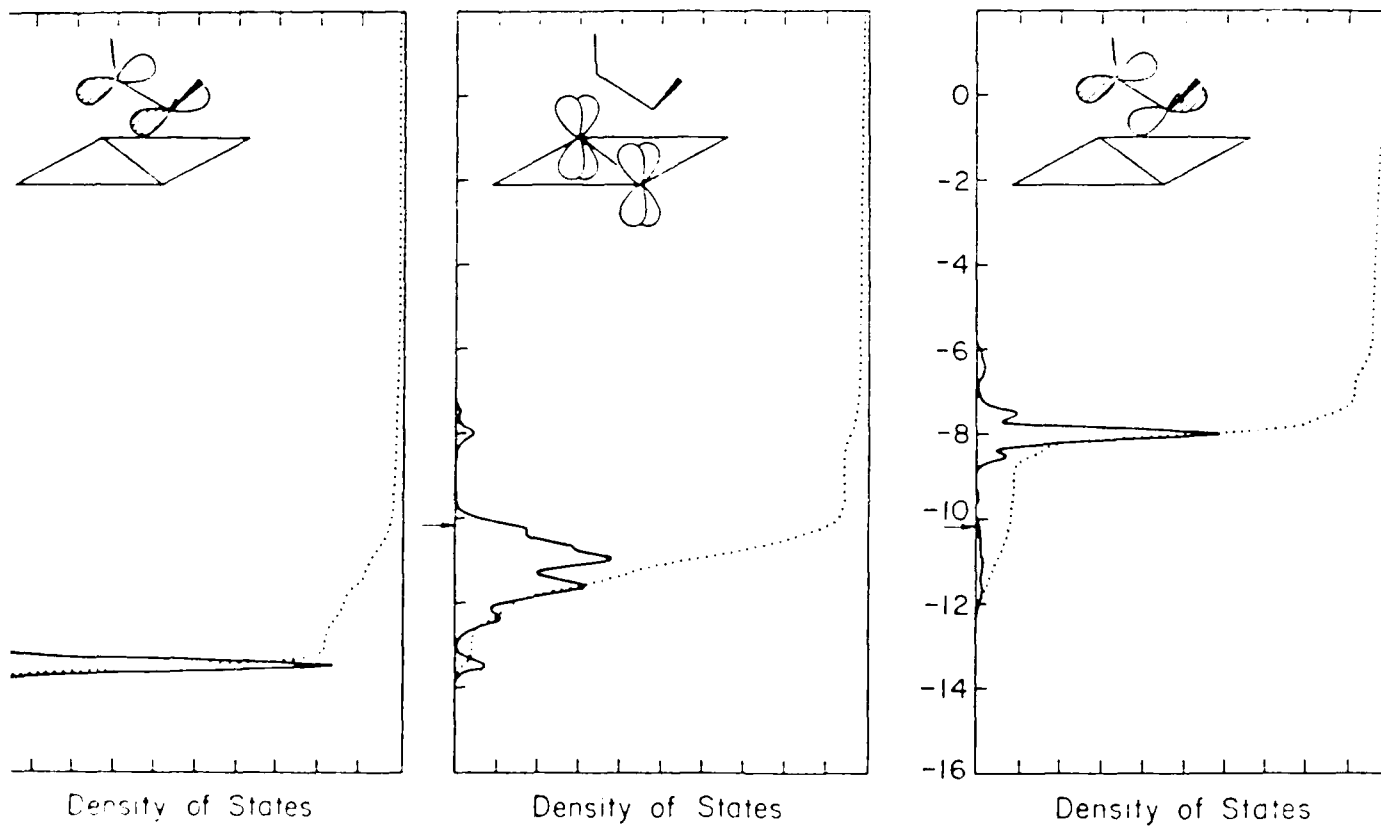
22

Density of States   Density of States   Density of States

Figure 2. From left to right: contributions of π, yz
(Pt_1, Pt_2) and π_σ^* to the DOS of the $C_2H_2/Pt(111)$
system in the 2-fold geometry. The curves are mag-
nified by a factor of 10.

from what was a secondary interaction in 16, depicted by 27.

Let us see how the empty levels of C_2H_2 are altered by the

proximity of Pt_3. This is shown for the π^* component in

Figure 10. At right is the projection of π^* once the acetylene

is on the 3-fold bridge 17. On the left-hand side is the

curve describing the distribution of the xz states on Pt_3.

Figure 10 here

This figure is very appealing because it illustrates so clearly

how perturbation theory and frontier orbital concepts trans-

late when one deals with a solid. Before interaction the

d-states are found in the -10.0 eV/-12.0 eV energy range

whereas the π^* states sit at the -8.3 eV energy mark. Upon

"contact" between the surface and C_2H_2, the d band spreads

out, but concentrates more heavily in the resulting bonding

states. Exactly the opposite situation occurs for the π^*

states. They emerge mostly in the antibonding states and some-

what pushed up in energy. A bar on the right plot stands for

the location of the π^* states before interaction. Note the

occupation of π^*; at the Fermi level it gets filled with

0.330 electrons, slightly more than twice its occupation in

the 2-fold geometry 16. Using again a localized M.O. picture

the bonding states between π^* and d_{xz} on Pt_3 may be depicted

as in 33(a). It is apparent that in this kind of combination

there is a significant contribution of the z^2 and yz states

on Pt_1 and Pt_2, 33(b-c).

Density of States   Density of States   Density of States
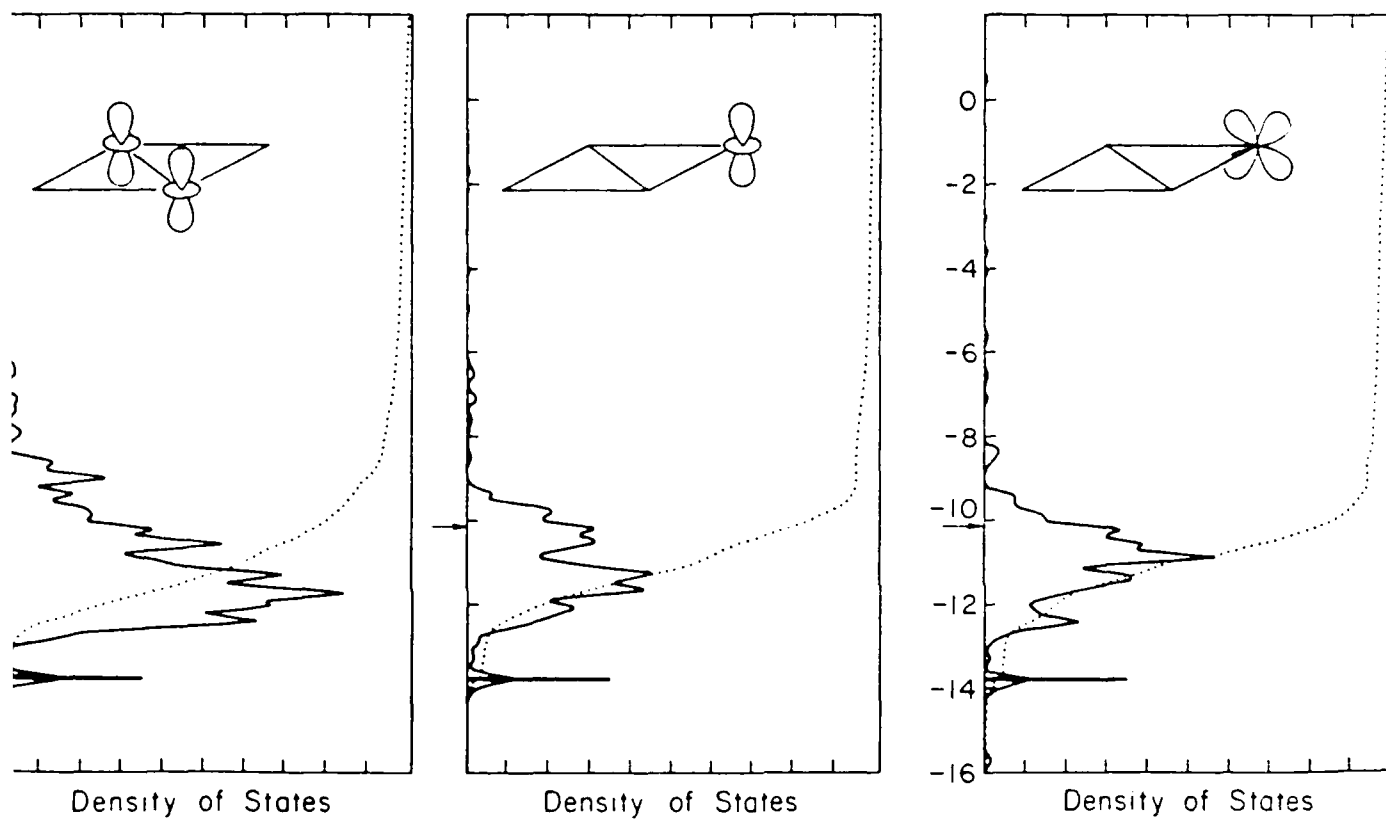
Figure 9. From left to right: contributions of $z^2(Pt_1, Pt_2)$, $z^2(Pt_3)$, $yz(Pt_3)$ to the DOS of the $C_2H_2/Pt(111)$ system at the 3-fold geomerty. The sticks refer to the location of 85% of the π and π_σ states. The curves are magnified by a ratio of 30.

at -13.9 eV is the location of 85% of the π and π_σ states.

Figure 9 here

These merge into a single line due to mixing induced by the reduced symmetry of geometry 17. This mixing of π and π_σ is significant in magnitude, primarily because they start close in energy, see Figure 2(d). The effect is less marked for π_σ^* and π^* for the initial energy gap between the two is much larger. The important feature of the Figure is the accumulation of levels occurring for all three type of states at -13.9 eV. The interaction at work here may be represented in a M.O. picture by 31 and 32. In these types of combinations,
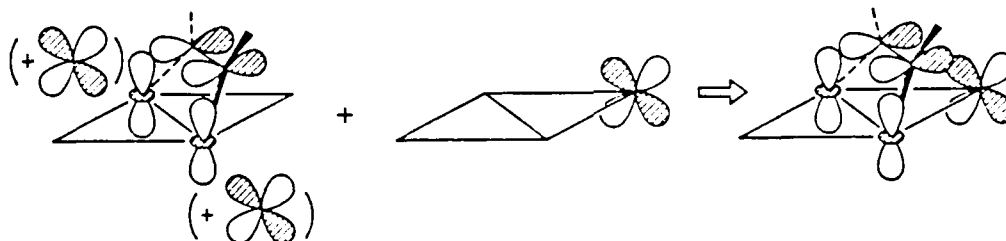
31
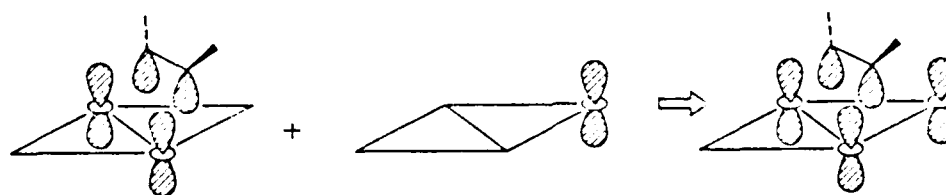
32

the crucial point is the stabilization of states centered on Pt_2, which was not present in the 2-fold geometry 16. Note that in 31 we also indicate the contribution of d_{yz} states from Pt_1 and Pt_2. We would like to emphasize that 31 descends

itself remote from any kind of action.   In 30, we show how

this translates in terms of the width of the states belonging

to Pt_1, Pt_2, Pt_3 and Pt_4.   Obviously Pt_1 and Pt_2 are equivalent
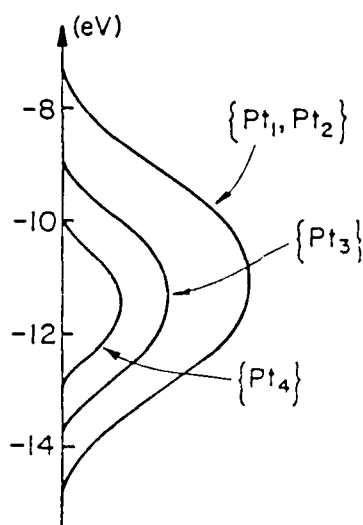
30

by symmetry and a single curve describes the envelope of the

corresponding DOS.

As may be anticipated, the details of what is happening

to Pt_1 and Pt_2 in 17 are not much different from those described

in the previous section for the 2-fold geometry 16.   For this

reason, we would like to focus rather on the new interactions,

those involving Pt_3.

Figure 9 shows how the d_{yz} and d_{z^2} states on Pt_3 enter

bonding with C_2H_2 .   We have displayed here from left to

right the projection of z^2 on Pt_1 and Pt_2, the z^2 states of

Pt_3 and the d_{yz} states of Pt_3.   Indicated with a bold stick

gests that a small geometrical distortion from 16 may increase
the bonding between say, Pt_3 and C_2H_2. We investigate this
possibility in the next section.

The 3-fold geometry, 17

Let us first say a few words about the atomic arrangement
in 17. From 16 to 17, one essentially moves the C-C bond over
the face of one triangle of Pt atoms and also inclines the
HCCH plane, so as to make an angle, with respect to the surface,

$$Pt_3-C=2.20\text{Å}$$

29
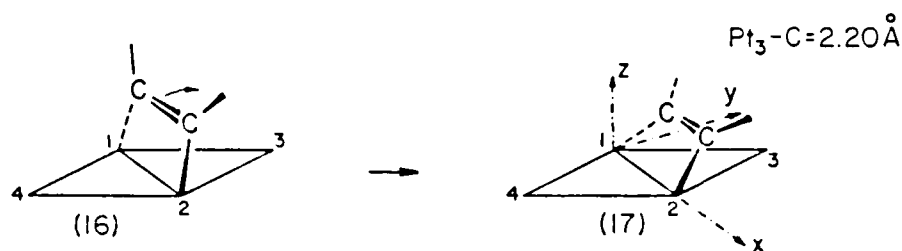
different from 90.0°. In 29 we illustrate this distortion.
Note that the $Pt_{1,2}-C$ distances are still 2.03Å. The carbon
atoms, however, are now at 2.20Å from the Pt the C_2H_2 leans
over, Pt_3. The coordinate system is still such that x lies
along the $Pt_1 - Pt_2$ bond and y is perpendicular to $Pt_1 - Pt_2$,
in the (Pt_1, Pt_2, Pt_3) plane. In 17, Pt_3 is involved in some
interaction with C_2H_2. The bending of C_2H_2 has the effect
of singling out Pt_4 in the unit cell. This metal atom finds

so strong that either the surface must break up or the triple
bond will be cleaved with essentially no barrier. Later we
shall find these last considerations particularly relevant.

In the description given so far, Pt_3 and Pt_4 were treated
as spectators. The computations justify this view. However,
one may ask via what kind of interaction they could enter the
picture. Based on local symmetry arguments, combination such
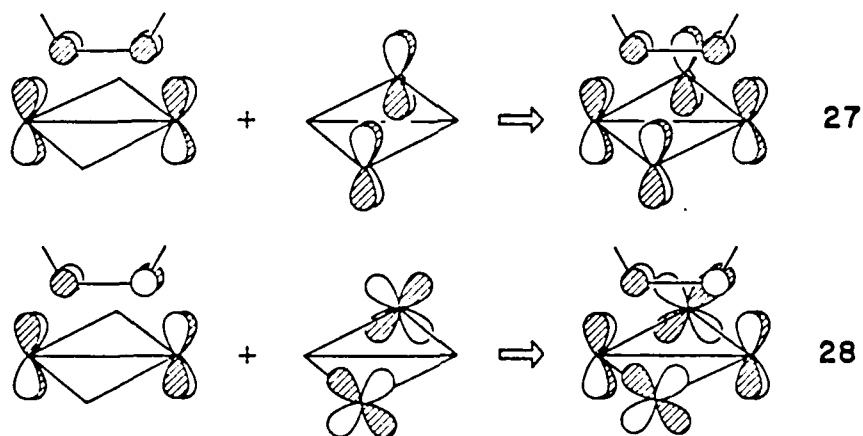
as 27 - 28 could have been a priori of some significance. In
geometry 16, because the overlap between any of the C_2H_2 M.O.'s
and any d-orbital of Pt_3 (or Pt_4) is small, the overall influence
of these 2 atoms remain small. Interestingly, however, the
overlap population between Pt_3 (or Pt_4) and the acetylene carbon
atoms is non-zero and positive: 0.0053. This obviously sug-

previously. Significance is attached to the origin of the
lines in the metal block. For example, the line issuing
from π_σ converges with one coming from the bottom of the
d_{z^2} band on Pt_1, Pt_2. The piece of volume the lines point
to in this case represents states of the type $\pi_\sigma + (z^2(1) +
z^2(2))$. The entire picture may be generated this way. The
squiggly lines refer to the states which are lost in the bulk
after the interaction is turned on. The horizontal dashed line
marks the Fermi level. From the earlier discussion, it is
clear that the d band of the slab is not 100% filled. For
simplicity, we omit the s and p states, the sources of
this hole in the d-block. Also for the sake of clarity, not
all lines are explicitly drawn. For example, a few high-
lying states in the d_{yz} band are pushed below ε_F by
π_σ^*, (see Figure 4), although the relevant line from π_σ^* is
not indicated.

Upon coordination to the surface, the acetylene triple
bond is significantly weakened. For the fixed bond length of
1.34Å, the overlap population falls from 1.703 down to 1.319.
One therefore realizes that upon chemisorption the two entities
see their intrinsic bonding decreased. The bonds within both
the surface and the adsorbate are weaker. The idea emerges
that strong adsorbate-surface bonding requires both entities
to pay the price in terms of their own stability. Along this
line, one may conceive cases where, depending upon the metal
and/or the adsorption site, the metal-carbon bonds formed are
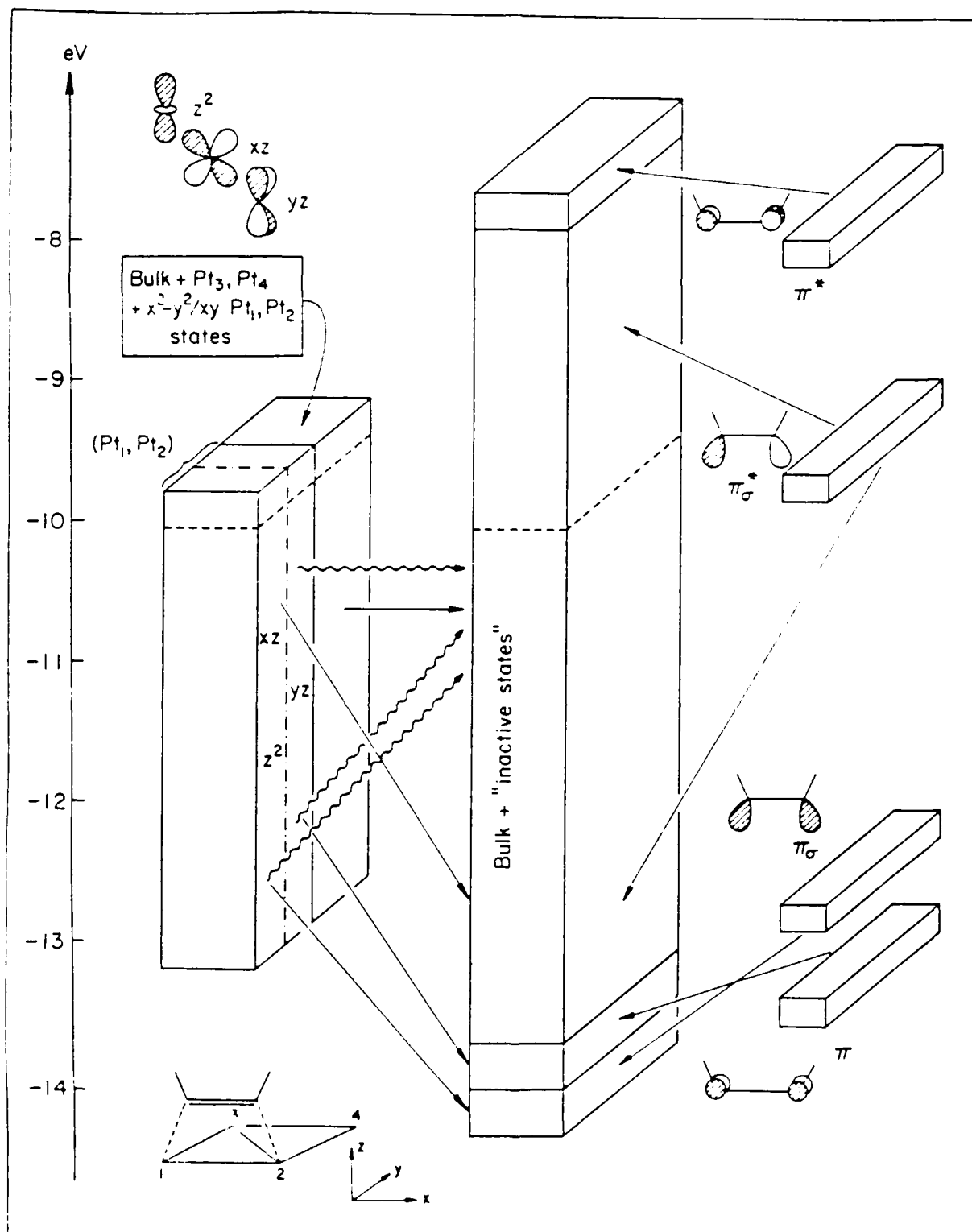
Figure 8. A generalized interaction diagram for C_2H_2 on Pt(111) in the 2-fold geometry.

structure picture. Molecular orbital π_g interacts with the part of the z^2 band which is near the zone <u>center</u> whereas the interaction with d_{xz} will be with those states lying close to the zone <u>edge</u>. This is a simple consequence of the topology of the d_{xz} orbital which is of "π" type rather than "σ" type, as is z^2.

We have gained up to this point an understanding of the bonding between C_2H_2 and the surface via a description of separated interactions ensuing from combinations of states of the surface and states of C_2H_2. What is the overall picture? Figure 8 tries to answer this question within the familiar framework of an interaction diagram. Although rather formidable-looking, the essence of Figure 8 is easily extracted. The inclusion of the depth-dimension is justified by our desire to partition the slab before interaction into "active" states (d_{z^2}, d_{xz}, d_{yz} on Pt_1, Pt_2) and the passive ones, those which will not play a direct role in the bonding. The dashed line in the left-hand volume further separates the (z^2, xz) from

---

Figure 8 here

---

the (yz) states in Pt_1 and Pt_2. The small volumes representing the C_2H_2 states could be viewed as single lines running into the plane of the paper; recall the shape of the DOS of the C_2H_2-layer only, Figure 2(d).

We now draw lines according to the interactions described

majority of the d states. What is happening here is shown in
25a. The z^2 interaction is negative, antibonding, in this
region but just above -13.0 eV all the rest of the atomic orbital
interactions between Pt_1 and Pt_2 are bonding. The net result is
25b, that is the curve of Figure 7(b). This situation is reminis-
cent of the effect of dilution of C_2H_2/surface bonding states
by the bulk discussed earlier in the text. The situation of
z^2 in 25 is equally applicable, albeit to a smaller extent
for overlap reasons, to d_{yz}.

We find that many states antibonding between the metal
atoms, which were empty before the interaction with C_2H_2, are
now pushed down well below the Fermi level. The net consequence
is a drop in the overlap population between Pt_1 and Pt_2 after
the adsorption of C_2H_2: 0.136 to 0.077. In more physical
terms, the bonding within the metallic surface is weakened.

We have concentrated so far on d_{z^2} and d_{yz} on the
metal. One should mention here the contribution made by d_{xz}
in the σ bonding between the surface and C_2H_2, via inter-
actions of the type shown in 26. The analysis of the influence

(a)   (b)
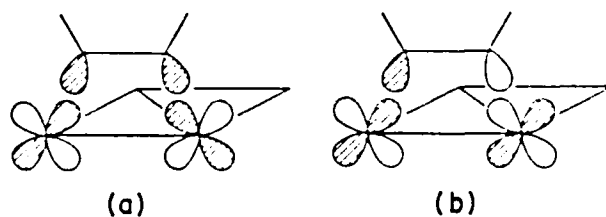
26

of the d_{xz} states closely follows that of d_{z^2} . The dif-
ference between d_{z^2} and d_{xz} would be apparent in a band

Figure 6. It is amusing to notice that the maxima in the
dotted and solid lines of Figure 7(a) do not coincide. The
C-C curve peaks at -13.5 whereas the Pt-C one peaks at -13.9 eV.
Each curve has its maximum where the other features a shoulder.
This comes from the fact that maximum C-C bonding is provided
by π rather than π_σ and maximum Pt-C bonding is the result
of the σ interaction rather than the π one. Between -13.0
and -12.0 eV are states bonding between the metal and C_2H_2 and
involving $\pi_\sigma^* : \pi_\sigma^* + (z^2(1) - z^2(2))$. One may wonder then
why the $Pt_1 - Pt_2$ curve, after a sharp peak in the negative
region at -13.0 eV, returns to bonding instead of describing
the antibonding nature of the interaction between the two z^2
orbitals. Recall that our curve sums up the overlap population
over <u>all</u> atomic orbitals. In other words, at -12.8 eV, even
though the z^2 interactions are antibonding, in this region one
finds states involved in σ bonding at the surface and the vast

(a)   (b)

25
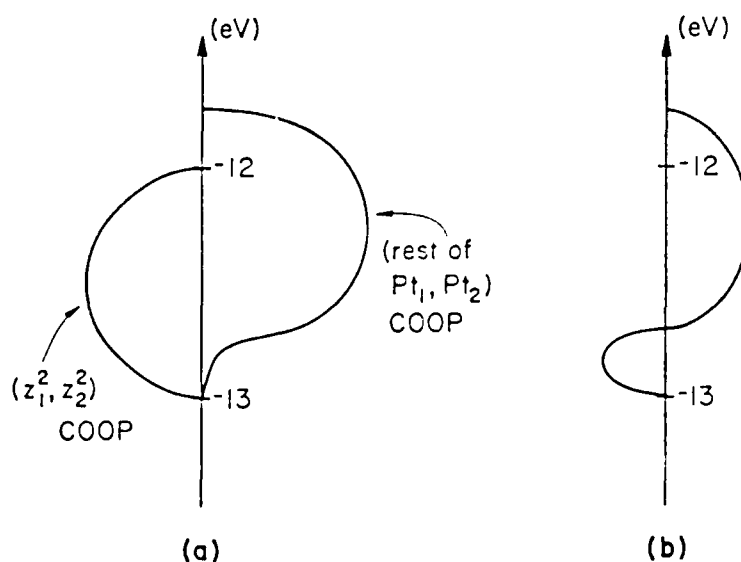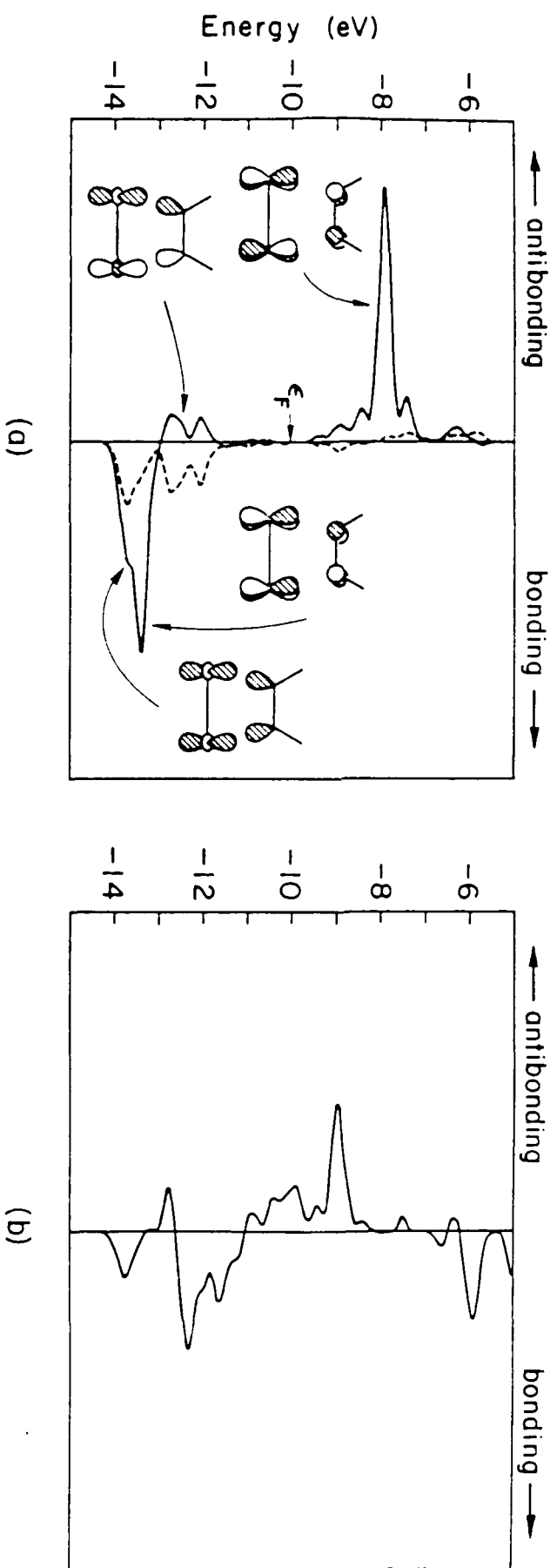
Figure 7. a) COOP curve for the C-C (solid line) and Pt-C (dotted line) bonds.
b) COOP curve for the Pt_1-Pt_2 bond.
Both plots refer to the C_2H_2/Pt(111) system in the 2-fold geometry.

or diluted in the massive center of the d-band. This is illus-
trated schematically in 24. The dashed line stands for metal-d
states. The nature of the interaction in each region of the
energy scale is indicated with the convention that + means
bonding, - refers to antibonding. This convention may be
understood, looking back at the interactions explicitly drawn
in 21, 22 and 23. The pattern of 24 is general. The d-bands
of a surface fall almost inevitably between the donor and the
acceptor states of the adsorbate.

Still greater insight into the bonding of an acetylene
to a surface may be obtained with the help of COOP curves.
Figure 7 at left shows on the same graph the overlap populations
between the two carbon atoms (solid line) and in the symmetry
related $Pt_{1,2}-C$ bonds, (dotted line). On the right is the over-
lap population between Pt_1 and Pt_2. Let us sweep through the

Figure 7 here

energy scale and enumerate the interactions that we encounter
along the way. Everything on the right (left) on the vertical
axis is bonding (antibonding) between the two specified atoms.
At -13.9 eV one finds $\pi_\sigma + (z^2(1) + z^2(2))$. These states
are bonding within the acetylene, bonding between Pt_1 and Pt_2,
and bonding between C_2H_2 and the substrate. They represent
the solid state equivalent to a discrete molecular $a_1 + \pi_-$
interaction in the binuclear system, see 8c. At -13.5 eV are
states of the type $\pi + (yz(1) + yz(2))$; please look back at

The reader will have noticed that in dealing with d_{z^2} and d_{yz} we have located the bonding combination between the bonding metal-d states and the bonding M.O of C_2H_2 and the antibonding combinations between antibonding metal-d states and the antibonding M.O of the C_2H_2. States of the type 23a-d are more

(a)   (b)   (c)   (d)
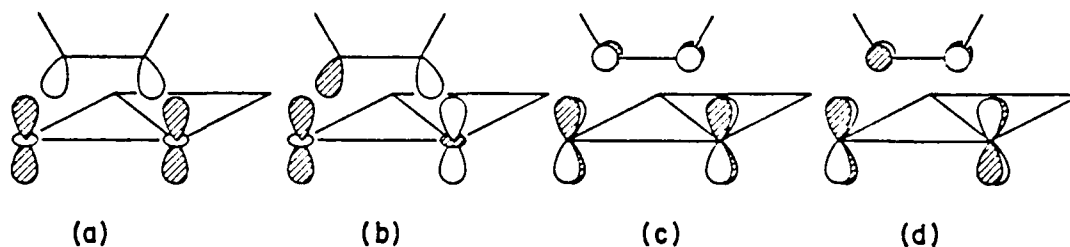
23

difficult to single out. The reason for this is that in each case, the center of gravity of the d-band lies between the two M.O.'s of the organic fragment. In other words, the lowest and highest states are concentrated on the acetylene. The levels corresponding to 23a-d are hidden among the bulk-like states. They form tails which are "drowned"

(M-M)-(C-C)

(M-M)+(C-C)

(M+M)-(C+C)

(M+M)+(C+C)
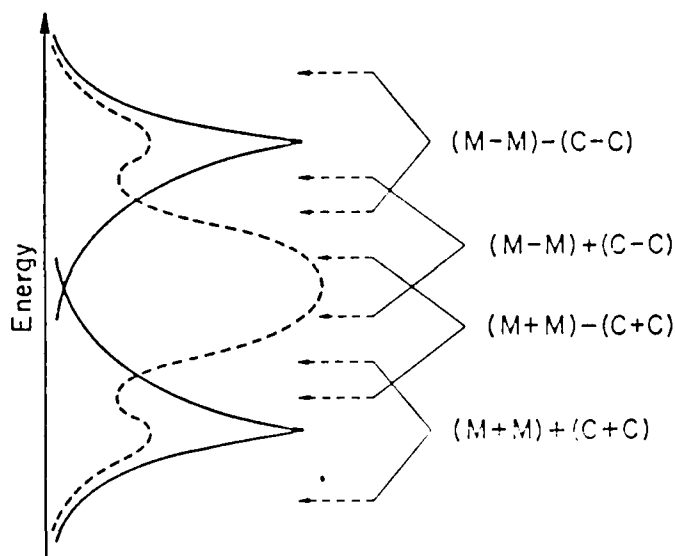
24
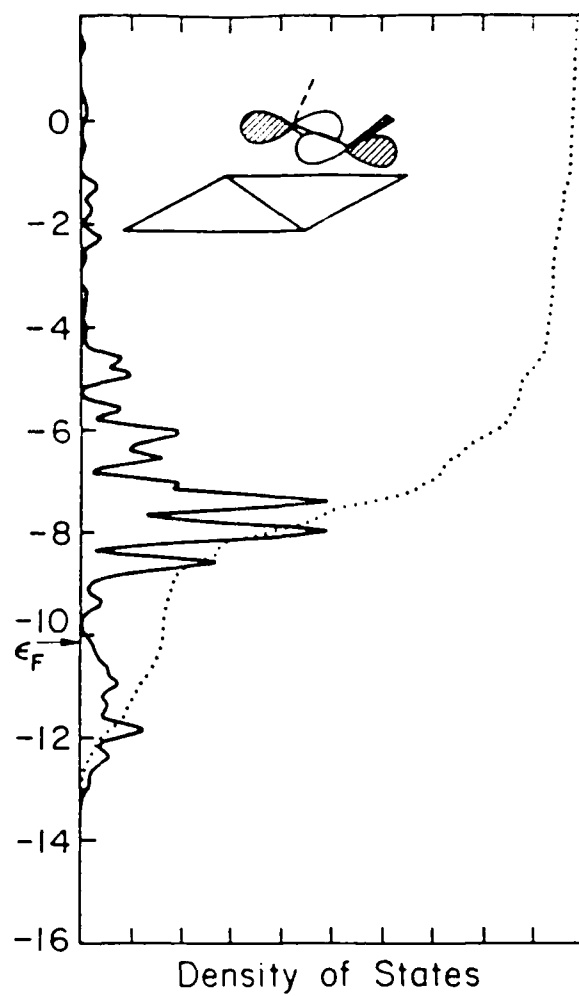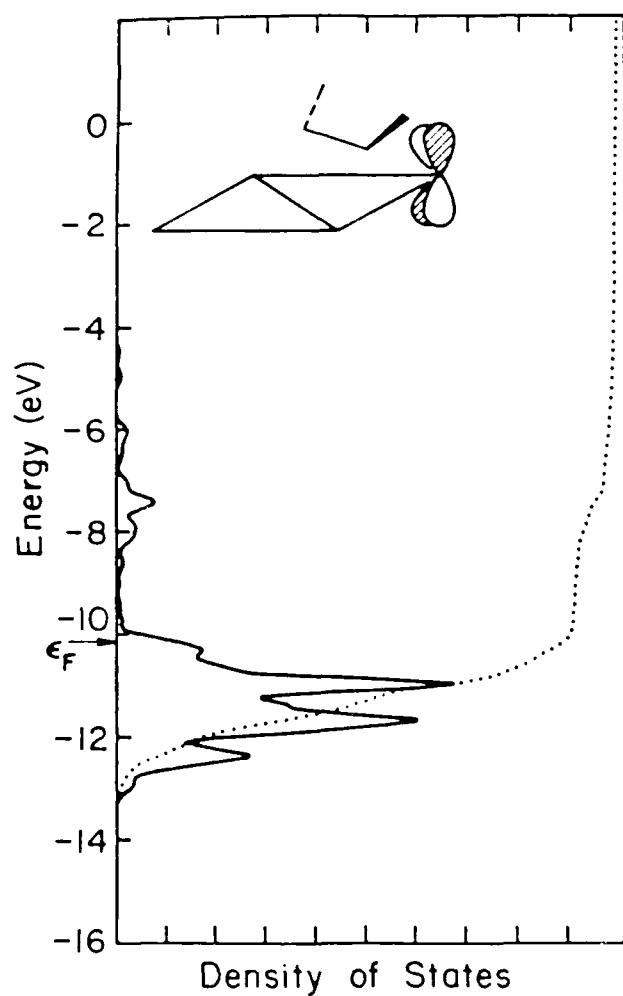
Figure 10. contributions of $xz(Pt_3)$ (left) and π^* (right) to the DOS of the $C_2H_2/Pt(111)$ system in the 3-fold geometry. The curves are magnified by a factor of 30.

(a)   (b)   (c)
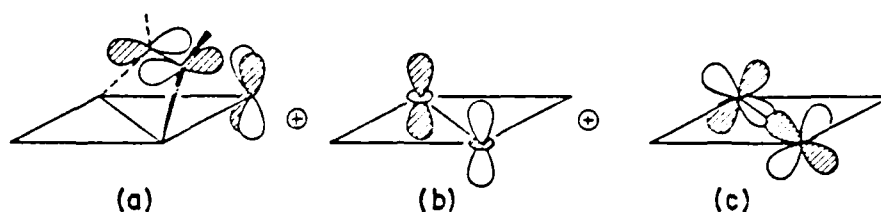
33

All this follows nicely what was anticipated in 28. The fact that interaction such as 31-33 provide some bonding between the acetylenic carbon and Pt_3 is further confirmed by the corresponding COOP curve shown in 34. Up to the Fermi level all interactions are basically bonding. The 3 peaks at -13.9, -13.0 and -12.0 eV match those of π (and π_σ), π_σ^* and π^*, respectively in Figure 10. As described earlier in the discussion of Figure 10, there is an accumulation of
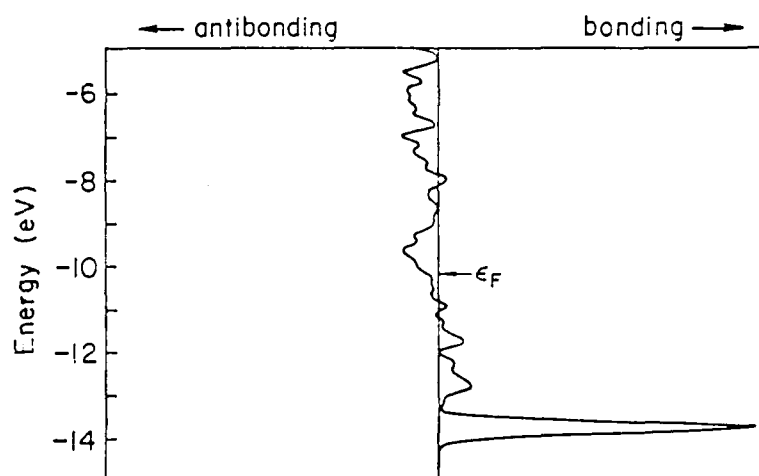
34

Pt_3-C antibonding states in the -8.0/ - 6.0 energy range. The overlap population between Pt_3 and C is 0.19 at ε_F

Although ultimately we will compare numerical results for all adsorption sites, it is worth pointing out here that in states such as the one generated in 33, antibonding character is induced between Pt_1 (and Pt_2) and Pt_3. The Pt_1 - Pt_3 overlap population which was 0.126 in 16 is now 0.067. Again we encounter the feature that the overlap population between atoms involved in bonding with the adsorbate diminish upon chemisorption. Conversely, the bonding between Pt_1 (and Pt_2) and the acetylene being slightly less in 17 than 16, the Pt_1-Pt_2 overlap population rises from 0.053 in 16 to 0.058 in 17.

We should conclude this section by taking note of the fact that 17 is favored over 16 by less than a tenth of an eV, (0.06 eV) per chemisorbed C_2H_2. This is a tiny difference, especially in view of the approximate nature of our calculations. We are inclined to think that a soft potential exists between 16 and 17; as noted above, 17 is the result of a small geometrical perturbation. Electronically, the preference obtained for 17 is the result of the gain of bonding between Pt_3 and C_2H_2, which is larger than the loss of interaction between Pt_1 (and Pt_2) and the acetylene. The choice of geometry makes the balance between these two counteracting effects a delicate one. Experimentally, spectroscopic studies of metastable C_2H_2 have indicated a tilted species analogous to 17, and methyl-acetylene was found by LEED to be in the three-fold bridging geometry 17.[4d,2a]

The On-top Geometry, 13

Because only one metal atom is involved with the adsorbed
C_2H_2 in this geometry, the situation is much simpler in this
case. It would be cumbersome to go through the details of all
the interactions between acetylene states and those of Pt_1.
We therefore rather want to focus on the similarity existing
between the present situation and that of a d^{10} - ML_2 acetylene
complex, discussed earlier in the text. Figure 11 shows on
the left the C-C (solid line) and the Pt_1-C (dotted line) COOP
curves for the 1-fold adsorption site. The Fermi level is
still indicated by an arrow. On the right-hand side is de-
picted the corresponding COOP curve that would be obtained in
a d^{10} - ML_2 system. Because in the latter case the levels
are discrete, the peaks in a DOS or COOP diagram are δ func-
tions. With the same convention as in the solid, the interactions

---

Figure 11 here

---

which are bonding give rise to a line at the right of the verti-
cal line, and for the antibonding ones, a line is drawn on the
left. For clarity the levels of the molecular system have
been sketched. The calculation was performed[32] on $(CO)_2Pt(C_2H_2)$.
The molecular diagram is schematic - only the important inter-
actions are shown. The length of the line on the right-hand
side plot corresponds to the computed overlap population con-
tributed by each M.O. to the bonding between the atoms under
consideration.
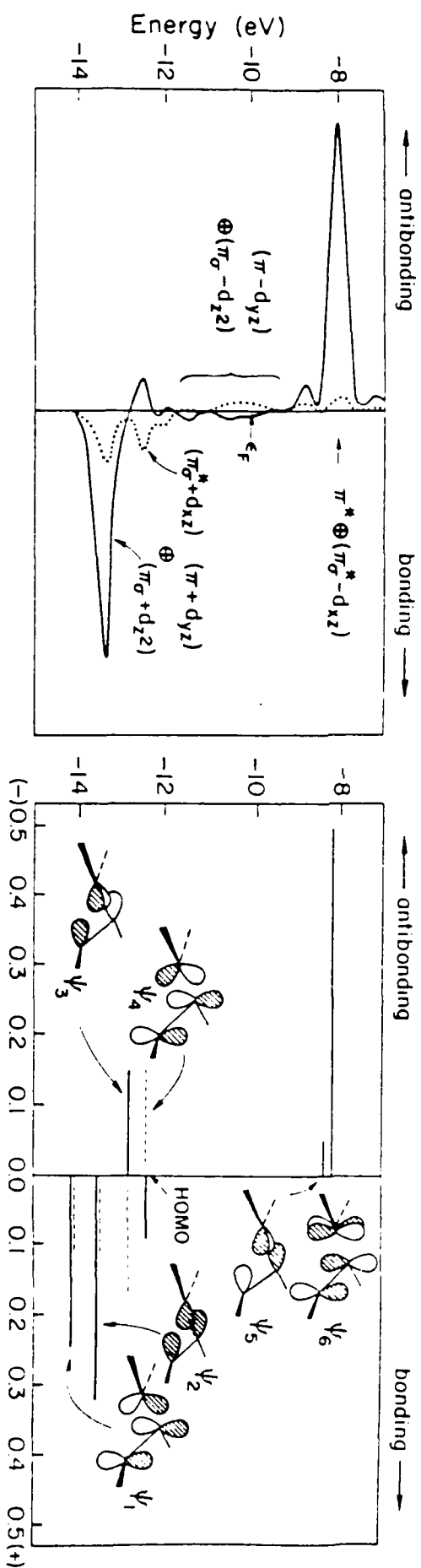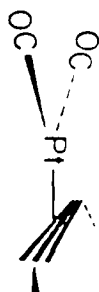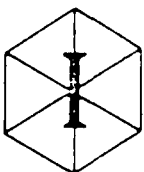
Figure 11. Left: COOP for the C-C (solid line) and Pt_1-C
(dotted line) bonds of the C_2H_2/Pt(111) system
in the 1-fold geometry.

Right: "COOP" for the C-C (solid line) and Pt -C
(dotted line) bonds of the $(CO)_2Pt(C_2H_2)$ system.

The assignment of the peaks in the left-hand side plot comes from a separate projection of the four components of the acetylene and the atomic orbitals of Pt_1 . A comparison between the left and right-hand side plots of Figure 11 is instructive: the patterns are virtually identical. This is particularly true up to ψ_3. A minor difference occurs because ψ_4 is filled in the complex whereas the corresponding states of the solid are spread around ε_F and therefore partially empty. The extended nature of the solid has its more crucial consequences around the Fermi level. Whereas all Pt-C σ antibonding states are unoccupied in the discrete system - ψ_5 is empty and the antibonding counterpart of ψ_2 is above -8.0 eV -, some $(\pi_\sigma - d_{z^2})$ states fall below ε_F and then are filled. To put it in another way, this mode of coordination of an acetylene to the Pt(111) surface is characterized by less σ-bonding than the corresponding $d^{10} - ML_2$ system.

Turning to the π interactions, it is clear from the position of π^* and π_σ^* on the COOP curve, that only a small amount of backdonation from the surface to C_2H_2 has occurred, 0.078 e⁻ in π^*. All these factors contribute to make the on-top geometry 18 substantially less stable, 1.2 eV higher in energy than both 16 and 17.

The 4-fold Geometry, 19

The adsorption site under consideration in this section is 19, and both the atom numbering and the coordinate system are shown in 35 in a top view. The first peculiar features of this
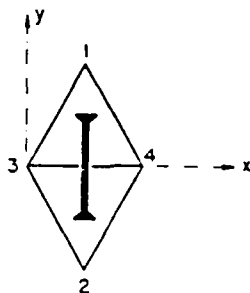
35

site are the geometrical requirements associated with it. For a Pt_1 (or equivalently Pt_2) - C distance of 2.03Å, the carbon atoms are rather close to Pt_3 and Pt_4: 1.87Å. In other words, all four metal atoms in the surface unit cell are expected to feel the adsorbate and all will be strongly involved in bonding with C_2H_2 . As a first consequence, the acetylene states are considerably spread out upon interaction with the surface: a width of over 10 eV is computed for the states associated with the 4 frontier orbitals of C_2H_2 . Because of the relatively high local symmetry (2 mirror planes are present[33]), the analysis of the bonding turns out to be relatively simple. In the following, we enumerate the principal interactions and dwell on the ones which are important to our overall conclusion. Starting with the initially empty π^* states, the middle

of Figure 12 shows how they spread upon interaction with
the metallic film. The stick stands for their initial position.

Figure 12 here

Note that ~30% of them now fall below the Fermi level. The
left and right of the Figure display the projections of the
Pt_1 (and Pt_2) xz states and the Pt_3 (and Pt_4) yz states,
respectively. Clearly, the levels of π^* at ~-12.5 eV in the
middle   of   the   Figure find some counterpart in both
types of metal d-states. The combinations grouped in this
energy region are of the kind displayed in 36. Spectacular
backbonding takes place in these. The behavior of the π_σ^*
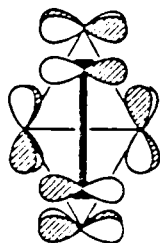
36

states can be analyzed along the same line. One finds 45%
of them below ε_F, which translates into a net occupation of
0.893 electrons. The levels are mainly concentrated (35%
overall) in a sharp peak at -13.5 eV, i.e., approximately 2.8 eV
lower than their initial location. On the metal side, it is
in z^2 of Pt_1 and Pt_2 that we find most of the states they
combine with. As expected from topological considerations,
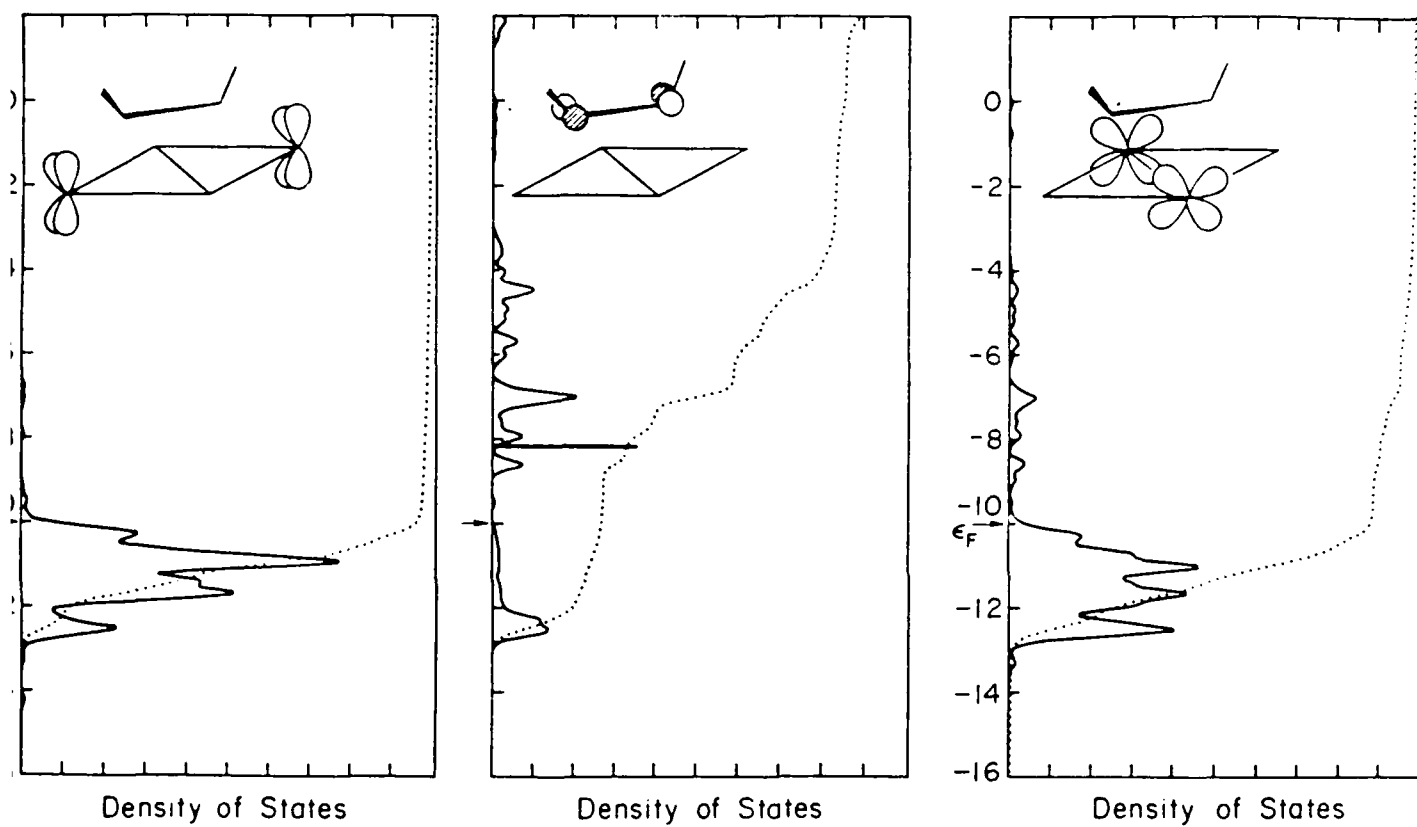
Figure 12. From left to right: contributions of xz(Pt$_1$, Pt$_2$), π^*, yz(Pt$_3$, Pt$_4$) to the DOS of the C$_2$H$_2$/Pt(111) system in the 4-fold geometry. The curves are magnified by a factor of 15.

the interactions here are those of the type 37, in a side view.
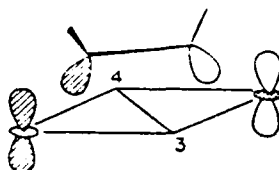
37

Obviously, a few yz states of Pt_3 and Pt_4 are mixed in combinations such as 37. For overlap reasons, their contribution is, however, of a lesser extent.

Conversely, the π_σ states are stabilized by z^2 on Pt_3 and Pt_4. Recall that the $Pt_{3,4}$-C distances are short. Interactions such as 38 are now predominant, with a smaller participation of z^2 from Pt_1 and Pt_2. A total of 60% of

38
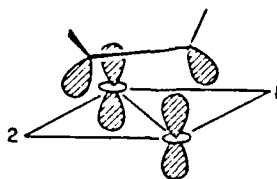
π_σ states are found in a sharp peak at -13.3 eV, pushed down by ~0.5 eV with respect to their position before adsorption.

The left-hand side of Figure 13 tells us what happens to the π states of C_2H_2. Almost 70% of them are stacked in

the peak at -14.2 eV. At the Fermi level, the π component
of the acetylene has, however, lost 0.470 electrons to the

Figure 13 here

---

surface. The mixing is primarily with xz states of Pt_3 and
Pt_4, whose distributions are indicated on the right-hand side of
the Figure. The interactions involved here are crucial and
39 gives a hint for why this is so. The d states implicated
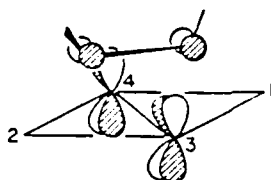
39

here are quite antibonding with respect to the Pt_3 - Pt_4 bond
and they get filled via forward donation from π of C_2H_2 .
The full consequence of this situation is better measured by
the overlap population between Pt_3 and Pt_4: -0.074, a
negative number. In other words, if C_2H_2 was to chemisorb
in this geometry, the Pt_3 - Pt_4 bond would be so much weakened
that surface reconstruction may occur via breakage of the
Pt_3 - Pt_4 bond.

From these considerations, it emerges that the 4-fold
geometry is characterized by a large electron density drift
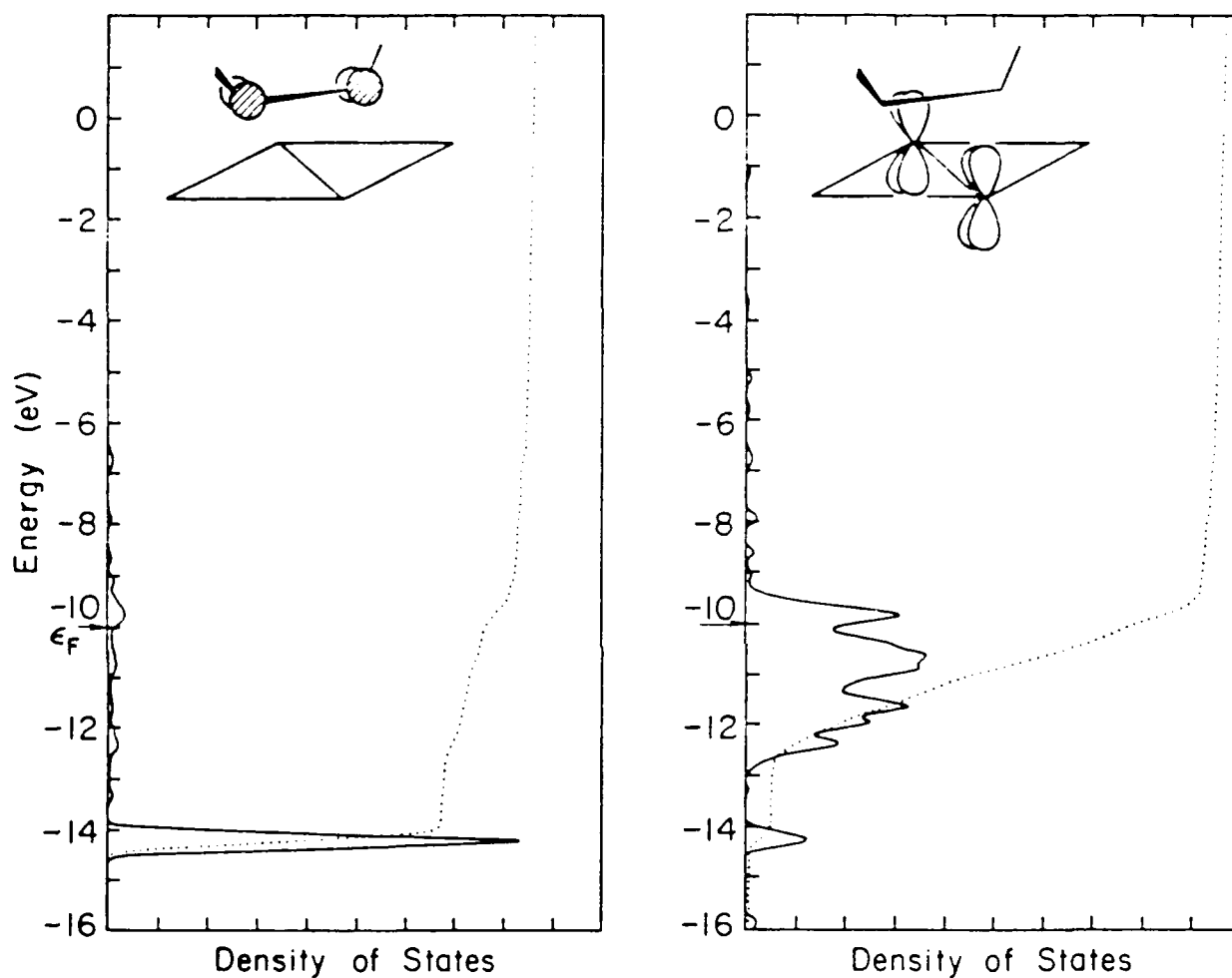
Figure 13. Left: contribution of π to the DOS.

Right: contribution of xz(Pt$_3$, Pt$_4$) to the DOS.

Both curves refer to the C$_2$H$_2$/Pt(111) system in

the 4-fold geometry and are magnified by a factor

of 15.

in both directions; metal - C_2H_2 and C_2H_2 - metal. As a
result, we have here an extremely strong interaction between
the surface and C_2H_2, at the expense of the stability of both
the surface and C_2H_2; the overlap population between the 2
carbon atoms drops abruptly from 1.703 before interaction
to 1.080 upon adsorption.

In contrast to the 1-fold geometry where the metal - C_2H_2
bonding is weak, it looks as if in the 4-fold site "too much"
of an interaction is turned on, destabilizing both the adsorbate
and the substrate. For this reason, and despite a strong
surface - C_2H_2 bonding, 19 is computed to be 0.22 eV (per C_2H_2)
higher in energy than 16 or 17. These results agree with pre-
vious calculations[11b] by Anderson suggesting that the 2-fold
and the 3-fold bridging sites are the most favorable geometries
for C_2H_2 onto Pt(111). The 3-fold site (2-fold as well)
achieves best the compromise required for optimum non-dissocia-
tive chemisorption of C_2H_2 on Pt(111): a good metal -
adsorbate interaction which does not ruin either the bonding
within the surface or that in the chemisorbed species itself.

Nevertheless, a 4-fold geometry is believed to be adopted
by C_2H_2 on Ni(111). Can this preference be reconciled with
the above considerations? We think that the source of the
problem for 4-fold site adsorption lies in the excessive
weakening of the surface bonding via 39. This very same inter-
action is likely to be less strong when the surface is made of
Ni atoms. We offer two reasons for this: a) the C_2H_2 is

more "centered" with respect to the 4 Ni atoms than in the Pt

case. For a $Ni_2 - C_1$ distance of 2.03Å in 40, the $C_2 - Ni_3 (Ni_4)$

40
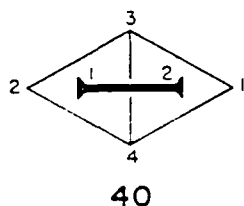
length is 1.99Å and not[34] 1.87Å as for the corresponding dis-

tance on Pt(111). This means that in interactions of type 39,

the surface will be involved through all 4 atoms more equally

and not preferentially through Ni_3 and Ni_4; b) the orbitals of

Ni are more contracted than those of Pt; therefore the overlap

between xz orbitals of Ni_3 and Ni_4 is smaller, hence reducing

the effect of the destabilization induced by filling these

antibonding (with respect to the 2 metal atoms) states. Thus,

we believe that a small geometrical difference in the Pt(111)

and the Ni(111) surface may translate into substantial elec-

tronic changes, which in turn dictate the choice of the adsorp-

tion site of C_2H_2 on these two surfaces.[35] Finally, it should

be noted that the reactivity of C_2H_2 on Ni(111)[5w], greater

than on Pt(111), is also consistent with the fact that the

4-fold geometry activates the triple bond of C_2H_2 more than

the 3-fold site.

The 2-fold Perpendicular Geometry 42
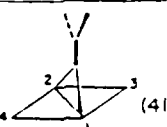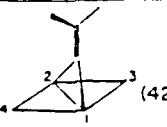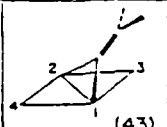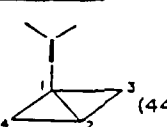
In this coordination mode the upper CH_2 unit is simply rotated by 90° with respect to its orientation in the parallel geometry 41. Topologically, the same kinds of interactions hold the vinylidene to the surface. However, the LUMO b_2 of CCH_2 is now combining with the bottom of $^{+}$ d_{yz} band, see 48. The energy difference between b_2 and this set of

48
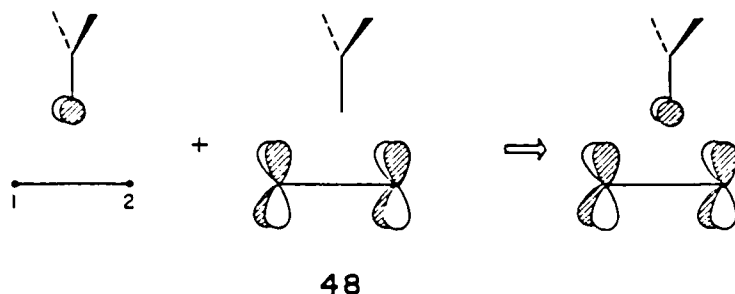
states is now larger than that between b_2 and the top of z^2 in the parallel geometry, see 46b. This translates into a less strong interaction between the surface and CCH_2. Similar reasoning may be used for π, which now interacts with the top of the d_{xz} band. We believe that these factors contribute heavily to the substantially higher energy of 42 compared to 41.

It is interesting to notice that the analogy between a 2-fold bridging site and a binuclear cluster is still operative in this system. A number of binuclear vinylidene complexes have been structurally characterized[38] and all display the parallel geometry. The α carbon in both the surface and

Table 4. Bonding Characteristics of Some Vinylidene Adsorption
Sites.

	$C_\alpha = C_\beta$	(41)	(42)	(43)	(44)
Binding Energy[a]		-6.13	-5.30	-5.85	-4.62
Fermi Level[a]		-10.11	-10.07	-10.07	-10.09
overlap populations — C-C	1.441	1.253	1.191	1.132	1.289
Pt_1/Pt_2-C		0.563	0.521	0.553	0.728
Pt_3-C_α		0.041	0.072	0.165	0.042
Pt_3-C_β		-0.006	-[b]	0.228	-
Pt_1-Pt_2		0.049	0.106	0.053	0.138
net occupations — π^*	0.0	0.300	0.426	0.356	0.130
b_2	0.0	1.136	0.998	1.130	1.278
a_1	2.0	1.551	1.551	1.581	1.571
π	2.0	1.971	1.899	1.716	1.992

a) in eV.

b) a dash means this quantity was not calculated.

47
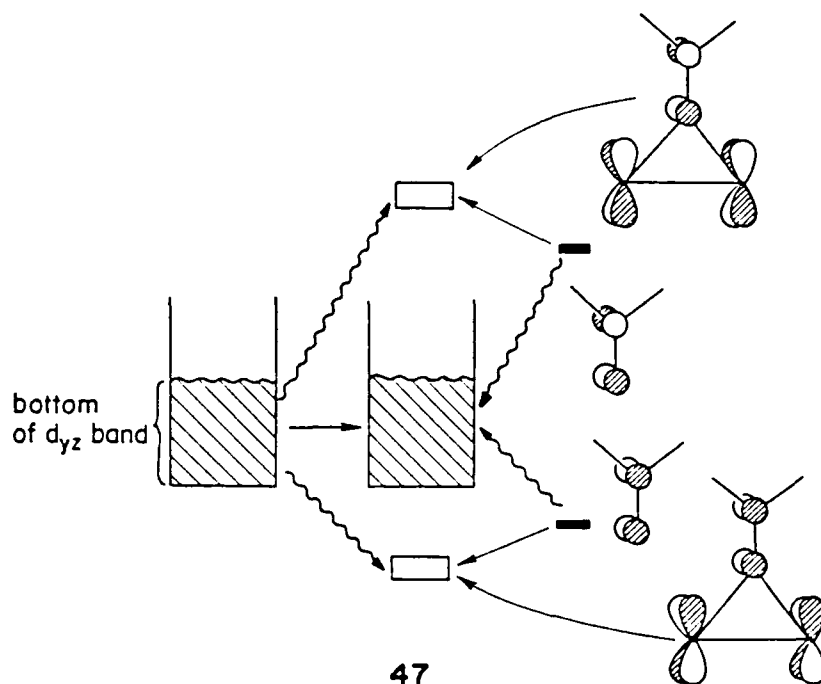
ture one would anticipate a C-C non-bonding character of
the states situated in the central region, just like the non-
bonding middle orbital of an allylic system. We see exactly
this in the carbon-carbon COOP curve. These states are pri-
marily located on the surface atoms and on the β carbon atom
and therefore are non-bonding between the surface and the
α - carbon.

Altogether, the vinylidene fragment achieves both good
σ and π bonding to the surface and we compute a binding
energy of 6.12 eV at this geometry. Table 4 provides the
numerical values obtained for some of the calculated quantities
in this geometry and the ones to be discussed next.

Table 4 here

illustrated in Figure 15. This state of affairs is clearly
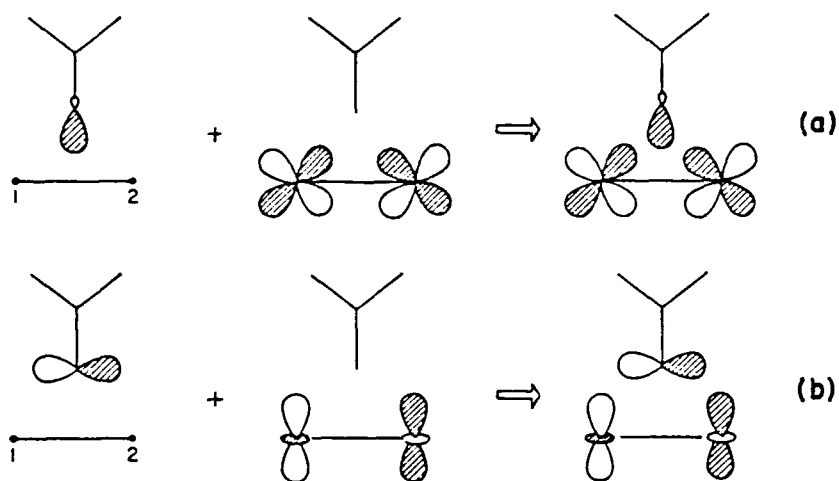
46

the consequence of strong overlap preferences.

The way π and π^* states enter the bonding picture of CCH_2 at this geometry is interesting for it parallels closely a pattern usually encountered in discrete molecules. The key is to notice that both orbitals can mix with a common piece of the d_{yz} band. More specifically, the π states are pushed down by the bottom of the d_{yz} band, and the same d states serve to destabilize slightly the π^* states. The interactions at work here are diagramatically depicted in $\underline{47}$. The familiar 3-orbital mixing pattern translates here into a 2-orbital/1-group of states one. The projection of the d_{yz} states, not presented here, shows indeed a main peak centered around two smaller peaks: one above, corresponding to most of the π^* states, and the other, lower in energy, matching the energy location of 70% of the π states. From this pic-
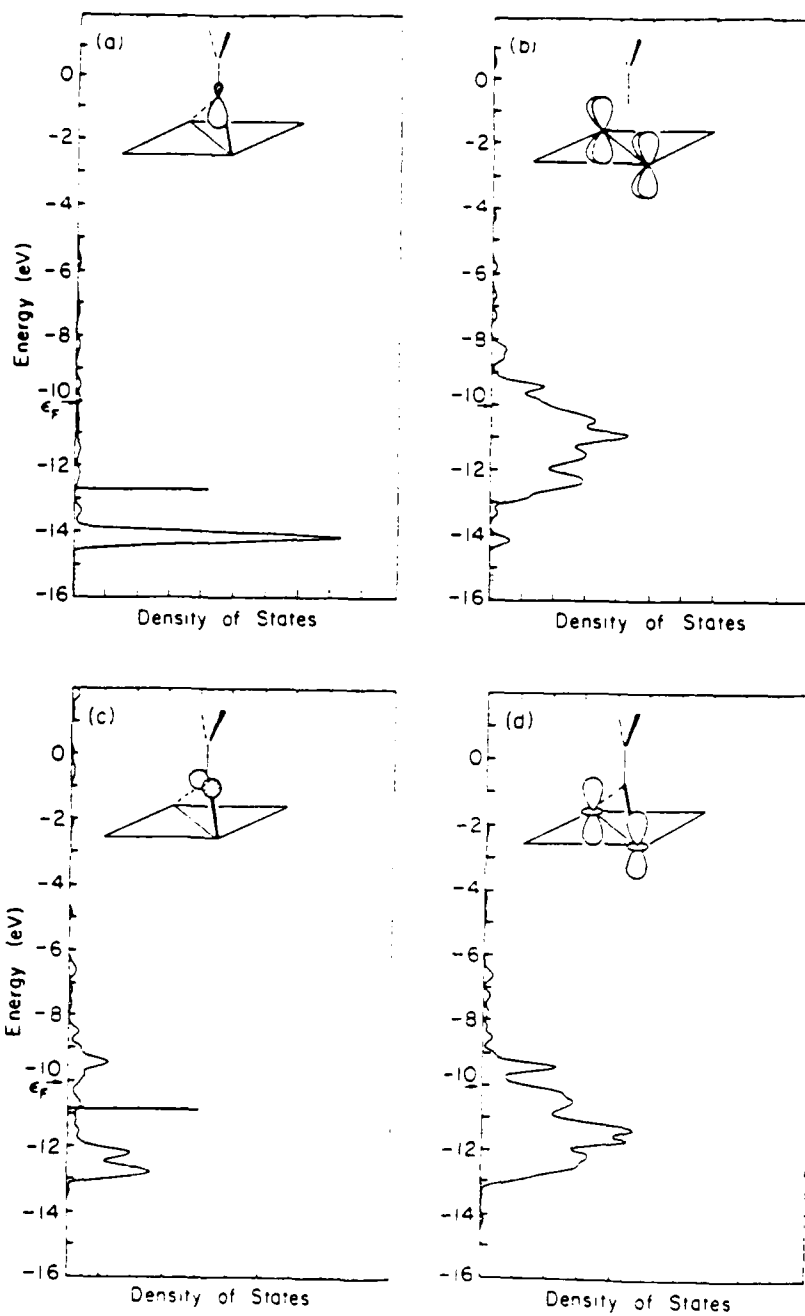
Figure 15. a) Contribution of CCH₂ a₁ states.

b) Contribution of xz(Pt₁, Pt₂) states.

c) Contribution of CCH₂ b₂ states.

d) Contribution of z²(Pt₁, Pt₂) states.

The 4 curves refer to the CCH₂/Pt(111) system in geometry 41, and are magnified by a factor of 10.
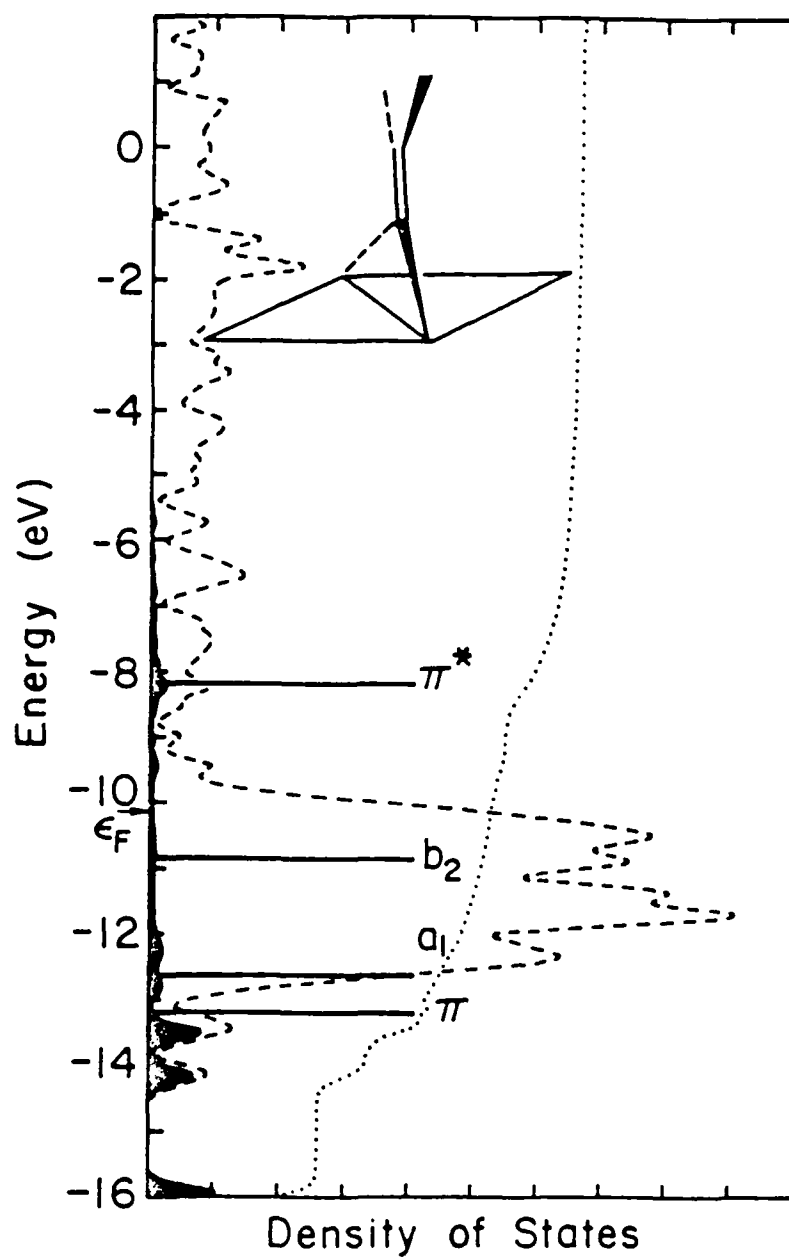
Figure 14. Total DOS (dashed line) and contributions to it of the
CCH₂ states (black area) for CCH₂ on Pt(111)
in geometry 41.

The 2-fold Parallel Geometry 41

Figure 14 displays the total DOS (dashed line) of the system upon chemisorption of CCH_2 in this geometry. The dark area represents those states contributed by the organic fragment only. We have indicated with straight lines the location of these states before interaction between CCH_2 and the

Figure 14 here

surface. Just as in the acetylene case, the adsorbate states are spread out dramatically in the process of chemisorption. This is particularly true for the levels generated by the LUMO of CCH_2, b_2. Both filled levels have been pushed down by a significant amount, whereas π^* still retains most of its states at ~-8.2 eV. Let us first focus on a_1 and b_2. The separate projections of states descending from a_1 and b_2, show that the lower peak in Figure 14 is not related to π but to a_1. Upon adsorption, the groups of states generated by the M.O.'s π and a_1 have switched their relative position on the energy scale. A similar unexpected pattern appears on plotting the z^2 and xz states of Pt_1 and Pt_2. The CCH_2 lone pair a_1 does not interact with the bottom of the z^2 band but with xz bonding states. It is the group of states descending from b_2 which combines with z^2 states. These interactions are shown in 46a-b and the above considerations

Figure 15 here

C_2H_2 , π_σ^* . One would anticipate then that b_2 should be more prone to backdonation from the surface than π_σ^* .

2-fold PAR	2-fold PER	2-fold bent	1-fold linear
41	**42**	**43**	**44**
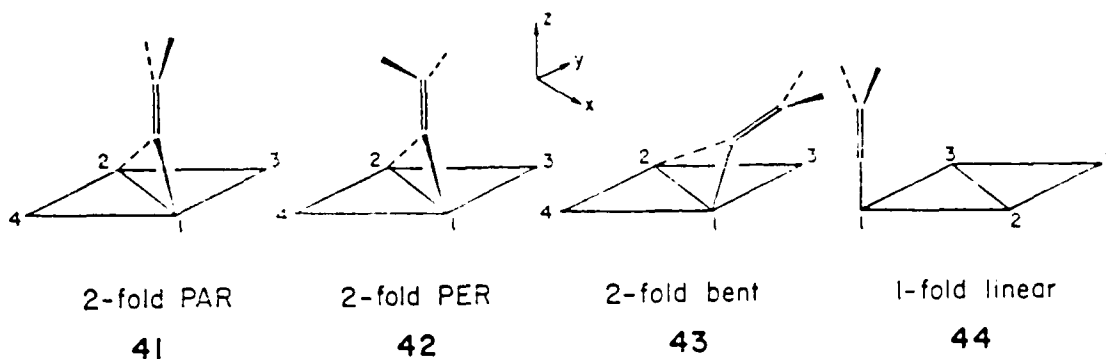
one CCH_2 unit is associated with a set of 4 surface Pt atoms.

Let us first go briefly through the frontier orbitals of the CCH_2 fragment. They are displayed in _45_ in increasing order of energy (in parentheses) from left to right. Only

$\pi(-13.22)$ $a_1(-12.67)$ $b_2(-10.82)$ $\pi^*(-8.24)$

45
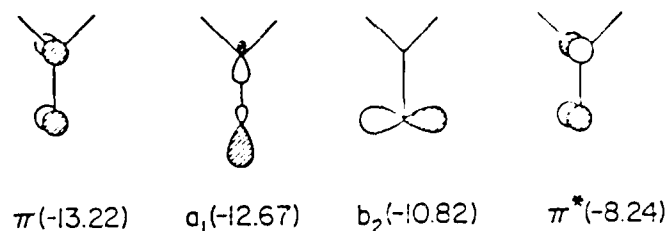
π and a_1 are filled in the free ligand. The a_1 and b_2 orbitals are the characteristic σ and p orbitals of any carbene. Interestingly enough, the topology of there orbitals is the same as those of the acetylene, see _6_. In this sense CCH_2 and C_2H_2 are isolobal. A second noteworthy point concerns the LUMO b_2. This orbital lies relatively low in energy; in particular it is much lower than the LUMO of

Vinylidene on Pt(111)

We mentioned briefly in the Introduction that the existence of a vinylidene fragment on Pt(111) has never been clearly established experimentally. However, it is strongly believed that the ultimate presence of an ethylidyne (CCH_3) on the surface can only be accounted for if a CCH_2 unit is initially adsorbed.[4d] The problem of the interconversion or rearrangement of a bound acetylene to a vinylidene fragment has been tackled by theoreticians. Simonetta and coworkers have assumed[12c] a concerted 1,2 hydrogen shift whereas Anderson and Kang[37] favor a mechanism involving scission of one acetylenic C-H bond and surface-hydrogen intermediates. We shall not dwell on this question here but rather focus on the electronic features of the CCH_2 chemisorbed state.

The vinylidene fragment is an interesting species for it represents one of those cases where the properties of a ligand are drastically altered (stability, reactivity) upon coordination to a transition metal center. This unit can attach to mono or polynuclear organometallic clusters and the growing amount of experimental information relevant to these systems was reviewed recently.[38]

In the following we discuss the bonding characteristics of CCH_2 in a 2-fold parallel, 2-fold perpendicular, 2-fold bent and 1-fold linear geometry on a Pt(111) surface. The adsorption sites are depicted schematically from a side view in 41-44. Again a coverage of ¼ was used in the computations;
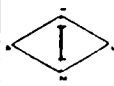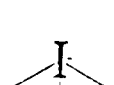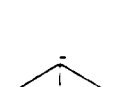
governing the bonding and the geometrical choice made by this system. We have also drawn conclusions about the electron reorganization associated with the chemisorption process. Next we apply these results and use the information obtained in this section to the chemisorption of a vinylidene and an ethylidyne fragment on the same surface.

negatively charged (the electron density is 10.125). From the numbers it is apparent that the more a surface atom is in contact with C_2H_2, the more electron density it loses. Furthermore, the partitioning of the charge among the different orbitals pointing towards the C_2H_2 is instructive in regard to the type of interaction which dominates at the geometry under consideration. For example, in 16, the σ interaction (via z^2 on Pt_1 and Pt_2) is the most important one. Turning to 17, Pt_3 is primarily involved in a π type of bonding through d_{yz}. In other words, the electron density loss from the surface atoms may be traced specifically to the orbitals locally more implicated in the bonding. A final remark deals with the fact that the amount of charge lost by the surface atom is larger than that gained by C_2H_2. As was mentioned before, the difference goes into the bulk. In the 4-fold geometry, the surface loses so much of its electron density (3.10 electrons over the 4 metal atoms) that there are not enough empty bulk-like states at the Fermi level to receive it. Consequently, some anti-bonding states are filled — they contribute to the weakening of the surface bonding — and the Fermi level in this geometry goes over the -10.0 eV mark. In our calculations, this excess of negative charge is found primarily in the bottom layer; each atom becomes even more negative than it is in the free surface.

We have gained from a detailed study of the acetylene adsorption on Pt(111) an understanding of some of the factors

Table 1 - Bonding Characteristics of Several Acetylene Adsorption Sites.

	bare surface	(16) z²	(16) xz	(16) yz	(16) Total	(17) z²	(17) xz	(17) yz	(17) Total	(18) z²	(18) xz	(18) yz	(18) Total	(19) z²	(19) xz	(19) yz	(19) Total
Binding energy [a]					-4.68				-4.74				-3.56				-4.46
Fermi level	-10.02				-10.09				-10.07				-10.00				-9.97
overlap populations																	
C - C	1.703				1.119				1.206				1.405				1.080
Pt₁ - Pt₂	0.136				0.077				0.088				0.126				-0.024
Pt₂ - Pt₃	0.136				0.126				0.067				0.139				0.062
Pt₁ - Pt₃	0.136				0.126				0.149				0.130				0.062
Pt₁ - C [c]					0.543				0.517				0.295				0.130
					0.005				0.193				0.001				0.266
occupations																	
n*	0.0				0.166				0.330				0.078				0.513
n°	0.0				1.059				1.028				0.811				0.893
σ	2.0				1.500				1.591				0.733				1.566
π	2.0				1.956				1.731				1.959				1.530
surf. atoms charges [d]																	
Pt₁	1.840	-0.440	-0.173	-0.069	-0.60	-0.260	-0.118	-0.192	-0.535	-0.425	-0.605	-0.037	-1.111	-0.215	-0.378	-0.165	-1.115
Pt₂	1.840	-0.440	-0.171	-0.064	-0.60	-0.260	-0.118	-0.192	-0.535	-0.010	-0.185	-0.046	-0.084	-0.215	-0.378	-0.165	-1.115
Pt₃	1.943	-0.055	-0.016	-0.021	-0.175	-0.160	-0.135	-0.209	-0.685	-0.080	-0.013	-0.017	-0.035	-0.158	-0.014	-0.177	-0.43
Pt₄	1.927	-0.025	-0.016	-0.021	-0.125	-0.034	-0.026	-0.003	-0.125	-0.080	-0.013	-0.017	-0.035	-0.158	-0.014	-0.177	-0.43

a) Taken as the difference: E(geometry) - E(slab) - E(C₂H₂) in eV. The negative signs means C₂H₂ is always bound.

b) The numbering system is different from that used in the text for 19.

c) The carbon atom here is the closest to the particular atom under consideration.

d) Total values are given for the free surface; differences are indicated for the different geometries. A negative sign means loss of electron density upon adsorption.

In Table 3 we give a numerical summary of our findings
for the chemisorption of C_2H_2 onto a Pt(111) surface. It
is obviously not our intention to discuss every one of these
numbers, but we rather want to comment on the trends and the
general picture which emerges. First, the 3-fold bridging
geometry is clearly the most favorable energetically. This
nicely agrees with recent spectroscopic results.[36] Looking
at the overlap population entry, one sees that in the sequence
1-fold, 2-fold, 3-fold, 4-fold the acetylene triple bond is

Table 3 here

---

more and more weakened; this holds also for the metal-metal
bonding within the surface layer. Summing all the Pt-C overlap
populations in each geometry, the surface-C_2H_2 bonding varies
in the reverse order. A large number is computed for more
bridging geometries. The consequence of these two counteract-
ing tendencies was discussed earlier in the text.

A glance at the occupation numbers gives a hint as to why
the 4-fold geometry is so strongly bound. In this geometry,
both the electron loss from C_2H_2 (π and π_σ depopulated)
and gain (π^* and π_σ^* populated) are the largest of all sites.
Also, it is easy to check that, overall, C_2H_2 gains electron
density in each geometry — slightly more than half of an elec-
tron on the average. This leads us to the next entry in
Table 3, the charges of the surface atoms. These are initially

cluster cases wants to retain its (planar) sp^2 hybridization. The π bond dictates the conformation of the CCH_2 fragment. With no π bond, a methylene fragment, CH_2, binds to a metal surface in a perpendicular fashion, the carbon atom being in a pseudo-tetrahedral environment.[39]

As indicated in Table 4, the $Pt_1 - Pt_2$ bond becomes weaker upon adsorption of CCH_2 in the parallel geometry than in the perpendicular conformation. This nicely matches an earlier conclusion drawn from the C_2H_2 study: a strong surface-adsorbate interaction translates into a weakening of the bonding within the surface layer.

The 2-fold Bent Geometry 43

This adsorption geometry is a simple distortion away from the 2-fold parallel one. We allowed the carbon-carbon double bond to lean over a third Pt atom (Pt_3) so that the 2 carbon atoms are 2.22Å from Pt_3, which should be a bonding distance. Calculations on trinuclear cluster systems have shown[40] that such a distortion is a stabilizing one. However, cluster-calculations on CCH_2 in this geometry have shown[39a] the existence of a repulsive interaction upon bending of the double bond. A $\mu^3 - \eta^2 - C = CH_2$ conformation was recently suggested to occur on Ni(111), based on vibrational frequencies data.[41] Ibach and Lechwald also proposed[5f] in their pioneering study a tilted CCH_2 on Pt(111).

Our computation unfortunately provide ambiguous results as far as this issue is concerned. As shown in Table 4, the bent geometry turns out to be energetically less favorable than the upright one. However, a substantial positive overlap population is computed for the $Pt_3 - C_\alpha$ and $Pt_3 - C_\beta$ bonds. In that respect, the contact between Pt_3 and the two carbon atoms does not appear to be repulsive. We can trace most of the interaction at work here to states of the type shown in 49, bonding between π and z^2 on Pt_3. Because of the approximate

49
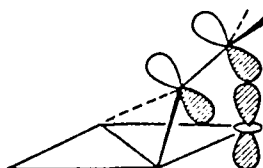
geometry used in this calculation and the lack of sophistica-
tion of our computational method, we place limited confidence
in the numerical values for the energy and tend to trust more
the indications provided by the overlap population values. In
particular, we believe that the repulsive interaction between
π and z^2 on Pt_3 (recall the latter is almost 100% filled
to begin with) is mitigated by mixing of π^* in the anti-
bonding combination of <u>49</u>. This argument may find some support
in the substantial occupation computed for π^* at this geometry,
$0.356 \, e^-$.

Backtracking a little, note that in the upright geometry
the Pt_3 - C_α overlap population is small but <u>positive</u> whereas
the Pt_3 - C_β one (also small) is <u>negative</u>.[42] We would like
to think that the bending motion from the linear geometry might
face initially a barrier, but that in fact the bent 2-fold
geometry is a minimum in the potential energy surface describing
the location of CCH_2 on Pt(111). It will take calculations
better than ours and careful geometry optimization to say
definitively if this is so.

The 1-fold Linear Geometry, 44

The adsorption of CCH_2 on top of a single Pt atom is easy to analyze because the number of interactions is limited by the geometry. Each combination of surface d orbitals stabilizing CCH_2 in the 2-fold linear geometry finds a topological counterpart in the d orbitals of the unique Pt atom at the 1-fold site. Representative bonding states are depicted in 50a-c. Notice again that the z^2/a_1 interaction

(a)	(b)	(c)
$z^2 + a_1$	$xz + b_2$	$yz + \pi$
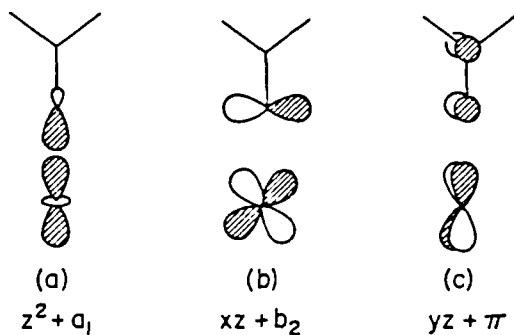
50

should be mainly repulsive due to the initial occupation of the corresponding antibonding states. However, the electrons which should enter z^2/a_1 antibonding states are ultimately housed in levels initially empty and lying near the Fermi level. These states (bulk-like, or centered in the in-plane orbitals of the surface atoms) constitute the empty reservoir mentioned in an earlier discussion. Consequently the z^2/a_1 interactions deplete both a_1 and z^2. The charge in the latter drops from 1.850 e^- to 1.260 e^- upon adsorption of CCH_2.

The xz/b_2 interaction (50b) represents a super back-donation from filled yz into empty b_2, as attested to by the ultimate occupation of b_2 (1.278 e^-). This electron density does not come from yz of Pt_1 only (see Table 4 for numbering system) but is the result of secondary interactions involving adjacent Pt atoms. This is illustrated in 51 and emphasized with arrows. This drawing also points out that
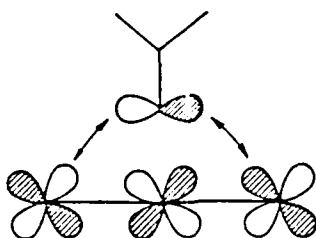
51

b_2 is more heavily filled by the bottom of the d_{xz} band.

The analysis of the yz/π interactions follows from that carried out for the 2-fold linear geometry. Just as in 47, the resulting states may be grouped into 3 sets of levels: bonding, non-bonding and antibonding. The partial occupation of the non-bonding levels induces a transfer of electrons into π^*.

The bonding of CCH_2 in this on-top adsorption site parallels that of carbon monoxide on surfaces in the same geometry. This is understandable since the two fragments are isoelectronic and isolobal. One noteworthy difference is the lesser involvement of the CO π orbitals. These lie deeper

in energy than π of CCH_2 with respect to the metal d band. A detailed analysis of this system is available elsewhere.[43]

As indicated in Table 4, our computations put the 1-fold geometry ~1.5 eV higher in energy than both the 2-fold linear and 2-fold bent conformations. We believe that the reason for this state of affairs is not that there is anything intrinsically wrong with the on-top site but rather than CCH_2 is altogether better bound in the other two geometries. The bonding between the α carbon and Pt_1 in 44 is excellent as evidenced by the overlap population of 0.728 in the corresponding bond. This may be calibrated incidentally by the $Mn - C_\alpha$ overlap population in $Cp(CO)_2Mn(C = CH_2)$ which is 0.480 for a $Mn - C_\alpha$ distance of 1.90Å. In the bridged geometries 41 and 42, the bonding is less strong in any of the Pt - C bonds, than in the $Pt_1 - C_\alpha$ bond of 44, but the sum of all Pt - C interactions is overall greater than in 44. More surface atoms are involved in bonding, hence more d states are pushed down: a lower total energy results.

Ethylidyne on Pt(111)

The ethylidyne fragment (CCH_3) has been detected on Pd(111) and Pt(111) surfaces both by LEED and by vibrational spectroscopic techniques.[4d,44] The species is formed after heating C_2H_2 or C_2H_4 on these surfaces. A general agreement has been reached in the recent past for the choice of the CCH_3 adsorption site: the 3-fold bridging conformation 54 appears to be the most favorable geometry as opposed to a 1-fold 52,

52   53   54
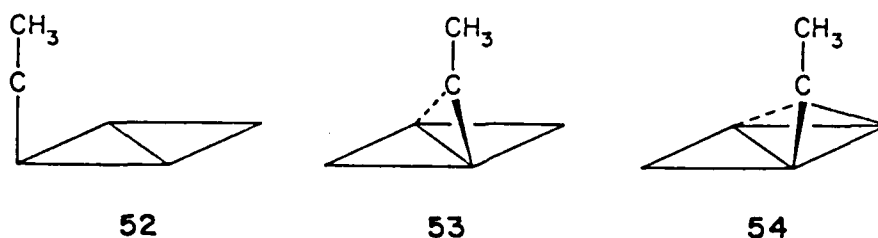
or a 2-fold 53, alternative. In their study of the cluster-surface analogy,[45] Sheppard and coworkers have correlated successfully spectroscopic data for CCH_3 on surfaces and trinuclear clusters[46] in a 3-fold geometry.

Ethylidyne (or more generally alkylidyne) fragments are presently known to bind to mono,[47] bi,[43] and trinuclear[49] organometallic frameworks. In this section we would like to understand the reasons for the inevitable preference of a 3-fold site coordination when CCH_3 adsorbs on the (111) face of a Pt surface.

In <u>55</u> are shown the familiar frontier orbitals of a

C - CH$_3$ unit. In increasing order of energy one finds a filled

M.O. of a$_1$ symmetry and a degenerate pair, e , composed of
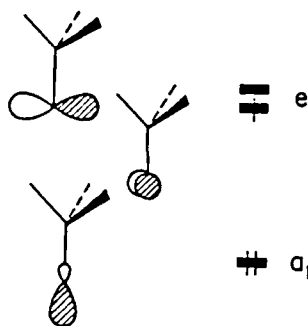
55

p$_x$ and p$_y$ on the unsaturated carbon atom. A single electron

is housed in the e set. The fragment is of C$_{3v}$ symmetry.

When it is chemisorbed in a 1-fold (<u>52</u>) or a 3-fold (<u>54</u>)

geometry, a local 3-fold axis of symmetry is retained. For

this reason we will deal with these 2 adsorption sites at the

same time. Then we examine the 2-fold geometry.

Ethylidyne in the 1-fold (52) and 3-fold (54) Geometry.

The left side of Figure 16 shows what has happened to the CCH_3 states upon adsorption in the 1-fold geometry. On the right-hand side of Figure 16 is the corresponding plot for the 3-fold geometry. The two pictures have been magnified and the total DOS omitted in both cases. We would like to concentrate on the differences and common aspects between these two

---

Figure 16 here

---

plots. First, their general shape is similar. More specifically, there is a common peak in the neighborhood of -14.0 eV, slightly lower for the 3-fold geometry. Separate projection of the individual fragment orbitals of CCH_3 (those shown in 55), make it clear that the peak under consideration is primarily composed of a_1 states. A glance at the stick-marks, which indicate the location of the CCH_3 states before interaction, tells us that the vast majority (70%) of a states are pushed down in energy by ~1.3 eV in both adsorption sites. The states concentrated in this region are combinations of the type 56a and 56b-c for 52 and 54 respectively, bonding between CCH_3 and the surface.

(a)   (b)   (c)

56
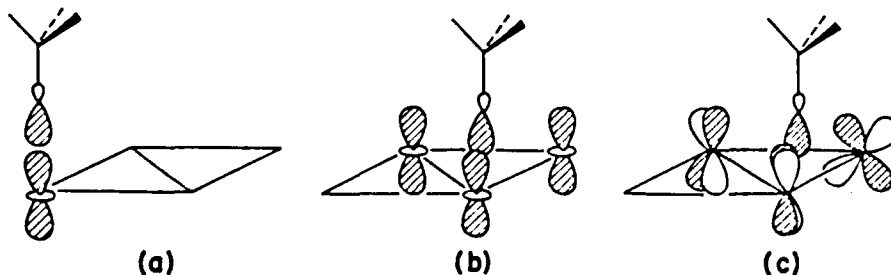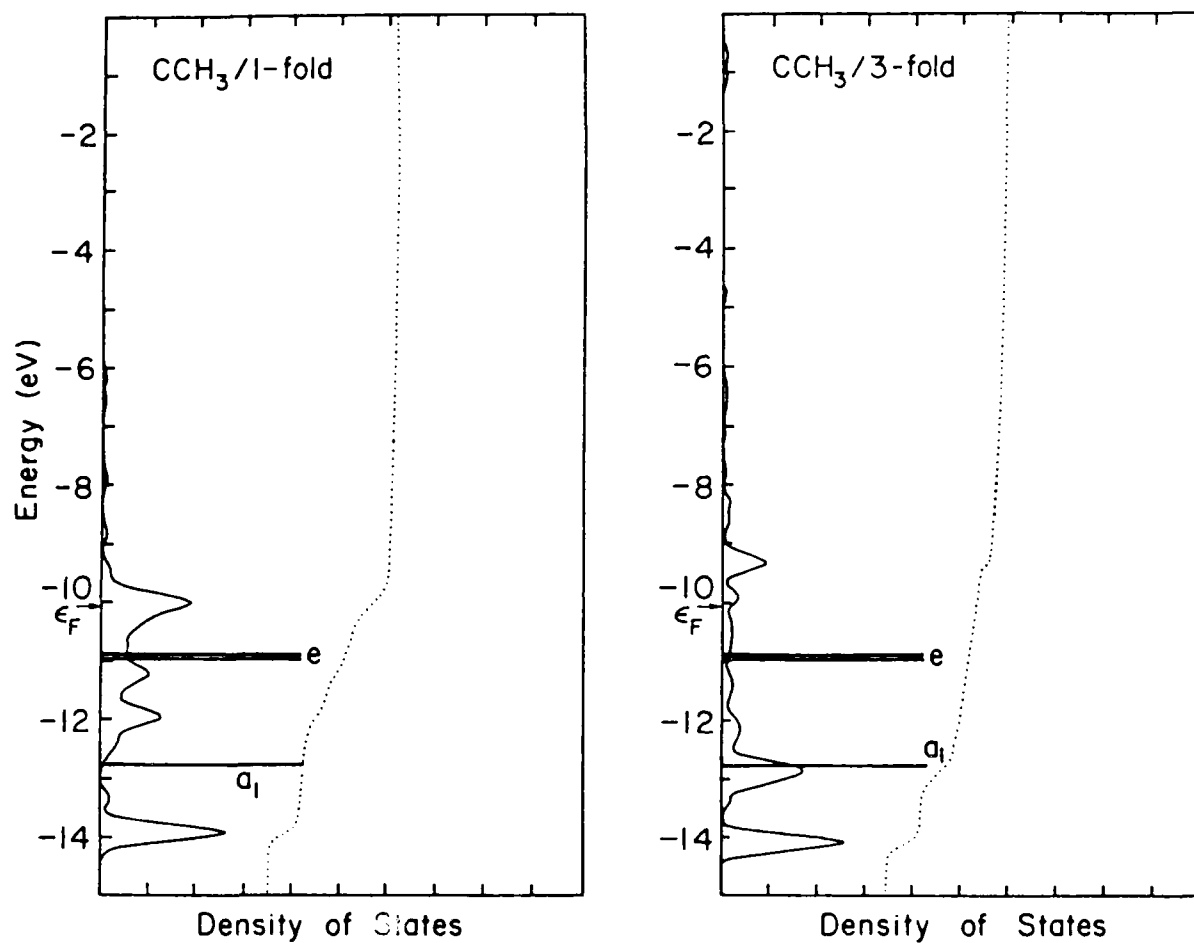
Figure 16. Left: Contributions of CCH₃ states of the

CCH₃/Pt(111) systems in the 1-fold geometry.

Right: Contributions of CCH₃ states of the

CCH₃/Pt(111) system in the 3-fold geometry.

The remaining part of the curves in Figure 16 describe the position of the states descending from the e set of CCH_3. We find here some important differences. A peak at -13.0 eV in the right plot is totally absent from the left-hand side picture. The states in the latter are packed in the -10.0/-12.0 eV region whereas they spread over a larger energy range in the 3-fold geometry. In particular, the existence of a peak at -9.5 eV for the 3-fold curve, <u>above</u> the Fermi level, contrasts with the location of a peak at -10.0 eV roughly centered at ϵ_F, therefore partially filled, in the 1-fold geometry. The states in question now are antibonding between the e set and the surface. Figure 17 illustrates this point. At left is the Pt - C COOP curve for the 1-fold geometry. On the right is displayed the COOP curve between <u>one</u> of the 3 equivalent Pt atoms in contact with CCH_3 and the unsaturated carbon atom. The crucial feature of these curves is the location of

Figure 17 here

the Fermi level. On the right-hand side plot, no Pt - C antibonding state is filled. This is not the case in the 1-fold geometry. In Figure 17 we indicate the type of interaction which generates the peaks in the two curves. Note in particular that the bonding interactions are concentrated lower in energy for the 3-fold geometry; this incidentally corroborates the fact that antibonding states lie higher in this case
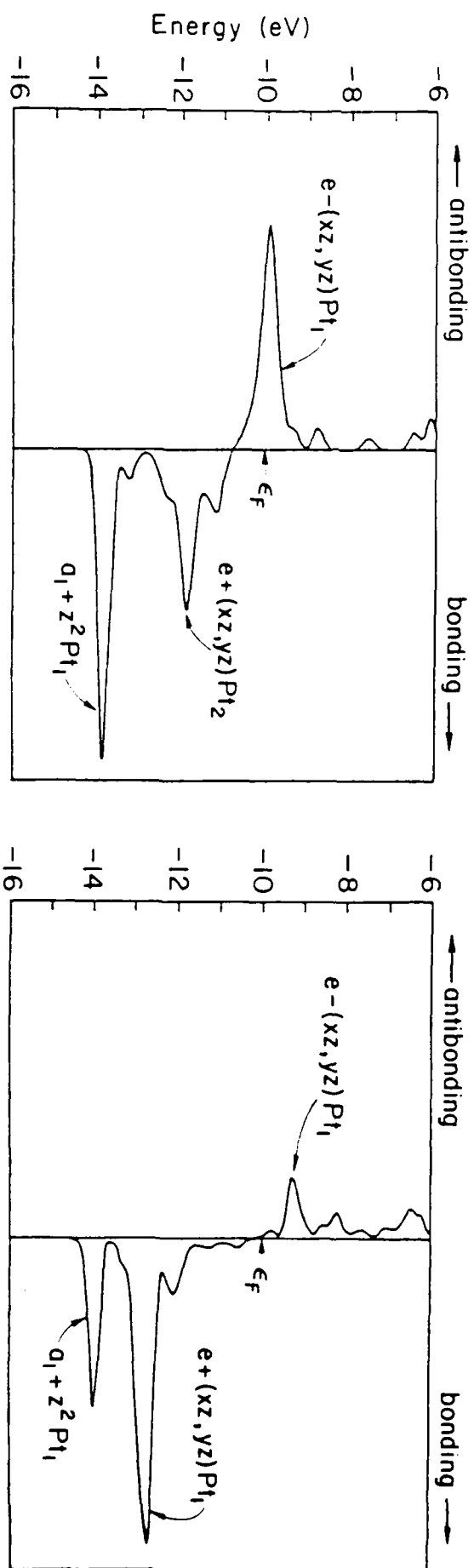
Figure 17. COOP curve for the (α-carbon)-Pt$_1$ bond in the 1-fold (left) and 3-fold (right) geometry of the CCH$_3$/Pt(111) system.

too. The e states initially at – 11.0 eV nicely split into
bonding and antibonding states in both adsorption sites. The
fundamental difference is that in the 1-fold geometry, the
splitting, which is essentially a measure of the interaction
with the surface orbitals, is not large enough so that all
antibonding states can be emptied. The interaction between
CCH_3 and 3 surface atoms is overall stronger than the inter-
action with 1 single atom. The reader may wonder where the
antibonding counterpart of the z^2/a_1 bonding combinations
are in Figure 17. As discussed earlier, these states are
simply diluted in the bonding states, between the e set of
CCH_3 and the surface orbitals, in the -10.0/-13.0 eV region.

Table 5 provides some of the numerical results obtained
for the adsorption of CCH_3 onto Pt(111) in the three geome-
tries 52-54. A point of particular interest is the larger

Table 5 here

overlap population between one Pt atom and C – CH_3 in the
1-fold geometry than the 3-fold one. This appears to contra-
dict our previous statement where we emphasized the filling
of Pt – C antibonding states in the 1-fold case and not in
the 3-fold geometry. However, what these numbers mean is that
the bonding between the unique Pt atom in 52 and the carbon
atom is larger than the bonding between one of the 3 equivalent
Pt atoms in 54 and the carbon atom; this is true notwithstanding
the filling of Pt – C antibonding states in 52. The reasons
for this situation are traced to the difference in the "quality"
of the bonding states in the 2 cases. In 52, the overlap between
the e set and d_{xz} and d_{yz} is extremely large; hence ex-
cellent bonding is achieved in the corresponding bonding states.

Table 5. Bonding Characteristics of Some Ethylidyne Geometries.

	$C-CH_3$	1-fold 52	2-fold 53	3-fold 54
Binding Energy (eV)		-5.46	-7.4	8.32
ϵ_F (eV)		-10.09	-10.05	-10.05
Pt - C overlap population		0.777	0.620	0.534
Surface/CCH_3 overlap population		0.777	1.241	1.600
occupation of e set	1.0	3.03	2.15	2.27

END

FILMED

DTI
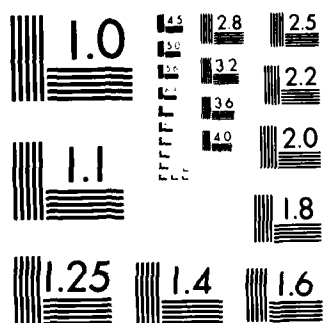
MICROCOPY RESOLUTION TEST CHART

NATIONAL BUREAU OF STANDARDS 1963 A

The bonding is even large enough so that it makes up for the filling of antibonding states and generates a bigger overlap population than that ensuing from the interaction of one Pt atom with CCH_3 in $\underline{54}$, even though in this last case no anti-bonding states are filled. The cooperative effect of the three equivalent Pt atoms in $\underline{54}$ provides extremely strong bonding and counterbalances the poorer overlap existing between the orbitals of the e set of CCH_3 and the $\underline{individual}$ atomic orbitals on each of the 3 Pt atoms compared to the overlap between the e set and $d_{xz}(d_{yz})$ of the unique Pt atom in $\underline{52}$.

A final comment to be made is that the numbers in Table 5 deal with the occupation of the e set after chemisorption. Electron transfer operates more efficiently in $\underline{52}$ than in $\underline{54}$. This results simply from partial occupation of CCH_3/surface antibonding states featuring the e set of the ethylidyne. In an exaggerated representation, the situation is that of $\underline{57}$ where the shaded areas correspond to filled states.

3-fold   **I-fold**

surface
d orbitals

e(CCH₃)   e(CCH₃)

57

The bonding is even large enough so that it makes up for the filling of antibonding states and generates a bigger overlap population than that ensuing from the interaction of one Pt atom with CCH_3 in 54, even though in this last case no anti-bonding states are filled. The cooperative effect of the three equivalent Pt atoms in 54 provides extremely strong bonding and counterbalances the poorer overlap existing between the orbitals of the e set of CCH_3 and the individual atomic orbitals on each of the 3 Pt atoms compared to the overlap between the e set and $d_{xz}(d_{yz})$ of the unique Pt atom in 52.

A final comment to be made is that the numbers in Table 5 deal with the occupation of the e set after chemisorption. Electron transfer operates more efficiently in 52 than in 54. This results simply from partial occupation of CCH_3/surface antibonding states featuring the e set of the ethylidyne. In an exaggerated representation, the situation is that of 57 where the shaded areas correspond to filled states.

3-fold   **I-fold**

$e(CCH_3)$ $e(CCH_3)$

surface
d orbitals

57

The 2-fold Geometry 53

We will not dwell on this adsorption site; as might have been anticipated, the results are in between those obtained for the 1-fold and 3-fold geometry. The bonding may be analyzed along the same lines as that of the 2-fold upright geometry of the vinylidene CCH_2. We may further recognize the similarity between the two systems by noting that the 2-fold geometry 53 is related to that occurring in binuclear ethylidyne complexes. Most of the latter are cationic, and assigning the positive charge to the unsaturated carbon of CCH_3 makes these systems analogous to binuclear vinylidene complexes.[50] From this standpoint, the bonding in 58a and 58b, where M-M represents a binuclear framework, is described by the same interactions.

(a)   (b)
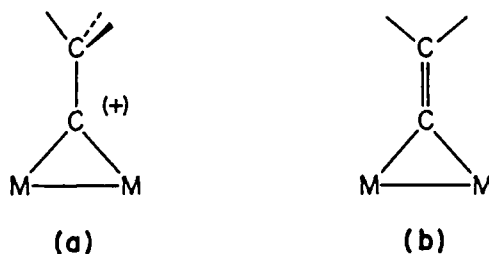
58

We should not then be surprised that, topologically, the interactions anchoring a CCH_3 and a CCH_2 unit to the same surface are similar.

Before concluding this section, we should point out that the hexagonal surface possesses two non-equivalent 3-fold hollows. These are distinguished by the presence or absence

of a second-layer atom below them. They are usually referred to as hcp (hexagonal close packing) or fcc (face centered cubic) hollows.[4d] Diffraction studies reveal that the CCH_3 is located atop of a fcc hollow. Our calculations put the two adsorption sites at the same energy, probably a consequence of the small number of layers used in this work.

Acetylene on Other Surfaces

The acetylene molecule is known to chemisorb on a number
of different surfaces, as was stated in the Introduction.
We now want to explore the reasons for i) the enhanced reactivity
of C_2H_2 when the latter is adsorbed on the (100) face of Fe,
ii) its lack of reactivity on Cu(111).

C_2H_2 on Fe(100)

The (100) face of iron is of square symmetry. Each layer
is translated by the $(\frac{1}{2}, \frac{1}{2}, 0)$ vector, with respect to the one
right above it. The unit cell of the 3-layer slab used for
this series of calculations is shown in 59. The surface layer

59   **60**
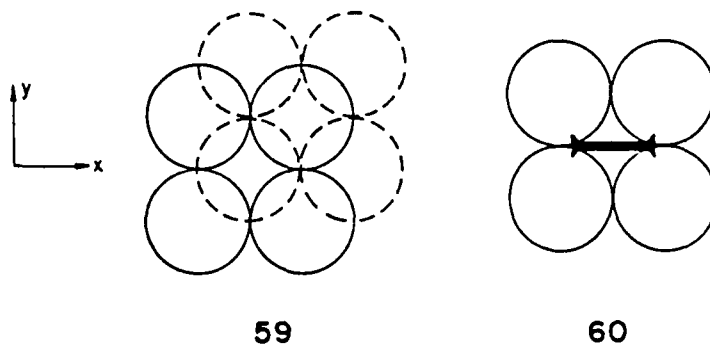
atoms are represented by solid lines whereas the next layer
atoms are dotted. The atoms of the third layer have identical
(x,y) coordinates to those of layer 1, but are 3.51Å below
them. The unit cell is in fact doubled in 59 because we are
to investigate the bonding of C_2H_2 in the geometry shown in
60. The coverage is again of $\frac{1}{4}$, i.e., one C_2H_2 for 4 surface

Fe atoms. No attempt will be made here to study the influence of the coverage. The interested reader is referred to a nice discussion of this topic in a recent article by Anderson.[51]

The previous sections of the present work have concentrated on the static interactions involved in the phenomenon of chemisorption. In the following, we look at the dynamics of C_2H_2 onto the surface starting with the 4-fold geometry 60. In particular we aim at understanding the role of the surface in making the cleavage of the acetylenic triple bond a process essentially free of activation energy.

Clearly, the bond must be weakened as soon as adsorption has taken place. Figure 18 shows at left the DOS of the naked surface, at right the DOS after the acetylene layer covers it. The dark area represents those states contributed by C_2H_2 . Note the location of the d states on the bare surface: -7.0 to -12.0 eV. The d bands are considerably shifted up

Figure 18 here

in energy as compared to those of the Pt surface, see Figure 3. The Fermi level is consequently found some 2.0 eV higher in energy, at -8.08 eV. The acetylene states spread over the -5.0 to -14.0 eV region as displayed on the right-hand side of the Figure. This large dispersion of the acetylene states leads one to think that C_2H_2 is strongly bound to the surface: indeed one computes an overlap population of 0.442 for each of
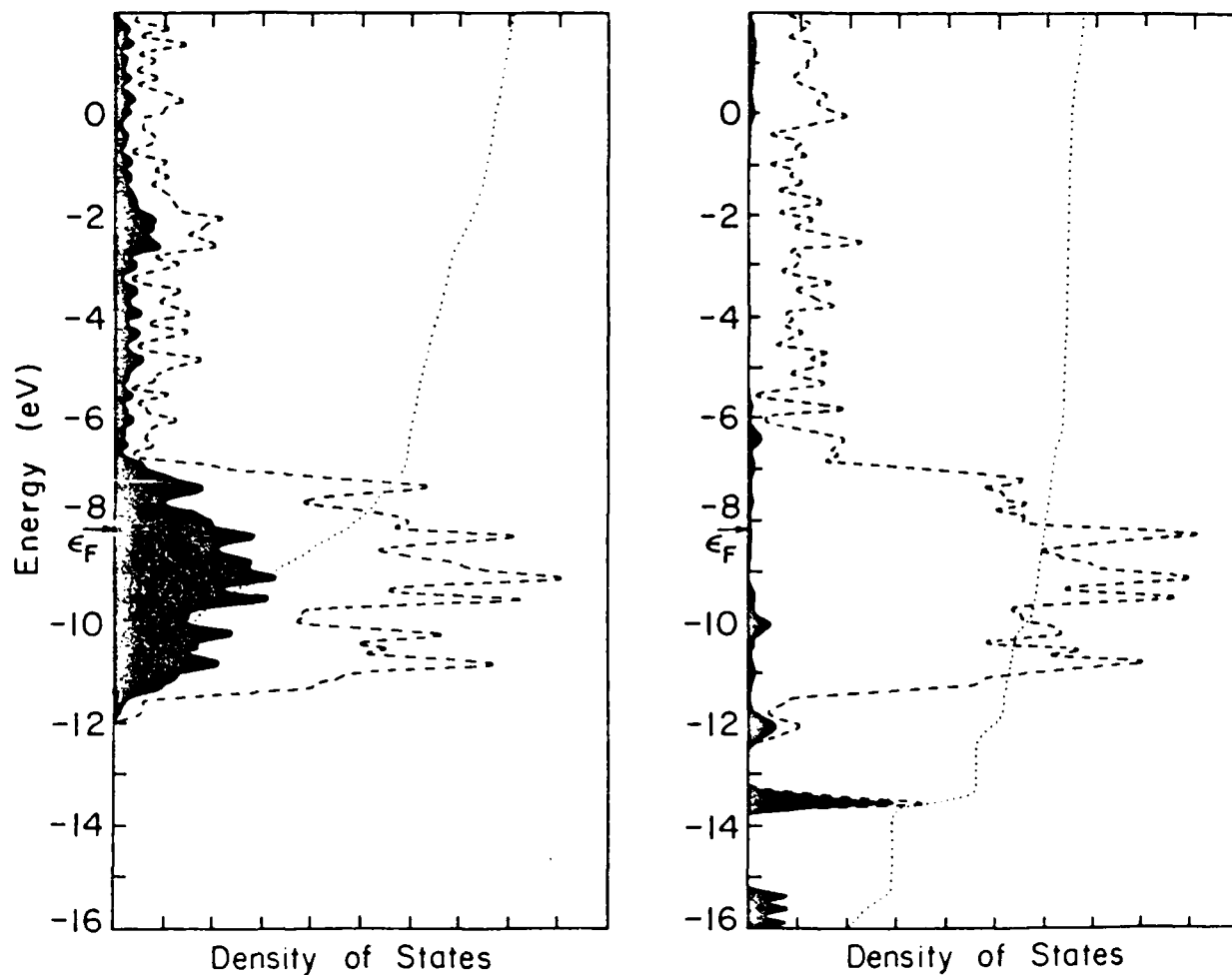
Figure 18. Left: Total DOS (dashed line) and contributions to it of the surface atoms (solid line) in the bare Fe(100) slab.

Right: Total DOS (dashed line) and contribution to it of the C_2H_2 states for the C_2H_2/Fe(100) system in the 4-fold geometry.

The areas under the contribution curves are darkened.

the 4 equivalent Fe - C interactions. However, the C-C overlap population, initially 1.703, drops dramatically to 0.965 electrons.

We have here the other extreme situation resulting from excessively strong bonding between the surface and the adsorbate: drastic weakening of the bonding within the adsorbate. The 4-fold adsorption of C_2H_2 on Pt(111), discussed in an earlier section, represented the case where it was the surface itself which had to pay the price of strong bonding to the adsorbate. Remember that surface reconstruction was anticipated in this case. The tremendous weakening of the C-C bond obviously will have important consequences <u>vis à vis</u> the ultimate reactivity of C_2H_2 on the surface. We return to this later. For now let us inquire which electron drift, $C_2H_2 \rightarrow$ metal or metal $\rightarrow C_2H_2$, causes this abrupt decrease in the C-C bond strength. Figure 19 deconvolutes the C_2H_2 states of Figure 18 with the contribution of each group of states according to their origin in the free acetylene. From left to right are the π, π_σ, π_σ^* and π^* states. Using the

Figure 19 here

now familiar convention of the sticks for the levels of C_2H_2 before interaction, one can measure the effects of chemisorption in each case. The Fermi level is also indicated.
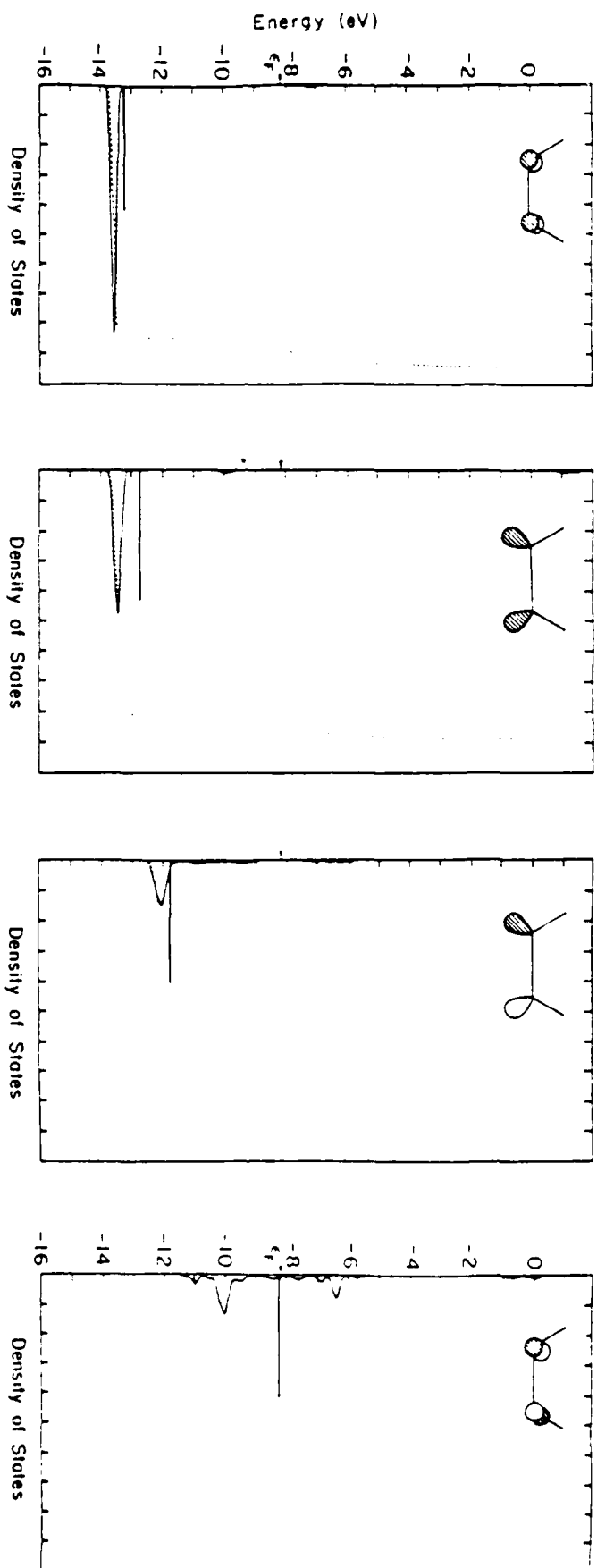
Figure 19. From left to right are the contributions to the DOS of π, π_σ, π_σ^* and π^* of C_2H_2 for the $C_2H_2/Fe(100)$ system in the 4-fold geometry. The sticks refer to the location of the corresponding states in the free C_2H_2. The curves are magnified by a factor of 4.2.

It is apparent that the π and π_σ states are pushed down upon interaction. Not that much though. For instance, the π states are sent down less in energy than in the 2-fold Pt(111) case. Recalling that the strength of the interaction is governed by the energy difference between combining orbitals, the fact that the d-block of Fe is moved up by ~2 eV with respect to that of Pt, i.e., further away from π (and π_σ), makes it clear why the C_2H_2 bonding orbitals are stabilized less by the Fe(100) surface than by Pt(111).

By the same argument, one anticipates stronger interactions involving $\pi_\sigma*$ and $\pi*$ in the iron case. A glance at the right-hand side plots of Figure 19 shows that this is indeed true. Please focus on the integration curves: at the Fermi level, $\pi_\sigma*$ is occupied by 1.35 electrons and $\pi*$ is filled with 1.065 electrons. These numbers are much larger than any of the corresponding ones encountered in Table 3 dealing with the C_2H_2/Pt(111) systems. The weakening of the acetylenic triple bond results from an enormous back-donation from the metal into C-C antibonding orbitals. Notice that this is particularly true for $\pi*$ of C_2H_2. The interactions at work here are combinations of the type shown in 61a-b. A similar discussion to the one presented here may be found in recent work from Anderson.[51]

(a)   (b)
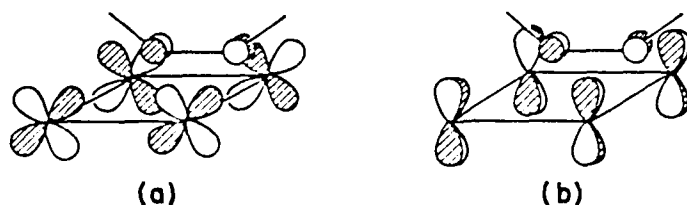
61

In order to anticipate the consequences of the bond
strength change during the process of chemisorption, we would
like to try to calibrate in terms of energy the difference in
C-C   overlap population before and after adsorption.
The acetylenic triple bond is worth ~200 kcal/mol.[52] The
overlap population computed for the chemisorbed species is
roughly that of single C-C   bond, worth ~85 kcal/mol.
What this means is that the energy required for dissociating
the chemisorbed C_2H_2 molecule into 2 CH fragments on the
surface has been decreased by a factor greater than 2.

Before turning to the actual cleavage of the C-C
bond on the surface, we describe rapidly the salient features
of the same process when the surface is absent. Most of the
information is obtained by the computation of a Walsh diagram
along the path taking C_2H_2 into 2 CH fragments. In 62
we depict schematically the evolution of the C_2H_2 orbitals
for this transformation. The analysis is straightforward and
we will not go into the details of it. Formally 3 bonds are

broken, 1 of σ type and 2 of π type. The corresponding bonding M.O.'s (σ, π_σ, π) see their energy rise whereas their
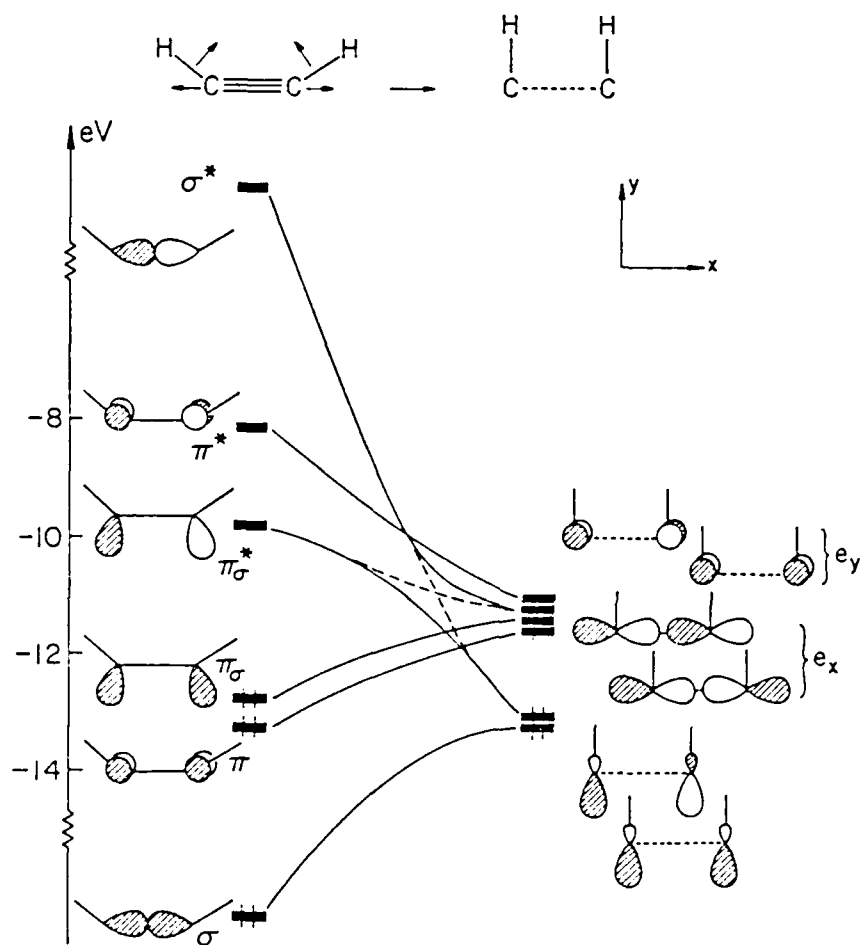
62

antibonding counterparts (π_σ*, π*, σ*) drop. For a large separation between the 2 CH units, one finds on the right hand side of 62 the symmetric and antisymmetric combinations

Appendix 1

The following geometrical parameters were used throughout: $C - C = 1.34\text{Å}$, $C - H = 1.09\text{Å}$, CCH angle = $140°$ in C_2H_2, $120°$ in CCH_2, $Pt - Pt = 2.775\text{Å}$, $Fe - Fe = 2.482\text{Å}$, $Cu - Cu = 2.556\text{Å}$. For the ethylidyne fragment, the $C - C$ and $C - H$ bonds were 1.54Å and 1.09Å and the β carbon was chosen tetrahedral. The metal to carbon distance was in all cases set at 2.03Å. The calculations performed on 12ab used $Pt - C(O)$: 1.85Å, $C - O = 1.14\text{Å}$.

of a compromise. The surface and the adsorbate see their intrinsic bonding weakened in the process. A non-dissociative chemisorption ensues when a balance between these two effects is reached. Surfaces composed of transition metals such as Fe or W have rather high-lying filled d-bands and are more prone to backbonding and therefore more likely to give rise to dissociative mechanisms than, say, Pt surfaces. We have in hand here the reason for the general high reactivity of these surfaces.

Acknowledgements

$\epsilon_F \rightarrow$

bulk empty

bulk·filled

adsorbate
donor states

(a)

metal
d states

adsorbate
acceptor states

bulk empty

bulk filled

ϵ_F

(b)
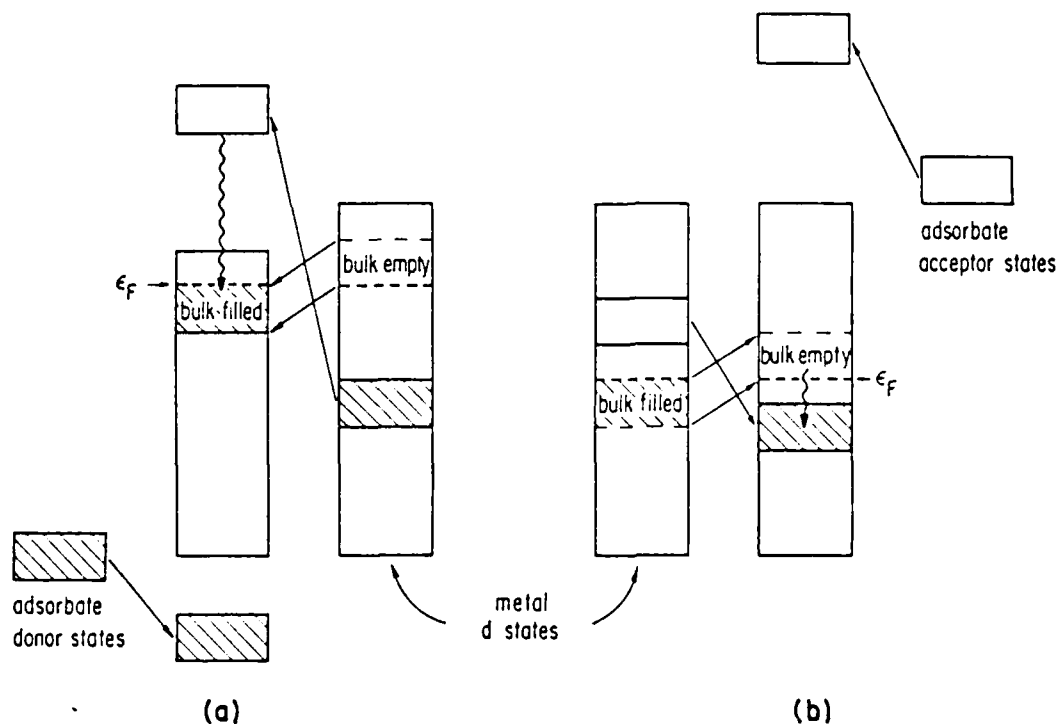
69

character of the surface: many metal-d states are empty prior

to chemisorption and accept electron density from filled orbitals

of the adsorbate. Secondary interactions now are between empty

states of the surface and empty states of the adsorbate. The

resulting bonding levels fall below the Fermi level. In turn,

those bulk states which are initially filled

transfer their electron density into these newly generated

bonding states. A graphic version of this discussion is shown

in 69b.

Another conclusion which emerges from this work is that

the possibility of non-dissociative chemisorption is the result

Conclusions

In this study, we have investigated the bonding of some unsaturated C_2 hydrocarbon fragments to metal surfaces. It is clear that in each adsorption site one finds similarities in the topology of the interactions in a molecule-cluster and adsorbate-surface system. The difference comes about in the electron reorganization following chemisorption. The existence of many states around the Fermi level of the surface in some sense allows a greater flexibility for the bonding of a molecule to a surface than to a discrete fragment. This reservoir of states can be either filled or emptied, depending on the metal involved and the adsorption site. The major contribution of these states to the overall bonding process is in secondary interactions. A surface featuring a high d-band filling will act as a donor towards the adsorbate in the primary interactions. The secondary interaction is a repulsive one between donor states of the adsorbate and filled metal d states. The reservoir of states has the crucial role of housing electrons which otherwise would enter highly antibonding states as a result of the repulsion. We should here perhaps emphasize the fact that these states are bulk-like in nature, being chiefly localized on inner-layer atoms of the surface. In 69a, we illustrate these considerations and show how bulk states get filled when an adsorbate interacts with an electron-rich surface. Turning to the case of a low d-band filling (electron-poor surface), the primary interaction involve the acceptor

chemisorbed and as Somorjai has put[57] it: "the activation

energy for reaction with the metal surface is significantly

larger than the heat of adsorption". This would mean that there

is a substantial barrier to going from a weakly bound C_2H_2

to the strongly bound state, i.e., the one investigated numer-

ically by us. To check this point, we ran a series of calcula-

tions, bringing the acetylene down in the 2-fold geometry with

a Cu - C distance decreasing from 2.50Å to 2.03Å. The energy

drops continuously but the curve features a slight shoulder

at 2.25Å. This may be a hint of the existence of a barrier,

which our calculations, which are poor at reproducing the

repulsive part of a chemisorption potential, do not model well.

We eagerly await more sophisticated computations on this system.

We should point out finally that previous experimental and

theoretical studies of C_2H_2 attach to a d^{11} - Cu atom have

suggested that only small backbonding from Cu to C_2H_2 is

taking place in these systems.[58]

between the d_{yz} states of the surface and p_x clearly drops to zero at the final geometry for symmetry reasons. As mentioned earlier, the p_x orbitals (or the e_x set) at point 5 can interact only with d_{xz} states with a relatively mediocre overlap, see 65b.

C_2H_2 on Cu(111)

The (111) face of copper is hexagonal, just like Pt(111). We carried out computations for C_2H_2 adsorbed in the 2-fold and 4-fold geometry, still using a 3-layer slab to model the surface. The Cu - C distances are 2.03Å. The 2-fold geometry is computed to be more stable than the 4-fold one by ~1.5 eV per C_2H_2. More importantly, the numerical results point to a strongly chemisorbed species with great back-bonding from Cu to C_2H_2. These findings do not agree with the experimental results discussed in the Introduction. We offer two reasons for this: first, the Fermi level of the bare surface is high in energy: -7.40eV. This is much higher than that of Pt(111) and does not compare well with what one would expect from the work function of Pt(111)[5b] (5.7 eV) and Cu(111)[56] (4.9 eV). In other words, our calculations may not reproduce well here the amount of penetration of the s-band into the d-block.

Secondly, the computations were performed assuming a strong C_2H_2/surface interaction with the use of a bonding Cu - C distance. In reality the C_2H_2 is only weakly
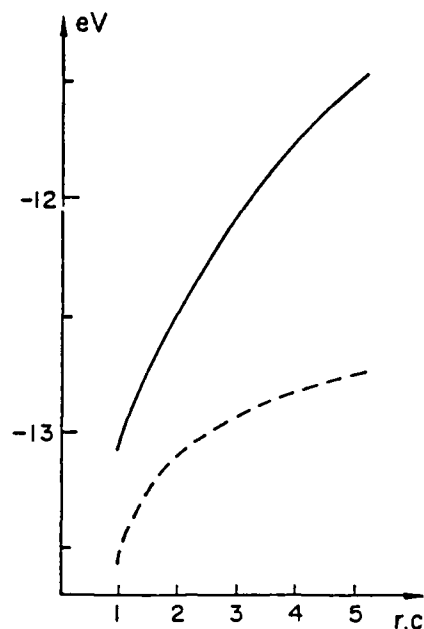
67

for molecular orbital σ. Note that at point 5 in <u>67</u>, the π orbital is at -11.4 eV, that is the energy of a pure p orbital of carbon. The π M.O. is at this point the symmetric combination of two p_y orbitals belonging to two non-interacting CH fragments.

Finally, it is interesting to look at the behavior of π_σ. This is a case where the overlap factor (in the perturbation term) wins over the energy one. Just as π, π_σ rises in energy when the C - C bond is stretched. However, instead of finding the π_σ states more stabilized in the process, we find them <u>less</u> stabilized. This is because the p_x orbital ultimately does not overlap well with the surface states. These ideas are illustrated in <u>68</u>, in a top view. The overlap

(a)   (b)
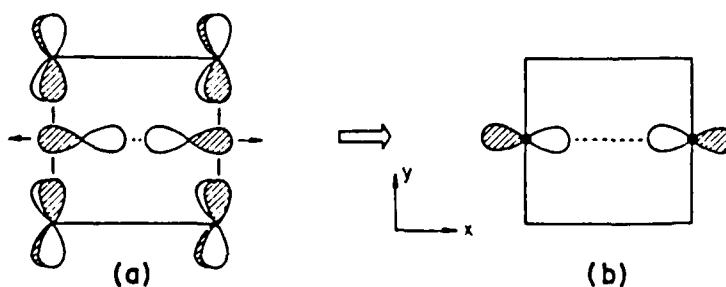
68

in many respects similar to that of the transition metal fragment in these systems. In the C_2H_2 - Fe(100) case, the surface does not act upon one molecular orbital but rather on groups of states.

Note that σ^* on the left-hand side plot of Figure 20 is not pushed up but stabilized. This appears to contradict the picture of 66. What happens here is that the σ^* states actually interact with the surface p states located in the -3.8 eV region, and are in fact stabilized. Would the σ^* states be involved only with lower lying metal d states, they would end up higher than the stick shown in the Figure. Recall that the latter indicates the energy of the σ^* orbital of the organic fragment in the absence of the surface at the geometry under consideration.

The picture discussed in 66 may however be used for the bonding π orbital of C_2H_2. In the free ligand it goes up in energy during the C - C bond breaking process. This means that in the course of the reaction, the π states will interact more and more with the d-bands and therefore are increasingly stabilized. The argument is illustrated in 67. The solid line shows the evolution of the energy of π in the ligand in the absence of the surface. The dashed line represents the energy below which one finds 50% of the π states in the total DOS of the whole C_2H_2/surface system. The dashed curve rises at a significantly lesser pace than the solid one. 67 is the solid state equivalent of what was described in 66

We can try to cast in more general terms how the surface assists the C - C bond breaking. The analysis of the projected DOS of both filled and empty C_2H_2 orbitals along the path 63 shows that rising filled orbitals are stabilized by the surface states with respect to their energy location in the free organic fragment. Imagine a hypothetical reaction where a σ bond is broken. A schematic version of the orbital changes and the energy profile for this reaction is given in 66. The role of a hypothetical catalyst for this transformation is defined by the two dashed lines: interaction with the catalyst pushes the rising filled orbital
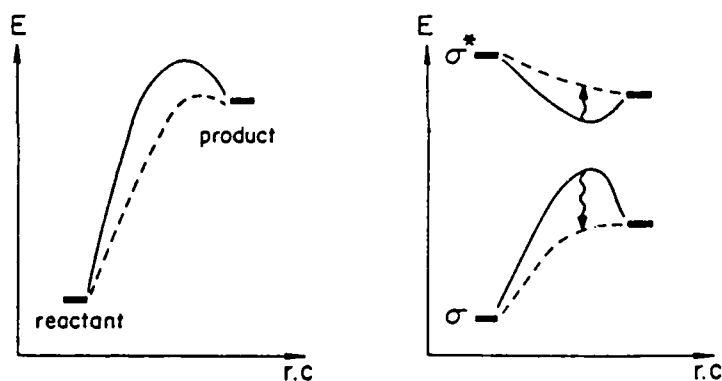
66

down in energy. In other words, some catalyst acceptor states enter bonding combination with σ, stabilizing this orbital. Conversely, σ^* acts as an acceptor towards some filled catalyst states. The latter are depressed in energy, whereas the σ^* is pushed up as indicated on the right-hand side of 66. The pattern in 66 is found for example in alkyl migrations[54] and hydrogen shifts[55] in organometallic chemistry. The influence of the surface on the C_2H_2 carbon-carbon cleavage is

via interactions such as 65a with surface d-states. Better overlap is achieved in these combinations than in those involving

(a)   **(b)**
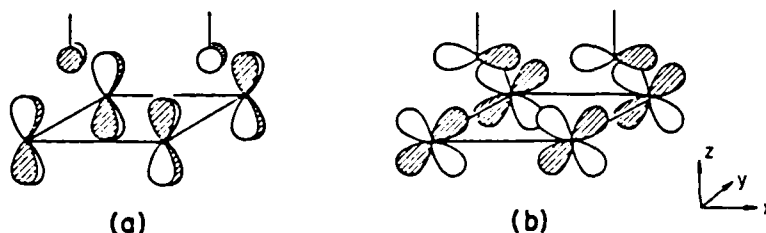
65

p_x, 65b for example. Therefore, the states generated by the degenerate set e_x, see 62, are found higher in energy than those descending from e_y: the splitting is small but significant: 0.7 eV.

The dismantling of the C – C bond on the Fe(100) surface perhaps illustrates what we call a principle of bonding transfer. The bonding inherent in the C – C bond is passed to the surface/CH fragment interactions. This idea also applies to non-dissociative chemisorption such as C_2H_2 on Pt(111). The surface to adsorbate bonding is in this case less strong but the C – C bond is weakened to a much lesser extent. The 4-fold adsorption of C_2H_2 on Pt(111), or more generally cases where surface reconstruction occurs on chemisorption, represent an alternative in which the surface-adsorbate bonding is paid for by loss of bonding within the surface.
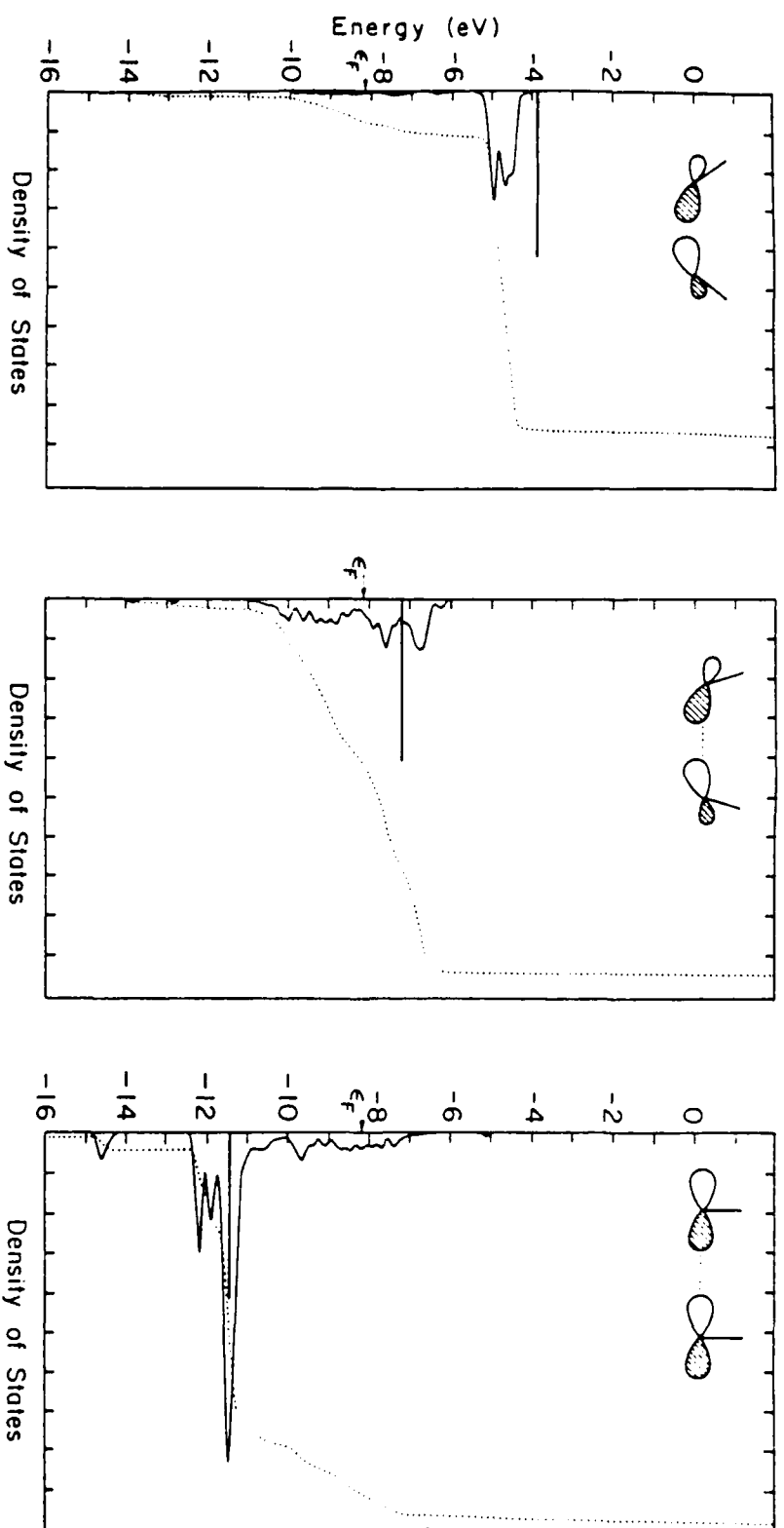
Figure 20. From left to right are the contributions of the carbon-carbon σ* states for different C-C distances, see text. The curves are magnified by a factor of 5.5.

Simultaneously, π^* and π_σ^* drop in energy and therefore increase their electron density content from back-donation. This serves as a driving force to elongate the C - C bond. Acting against this is rising σ . However, the σ M.O. will present two lobes towards the surface during the reorientation of the C - H bonds. These lobes will interact with the bottom of the d-band and further enhance Fe - C bonding. In the later stages of the process, σ^* comes into play. Figure 20 shows the DOS contribution of σ^* in the last 3 steps of our idealized surface. From left to right the C - C distance goes from 1.94 to 2.20 to 2.48Å, and again the Fe - C distance is constant. The states generated by σ^* , which ultimately evolves into the antisymmetric combination of the p_x orbitals

Figure 20 here

on the 2 carbons, mix more and more with the d-bands. Look especially at the shift in position of the integration curve. The stick marks locate the σ^* orbital in the organic fragment without the surface. Notice that when σ^* hits the energy range containing the d-band, the states resulting form inter-action are extremely disperse. Once σ^* is below -8.0 eV (the bottom of the d-band), the states which are surface-CH bonding in character emerge as a much narrower peak.

Along the same lines, σ^* becoming the antisymmetric combination of the p_y orbitals, which enter strong bonding

creased bonding of each Fe - C bond. A plot of the overlap

population of one of the 4 equivalent Fe - C bonds is shown

in <u>64</u>. The reaction coordinate is the 5-step sequence mentioned

above. The increase in bond str .gth must be multiplied by 4

overlap population

64
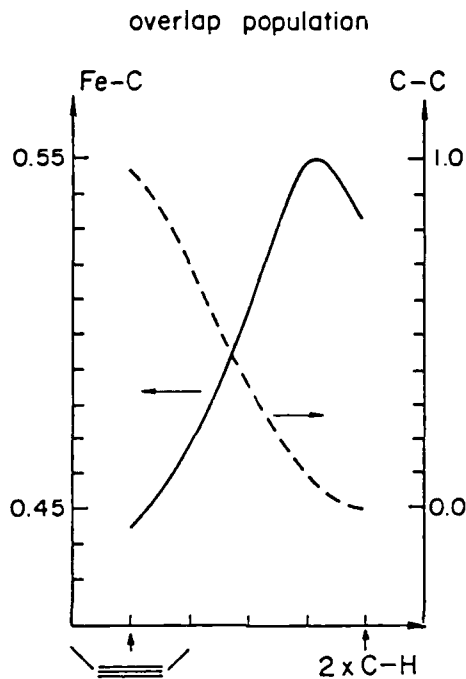
to reflect what is happening per unit cell. On the same plot

and referred to the right-hand side axis is the C - C overlap

population. Note that the Fe - C line curves slightly down

at the end point; we have not yet succeeded in explaining this.

To understand how the increase in the Fe - C bond strength

comes about, it is useful to return temporarily to <u>62</u>. In

the initial stages of the reaction π and π_σ go up and there-

fore get closer in energy to the d-block. In turn this trans-

lates into stronger bonding interactions between these states.

of the sp hybrid and the e set. These combinations are

degenerate if no overlap exists between the 2 fragments. The

large activation energy associated with the cleavage of the

triple bond is clearly generated by filled σ, π and π_σ,

all rising sharply up during the process. We compute a

9 eV barrier for the dissociation 62.

What happens when the same reaction occurs on Fe(100)?

We divided the transformation shown in 63 in 5 steps, keeping

the Fe to C distance at a fixed value[53] of 2.03Å. The

energy of the system exhibits a continuous decrease and the

dissociated C_2H_2 system 63b is stabilized by 5.2 eV over the

top view

$\odot \equiv C-H$
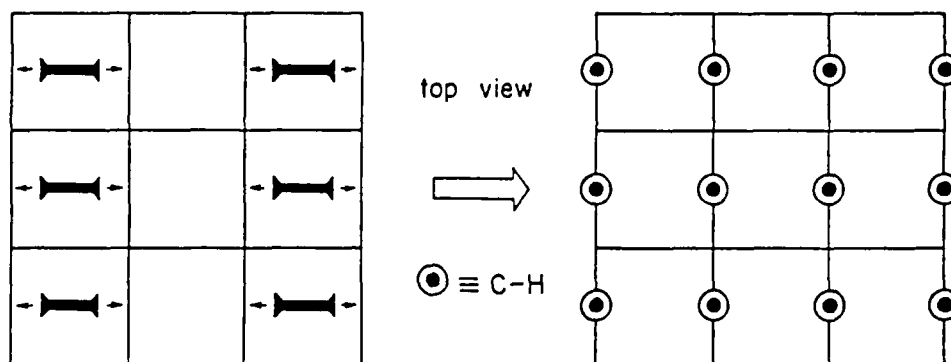
63

non-dissociated one, 63a. Experimentally, the process occurs

spontaneously at 95K which translates into a small barrier, if

any.

The calculations therefore show that the C_2H_2/Fe(100)

system as a whole moves to lower energy upon cleavage of the

carbon-carbon bond. The reason for this is found in the in-

Appendix 2

The parameters used in the computations are listed in Table 6. For the molecular calculations, the Pt parameters come from earlier work.[17b] The metal H_{ii}'s for the surface calculations were obtained by a charge iteration procedure on the bulk in each case.[59] The average on the hexagonal (111) surface were performed using a 9k-point set[60] appropriately reduced when symmetry factors allowed to do so. A 16k-point set[61] was used for the (100) cubic face of Fe.

Table 6. Extended Hückel Parameters.

orbital		H_{ii}, eV	ζ_1	ζ_2	$C_1{}^a$	$C_2{}^a$
Pt[b]	5d	−12.59	6.013	2.696	0.6334	0.5513
	6s	−9.077	2.554			
	6p	−5.475	2.554			
Pt[c]	5d	−11.260	6.013	2.696	0.6333	0.5512
	6s	−9.29	2.554			
	6p	−4.48	2.554			
Fe	3d	−9.2	5.35	1.80	0.5366	0.6678
	4s	−7.6	1.90			
	4p	−3.8	1.90			
Cu	3d	−11.9	5.95	2.30	0.5933	0.5744
	4s	−8.4	2.20			
	4p	−3.9	2.20			
C	2s	−21.4	1.675			
	2p	−11.4	1.625			
O	2s	−32.3	2.275			
	2p	−14.8	2.275			
P	3s	−18.6	1.6			
	3p	−14.0	1.6			
H	1s	−13.6	1.30			

[a]These are the coefficients in the double ζ expansion.

[b]Molecular calculations.

[c]Surface calculations.

References

1. a) G. Ertl and J. Kuppers in: "Low Energy Electrons and Surface Chemistry", Verlag Chemie, Weinheim, 1974.

   b) "Structural Studies of Surfaces", Springer Tracts in Modern Physics; V. 91; ed. G. Höler, Berlin, 1982.

   c) C.R. Brundle, Surf. Sci. 48, 99 (1978).

   d) M.W. Roberts and C.S. Mackee in "Chemistry of the Metal Gas Interface", Oxford University Press, London, 1978.

   e) "Electron Spectroscopy for Surface Analysis", ed. H. Ibach, Springer Verlag, Heidelberg, 1977.

2. a) "The Chemical Physics of Solid Surfaces and Heterogeneous Catalysis", ed. D.A. King, V. 4; Elsevier Scientific Company; Amsterdam. 1982.

   b) "Catalysis, Science and Technology", ed. J.R. Anderson and M. Beudart, Springer Verlag, Heidelberg, 1984.

3. N.D. S. Canning and R.J. Madix, J. Phys. Chem. 88, 2437 (1984).

4. a) E.L. Muetterties and J. Stein, Chem. Rev. 79, 479 (1979).

   b) E.L. Muetterties, Chem. Soc. Rev. 11, 283 (1982).

   c) E.L. Muetterties, T.N. Rhodin, E. Rand, C.F. Brucker and W.R. Pretzer, Chem. Rev. 79, 91 (1979).

   d) R.J. Koestner, M.A. Van Hove and G.A. Somorjai, Chem. Tech. 13, 376 (1983); J. Phys. Chem. 87, 209 (1983); G.A. Somorjai, Chem. Soc. Rev. 13, 321 (1984).

   e) H.F. Schaefer III, Acc. Chem. Res. 10, 287 (1977).

5. a) R.J. Koestner, J.C. Frost, P.C. Stair, M.A. Van Hove and G.A. Somorjai, Surf. Sci. 116, 85 (1982); P.C. Stair and

G.A. Somorjai, <u>Chem. Phys. Lett.</u> 41, 192 (1986); L.L.
Kesmodel, P.C. Stair, R.C. Baetzold and G.A. Somorjai,
<u>Phys. Rev. Lett.</u> 36 1316 (1976); L.H. Dubois, D.G. Castner
and G.A. Somorjai, <u>J. Chem. Phys.</u> 72, 5234 (1980); L.L.
Kesmodel, P.C. Stair, R.C. Baltzold and G.A. Somorjai,
<u>Surf. Sci.</u> 66, 299 (1977); W.J. Lo, Y.W. Chung, L.L.
Kesmodel, P.C. Stair and G.A. Somorjai, <u>Sol. Stat. Comm.</u>
22, 335 (1977); L.L. Kesmodel, L.H. Dubois and G.A.
Somorjai, <u>J. Chem. Phys.</u> 70, 2180 (1979); R.J. Koestner,
J.C. Frost, P.C. Stair, M.A. Van Hove and G.A. Somorjai,
<u>Surf. Sci.</u> 117, 491 (1982); A.E. Morgan and G.A. Somorjai,
<u>J. Chem. Phys.</u> 58, 3309 (1969).

b) J.E. Demuth, <u>Surf. Sci.</u> 80, 367 (1979), <u>I.B.M. J. Res.
Develop.</u> 22, 265 (1978), <u>Surf. Sci.</u> 84, 315 (1979);
J.E. Demuth and H. Ibach, <u>ibid</u> 85, 365 (1979), 78, L238
(1978); J.E. Demuth, <u>Chem. Phys. Lett.</u> 45, 12 (1977),
<u>Surf. Sci.</u> 93, 127 (1980), 69, 365 (1977).

c) T.E. Felter and W.H. Weinberg, <u>Surf. Sci.</u> 103, 265 (1981);
W.H. Weinberg, H.A. Deans and R.P. Merrill, <u>ibid</u> 41, 312
(1974).

d) H. Ibach, H. Hopster and B. Sexton, <u>Appl. Phys.</u> 14, 21
(1977); K.J. Rawlings, B.J. Hopkins and S.M. Foulias,
<u>Surf. Sci.</u> 77, 56 (1978); M.A. Chesters, B.J. Hopkins
and R.J. Winton, <u>ibid</u> 83, 181 (1979); H. Ibach, H. Hopster
and B. Sexton, <u>Appl. Surf. Sci.</u> 1, 1 (1977); A.M. Baro
and H. Ibach, J. Chem. Phys. 74, 4194 (1981); W. Erley,

A.M. Baro and H. Ibach, Surf. Sci. 120, 773 (1982); S.D. Foulias, K.J. Rawlings and B.J. Hopkins, ibid 114, 1 (1982).

e) N.D.S. Canning. M.D. Baker and M.A. Chesters, ibid 113, 441 (1981).

f) H. Ibach and S. Lehwald, J. Vaccum Sci. Technol. 15, 407 (1978).

g) S.D. Foulias, K.J. Rawlings and B.J. Hopkins, Surf. Sci. 133, 377 (1983).

h) L.L. Kesmodel, J. Chem. Phys. 79, 4646 (1983); L.L. Kesmodel, L.H. Dubois and G.A. Somorjai, Chem. Phys. Lett. 56, 267 (1978); J.A. Gates and L.L. Kesmodel, J. Chem. Phys. 76, 428, (1982), Surf. Sci. 124, 68 (1983).

i) W.T. Tysoe, G.L. Nyberg and R.M. Lambert, Surf. Sci. 135, 128 (1983).

j) G. Casalone, M.G. Cattania, R. Merati and M. Simonetta, ibid 120, 171 (1982).

k) R. Rye and R.S. Harrisen, J. Chem. Phys. 50, 3585 (1969).

l) D.L. Smith and R.P. Merrill, ibid 52, 5861 (1970).

m) R. Mason, M. Textor, Y. Iwasawa and I.D. Gray, Proc. Roy. Soc. (London) A-354, 171 (1977).

n) C. Brucker and T.N. Rhodin, J. Catal. 47, 214 (1977); C. Broden, T.N. Rhodin and W. Capehart, Surf. Sci. 61, 193 (1976).

o) T.N. Rhodin, C.B. Brucker and A.B. Anderson, J. Phys. Chem. 82, 894 (1978).

p) M.R. Albert, L.G. Sneddon, W. Eberhardt, F. Greuter, T. Gustafsson and E.W. Plummer, Surf. Sci. 120, 19 (1982).

q) N. Freyer, G. Pirug and H.B. Bonzel, _ibid_ 125, 327 (1983).

r) W.L. Parker, A.R. Siedle and R.M. Hexter, submitted.

s) B.J. Bandy, M.A. Chesters, M.E. Pemble, G.S. McDougall and N. Sheppard, _Surf. Sci._ 139, 87 (1984).

t) S. Lehwald, W. Erley, H. Ibach and H. Wagner, _Chem. Phys. Lett._ 62, 360 (1979).

u) J.C. Bertolini and J. Rousseau, _Surf. Sci._ 83, 531 (1979).

v) R.C. Baetzold, _ibid_ 95, 286 (1980).

w) U. Seip, M.-C. Tsai, J. Küppers, G. Ertl, _ibid_, 147, 65 (1984).

x) M.R. Albert, J.G. Sneddon, E.W. Plummer, _ibid_, 147, 127 (1984).

6. G.A. Somorjai in ref. 2a.

7. See for example: W. Bernhardt and H. Vahrenkamp, _Angew. Chem._ 96, 139 (1984).

8. P.-K. Wang, C.P. Slichter and J.H. Sinfelt, _Phys. Rev. Lett._ 53, 81 (1984).

9. K.Y. Yu, W.E. Spicer, I. Lindau, P. Pianelta and S.F. Lin, _Surf. Sci._ 57, 157 (1976).

10. See reference 5s for a discussion of this point.

11. a) For Ni; A.B. Anderson, _J. Chem. Phys._ 65, 1779 (1976)

   b) For Pt; A.B. Anderson, _J. Am. Chem. Soc._ 100, 1153 (1978); A.B. Anderson and A.T. Hubbard, _Surf. Sci._ 99, 384 (1980); S.P. Mehandru and A.B. Anderson, _Appl. Surf. Sci._, in press.

   c) For Fe; A.B. Anderson and S.P. Mehandru, _Surf. Sci._ 136, 398 (1984); A.B. Anderson, T.N. Rhodin and C.F. Brucker. Physical Electronics Conference. _Bull. Am. Phys. Soc._ 21,

940 (1976); A.B. Anderson, J. Am. Chem. Soc. 99, 696 (1977);   A.B. Anderson, J. Catal. 67, 129 (1981).

12. a) A. Gavezzotti and M. Simonetta, Surf. Sci. 99, 453 (1980).

    b) A. Gavezzotti, E. Ortoleva and M. Simonetta, J. Chem. Soc., Faraday Trans. I 78, 425 (1982).

    c) M. Simonetta and A. Gavezzotti, J. Mol. Struct. (Theochem), 107, 75 (1984).

    d) A. Gavezzotti and M. Simonetta, Chem. Phys. Lett. 48, 434 (1977); 61, 435 (1979).

    e) A. Gavezzotti, E. Ortoleva and M. Simonetta, Theor. Chem. Acta. 52, 209 (1979); Nouv. J. Chim. 7, 137 (1983).

    f) M. Simonetta, Nouv. J. Chim. 6, 65 (1982).

13. Other calculations of the cluster-type on this subject may be found in: a) H. Kobayashi, H. Teramae, Y. Yamabe and M. Yamagushi, Surf. Sci. 141, 580 (1984); b) R.C. Baetzold, Chem. Phys. 38, 315 (1979).

14. Numerous textbooks are available for an introduction to the tight-binding approximation: N.W. Ashcroft and N.D. Mermin, "Solid State Physics", Saunders, Philadelphia, 1976; J. Callaway, "Energy Band Theory", Academic Press, New York, 1964; W.A. Harrison, "Solid State Theory", Dover Publications Inc., New York, 1980.

15. a) R. Hoffmann, J. Chem. Phys. 39, 1397 (1963).

    b) R. Hoffmann and W.N. Lipscomb, ibid 36, 2176 (1962).

    c) For the implementation of the E.H. formalism to generate band structures, see: M.-H. Whangbo, R. Hoffmann and R.B. Woodward, Proc. Roy. Soc. (London) A-366, 231 (1979).

16. For a discussion of the active sites on Pt(111), see: G.A. Somorjai, _Adv. Cat._ 26, 1 (1977).

17. a) For ML_n see: S. Otsuka and A. Nakamura, _Adv. Organomet. Chem._ 14, 245 (1970).

    b) For M_2L_{2n} see: D.M. Hoffman, R. Hoffmann and C.R. Fisel, _J. Am. Chem. Soc._ 104, 3858 (1982) and references therein.

    c) For M_3L_{3n} see: E. Sappa, A. Tiripicchio and P. Braunstein, _Chem. Rev._ 83, 203 (1983).

18. For the derivation of the pattern displayed in Figure 1, see, T.A. Albright, _Tetrahedron_ 38, 1339 (1982).

19. B.E.R. Schilling and R. Hoffmann, _J. Am. Chem. Soc._ 101, 3456 (1979).

20. a) M.J.S. Dewar, _Bull. Soc. Chim. Fr._ 18, C71 (1951).

    b) J. Chatt and L.A. Duncanson, _J. Chem. Soc._ 2939 (1953).

21. K. Tatsumi, R. Hoffmann and J.L. Templeton, _Inorg. Chem._ 21 466 (1982).

22. This argument assumes that overlap in all cases is comparable in magnitude.

23. This statement holds when the chemisorbed species adsorbs in an ordered fashion.

24. By construction!

25. More rigorously, there are as many levels, hence k-points as there are microscopic unit cells in the macroscopic crystal.

26. Detailed expositions of the ideas developed here may be found in books listed in reference 14.

27. This holds for non degenerate bands at the zone edges. See: M. Lax "Symmetry Principles in Solid State and Molecular Physics", Wiley-Interscience, New York, 1974.

28. T. Hughbanks and R. Hoffmann, J. Am. Chem. Soc. 105, 1150 (1983); S.D. Wijeyesekera and R. Hoffmann, Organometallics 3, 949 (1984).

29. For recent reviews see: J.C. Bertolini and J. Massardier in "The Chemical Physics of Solid Surfaces and Heterogeneous Catalysis", ed. D.A. King. V. 3; Elsevier Scientific Company, Amsterdam, 1982; see also reference 4d.

30. For a comparative discussion of cluster and slab-type of computations see: R.P. Messmer, J. Vaccum Sci. Technol. A2, 899 (1984). For a survey of cluster-type calculations see: M. Simonetta and A. Gavezzotti, Adv. Quant. Chem. 12, 103 (1980).

31. J.-Y. Saillard and R. Hoffmann, J. Am. Chem. Soc. 106, 2006 (1984) and references therein.

32. A common energy scale is used for practical purposes. The parameters of Pt are different for the surface and molecular calculations, see Appendix.

33. In fact, only yz is a true element of symmetry. The xz plane is not, because of the finite thickness of the slab. For purposes of our discussion we can use the two mirror planes of the real surface/adsorbate system.

34. This follows simply from the Ni - Ni distance which is 2.492Å in the metal whereas the Pt atoms are spaced by 2.775Å.

35. The geometrical problem associated with C_2H_2 in a 4-fold geometry on Pt(111) was pointed out recently by Sheppard and coworkers, (ref. 5s).

36. C.E. Anson, B.T. Keiller, I.A. Exton, D.B. Powell and N. Sheppard, J. Chem. Soc., Chem. Comm. 470 (1983).

37. D.B. Kang and A.B. Anderson, submitted for publication.

38. M.I. Bruce and A.G. Swincer, Adv. Organomet. Chem. 22, 59 (1983).

39. a) C. Minot, M.A. Van Hove and G.A. Somorjai, Surf. Sci. 127, 441 (1982).

    b) C. Zheng, Y. Apeloig and R. Hoffmann, to be published.

    c) The reverse conclusion was drawn by Muetterties and coworkers in: R.M. Gavin, Jr., J. Reutt and E.L. Muetterties, Proc. Natl. Acad. Sci. USA 78, 3981 (1981).

40. B.E.R. Schilling and R. Hoffmann, J. Am. Chem. Soc. 100, 6274 (1978).

41. J. Evans and G.S. McNulty, J. Chem. Soc., Dalton Trans. 79 (1984).

42. This could lead one to think that a 3-fold upright geometry is the best one. This was tested numerically and the energy for this geometry is the highest of all sites, primarily due to weakening of the surface - CCH_2 σ bonding.

43. S.-S. Sung and R. Hoffmann, J. Am. Chem. Soc. in press.

44. L.L. Kesmodel, J. Vacuum Sci. Technol. A2, 1082 (1984).

45. a) N. Sheppard, _J. Mol. Struct._ 80, 163 (1982).

    b) M.A. Chesters and N. Sheppard, _Chem. Brit._ 17, 521 (1981).

    c) I.A. Oxton, D.B. Powell, N. Sheppard, K. Burgen, B.F.G. Johnson and J. Lewis, _J. Chem. Soc., Chem. Comm._ 719 (1982).

    d) M.W. Howard, S.F.A. Kettle, I.A. Oxton, D.B. Powell, N. Sheppard and P. Skinner, _J. Chem. Soc., Faraday Trans. II_ 2, 77 (1981).

46. P. Skinner, M.W. Howard, I.A. Oxton, S.F.A. Kettle, D.B. Powell and N. Sheppard, _J. Chem. Soc., Faraday Trans. II_ 2, 1203 (1981).

47. a) E.O. Fisher and U. Schubert, _J. Organomet. Chem._ 100, 59 (1975).

    b) S.J. McLain, C.D. Wood, L.W. Messerle, R.R. Schrock, F.J. Hollander, W.J. Yongs and M.R. Churchill, _J. Am. Chem. Soc._ 100, 5962 (1978).

    c) K.R. Birdwhistell, S.J. Burgmeyer Nietzer and J.L. Templeton, _ibid_ 105, 7789 (1983).

    d) M.H. Chisholm, J.C. Huffman and N.S. Marchant, _ibid_ 105, 6162 (1983).

48. a) C.P. Lasey, S.R. Marder and P.J. Fajan, _ibid_ 104, 4950 (1982).

    b) D.L. Davies, A.F. Dyke, A. Endesfelder, S.A.R. Knox, P.J. Naish, A.G. Orpen, D. Plaas and G.E. Taylor, _J. Organomet. Chem._ 98, C43 (1980).

49. a) J.T. Park, J.R. Shapley, M.R. Churchill and C. Bueno,
    J. Am. Chem. Soc. 105, 6182 (1983).

    b) A.J. Canty, B.F.G. Johnson, J. Lewis and J.R. Norton,
    J. Chem. Soc., Chem. Comm., 1331 (1972).

    c) R. Markby, J. Wender, R.A. Friedel, F.A. Cotton and
    F.W. Sternberg, J. Am. Chem. Soc. 80, 6529 (1958).

    d) K.S. Wong, K.J. Haller, J.K. Dutta, D.M. Chipman and
    T.P. Fehlner, to be published.

50. R. Hoffmann, Angew. Chem., Int. Ed. Engl., 12, 711 (1982).

51. See first paper in reference 11c. Also, the influence of
    the metal d-band position and the orbital size effect
    are discussed in a paper dealing with C_2H_2 on vanadium
    surfaces: D.B. Kang and A.B. Anderson, to be published.

52. These bond energies are extracted from: J. March, "Advanced
    Organic Chemistry", 2nd Ed., McGraw-Hill, 1977, p. 28.

53. This does not change our conclusions. The
    reader should also be aware of the fact that experimentally
    the Fe - C distances decrease. At the end point, these
    are 1.75Å. In this study, we used 2.03Å throughout to
    keep the meaningfulness of the changes in overlap popula-
    tions.

54. H. Berke and R. Hoffmann, J. Am. Chem. Soc. 100, 7224 (1978).

55. J. Silvestre and R. Hoffmann, submitted.

56. P.O. Gartland, S. Berge, B.J. Slagurold, Phys. Rev. Lett.
    28, 738 (1972).

57. First paper in reference 4d.

58. G.A. Ozin, D.P. McIntosch, W.J. Power and R.P. Messmer,

   Inorg. Chem. 20, 2623 (1981); see also A.J. Lee, G.A.

   Ozin and W.J. Power, ibid 17, 3648 (1978); P.H. Kasai

   and D. McLeed, Jr., J. Am. Chem. Soc. 100, 625 (1978);

   R.W. Zoellner, K.J. Klabunde, Chem Rev. 84, 554 (1984).

59. For Fe, the parameters are from reference 31.

60. J.D. Pack and J.J. Monkhorst, Phys. Rev. B 16, 1748 (1977).

61. S.L. Cunningham, Phys. Rev. B 10, 4988 (1974).

END

FILMED

4-85

DTIC